START

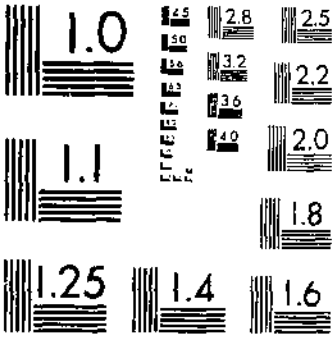

MICROCOPY RESOLUTION TEST CHART
NATIONAL BUREAU OF STANDARDS-1963-A

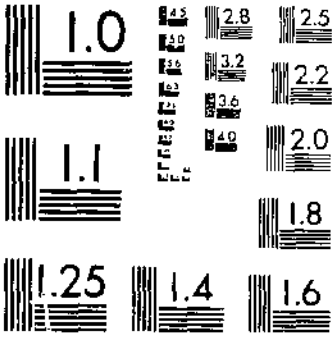

MICROCOPY RESOLUTION TEST CHART
NATIONAL BUREAU OF STANDARDS-1963-A

TECHNICAL BULLETIN NO. 577 OCTOBER 1937

FLOW OF WATER THROUGH 6-INCH PIPE BENDS

By

DAVID L. YARNELL

Senior Drainage Engineer, Division of Drainage
Bureau of Agricultural Engineering

UNITED STATES DEPARTMENT OF AGRICULTURE, WASHINGTON, D. C.
IN COOPERATION WITH THE UNIVERSITY OF IOWA COLLEGE OF ENGINEERING

Technical Bulletin No. 577 October 1937

UNITED STATES DEPARTMENT OF AGRICULTURE
WASHINGTON, D. C.

FLOW OF WATER THROUGH 6-INCH PIPE BENDS[1] [2]

By DAVID L. YARNELL
Senior drainage engineer, Division of Drainage, Bureau of Agricultural Engineering

(United States Department of Agriculture, Bureau of Agricultural Engineering, in Cooperation with the University of Iowa College of Engineering)

CONTENTS

INTRODUCTION

This bulletin presents the results of a series of experiments on the flow of water through bends in 6-inch circular pipe with various amounts of total curvature, on 90° bends of hyperbolic and elliptical cross section, on a 90° bend of circular cross section with varying radius of curvature, and on a 90° miter bend. The research included cases with uniform and with nonuniform velocity distribution in the pipe approaching the bend.[3]

Designers of pumping plants and hydroelectric plants are constantly endeavoring to increase the efficiencies of plant operation. Any change in design that reduces the loss of head in the pipes and bends means increased efficiency. A bend acts as an obstruction to flow, causing loss of head, both in open and in closed conduits. Certain types of bends cause internal changes in velocity to such a degree that the capacity of the bends as hydraulic conduits is reduced con-

[1] Received for publication Apr. 12, 1937.
[2] Experiments on 180° bends of square and rectangular cross section have been previously reported. (See U. S. Dept. Agr. Tech. Bull. 520, Flow of Water Around 180-degree Bends.)
[3] The investigation was carried on at the hydraulics laboratory of the University of Iowa. Sherman M. Woodward acted as consultant during the investigation. The late Floyd A. Nagler, and Frederic T. Mavis, head of the department of mechanics and hydraulics, advised with regard to the method of computations and the report.

siderably. As a rule, disturbed flow means inefficient flow, and the maximum usefulness of the entire cross section of the channel is not realized.

The studies here reported have developed new data on velocity and pressure changes in bends and in the tangents adjacent. The data will be useful to designers of new plants and to engineers engaged in making efficiency tests of irrigation pumping plants, because they show the effects that may be expected when piezometer connections are made at different points on a pipe. The data also demonstrate the necessity of taking into consideration the disturbing effects of bends upon the performance of the downstream tangents. Such conditions are often encountered in penstock and spiral casings approaching water turbines as well as in draft-tube conduits of the elbow type.

The investigation described herein was undertaken for the purpose of exploring the changes in pressure and velocity in different parts of the flowing stream, as the water undergoes the transition from motion along a straight path to motion around a curve and the opposite transition back to straight-line motion. The conditions disclosed in this study may be considered as representing what always occurs when water flows in a bend or a crooked channel, or when it meets a bridge pier or other form of obstruction. A knowledge of these changes is fundamental to an understanding of the effects, harmful or otherwise, of crooked and obstructed channels on the flow of water, and to a determination of the best means for diminishing any objectionable or troublesome effects.

SCOPE OF THE INVESTIGATION

The investigation was planned to cover measurement of (1) velocity distribution in the bend and in approach and discharge tangents, (2) pressure changes at various sections in the bend and the tangents, (3) energy changes as the water passes around the bend, (4) loss of head due to the bend, (5) directions of the filaments of flow as the water moves around the bend, and (6) friction losses occurring in the approach and discharge tangents.[4]

The experiments were conducted on bends of 6-inch pipe, the bends and the approach and discharge tangents being of transparent celluloid. The bends tested comprised round pipe bent to circular arcs of 45°, (pl. 1, *A*) 90°, and 180° continuous curvature (pl. 2, B), 180° with curvature once reversed (pl. 1, *B*), 270° with curvature twice reversed (pl. 2, *A*), three special-shape 90° (pl. 1, *C*) bends, and a 90° miter bend (pl. 2, *C*).

Determinations of loss of head were made on all the bends, with mean velocities of 2, 4, 5, 6, 7, 8, 10, 12, and 14 feet per second and uniform velocity distribution [5] in the approach tangent, by piezometer measurements of peripheral pressures. Changes in velocity distribution were studied with mean velocities of 5, 8, and 12 feet per second by means of pitot-tube traverses.

[4] Frank W. Edwards, H. P. Evans, Jr., O. J. Baldwin, G. A. Marston, Roland A. Kampmeier, Ross N. Brudenell, Cecil H. Morris, Edward Soucek, Charles W. Kinney, Carlos Kampmeier, L. B. Wuemer, H. B. Vasey, Kenneth M. Smith, Andreas Luksch, Arthur Ippen, and Edwin Thomas assisted in making the tests.

[5] Uniform velocity distribution, in this bulletin, means velocity distributions as for undisturbed flow in straight pipe, approximately symmetrical about the center line of the pipe.

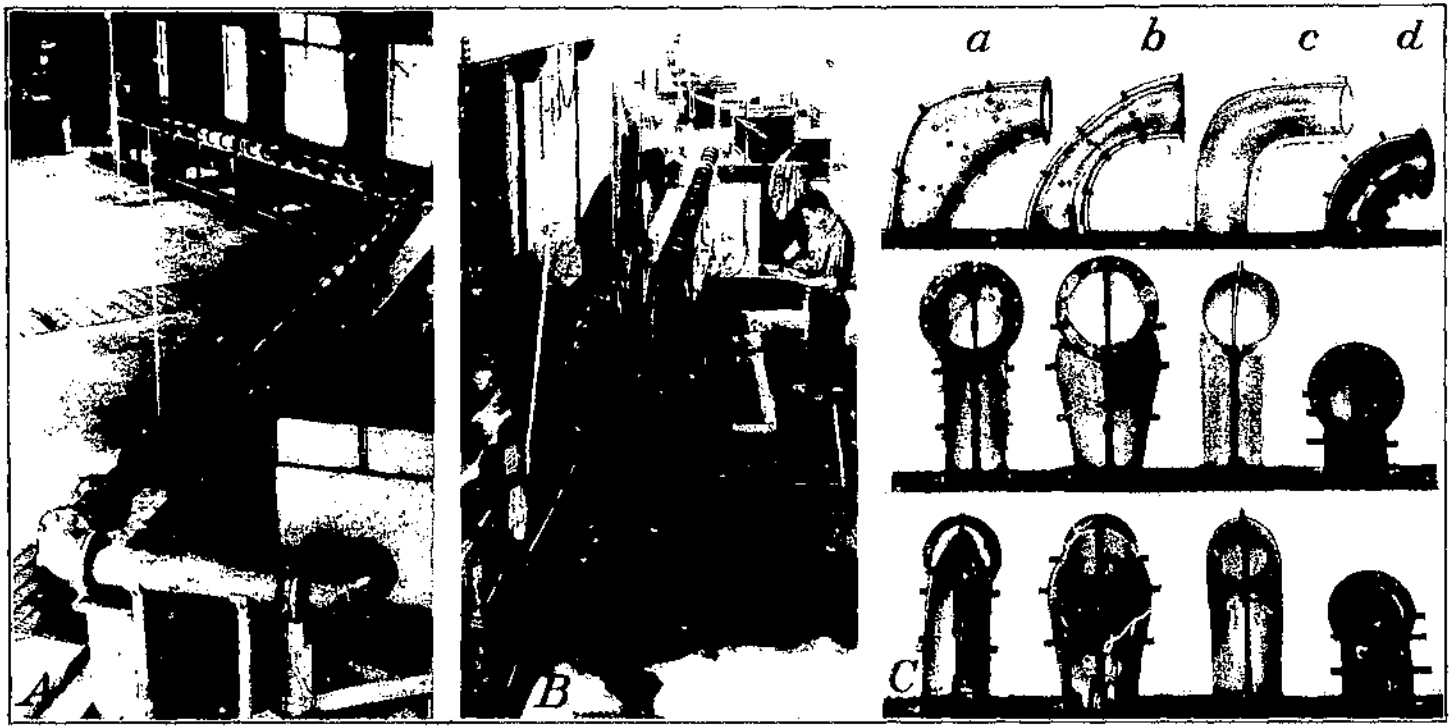

FLOW OF WATER IN 6-INCH PIPE BENDS.

A, 45-degree bend and tangents set up for test, with weir box in foreground; *B*, 180-degree reverse-curvature bend and tangents set up for test; *C*, special-shape and standard bends tested: *a*, Type M; *b*, type N; *c*, type W; *d*, standard.

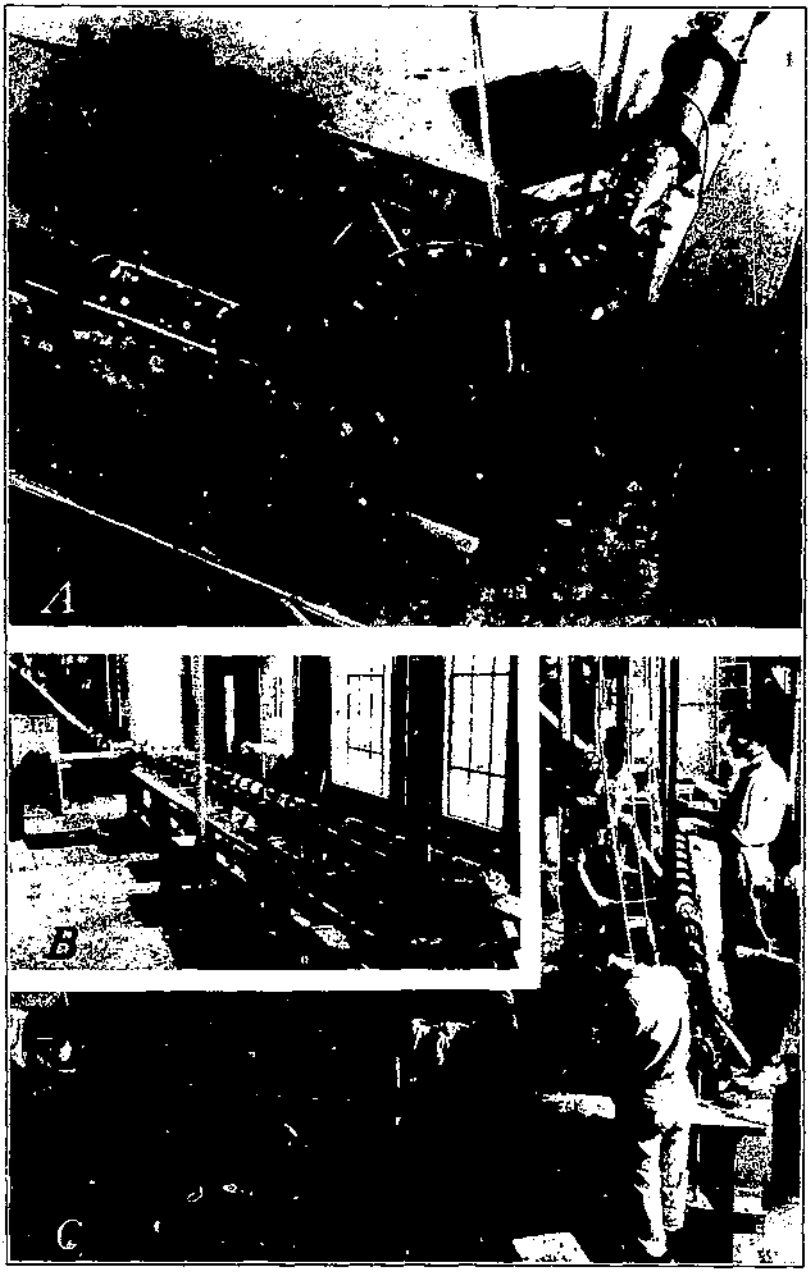

FLOW OF WATER IN 6-INCH PIPE BENDS.

A, 270-degree bend arranged for test; *B*, 180-degree continuous-curvature bend and tangents set up for test; *C*, miter bend and tangents set up for test.

The effect of nonuniform velocity distribution in the approach tangent was studied, at a mean velocity of 8 feet per second. High velocity was induced first at the top of the pipe, then toward the inner side of the bend, then at the bottom, and lastly toward the outer side of the bend. The high velocity along one side of the approach tangent was three to four times the low velocity along the opposite side.

BENDS TESTED

The "standard" 90° bend was of uniform cross section approximately 6 inches inside diameter, and the radius of curvature of the center line was 8¼ inches. The length of the center line thus was 12.96 inches, and the cross-section area 28.27 square inches. The 45° bend was like half the standard bend; the 180° and 270° bends were made of two and three standard bends (pl. 1 and 2.)

The three special-shape bends[6] are shown in plate 1, *C*, and their general characteristics are given in table 1. All were 6 inches in diameter and circular in cross section at the ends. Type M gradually changed to an oval section at midlength with major axis 9.87 inches and minor axis 6 inches (fig. 36). In transverse view, the inner and outer boundary curves were hyperbolas. Type N had a constant curvature radius of 15 inches. The cross section gradually changed to elliptical at midlength, with major axis 10 inches and minor axis 3.60 inches, maintaining a constant cross sectional area (fig. 43). Type W was of circular cross section throughout, but increased to approximately 7 inches diameter at midlength (fig. 50). The radius of curvature decreased from infinity at the points of tangency to 5 inches at midlength.

The miter bend was made by joining directly two straight pieces of pipe cut obliquely, with no intervening curved section. Its length on the center line was 16½ inches, so when it was placed upon the standard bend the ends of the two bends coincided.

TABLE 1.—*Characteristics of special-shape 90° bends* [1]

Bend [2]	Cross-section area at vertex	Length on center line	Radius of curvature of center line at vertex
	Square inches	*Inches*	*Inches*
Type M	47.00	23.0	12
Type N	28.27	23.6	15
Type W	38.15	26.4	5

[1] MOCKMORE, C. A. FLOW CHARACTERISTICS IN ELBOW DRAFT TUBES. Amer. Soc. Civ. Engin. Proc., 63: [251]-280, illus. 1937. See p. 269.

[2] Professor Mockmore designated types M, N, and W as numbers 2, 4, and 3, respectively.

The tests included 50 feet of straight celluloid pipe with which was determined the loss of head in straight pipe of the same kind as used for the bends, and which was utilized also for approach and discharge tangents in testing the bends.

[6] These bends had been made by Charles A. Mockmore for his special studies on draft tubes, and were loaned for use in this investigation.

The standard bends and about 30 feet of the straight celluloid pipe were obtained by purchase, and some 20 feet of the straight pipe was made in the laboratory. As a result of the continued drying out of the solvent used in making the celluloid, there was some slow shrinkage in the pipe diameter, but the amount in most cases did not exceed three thirty-seconds of an inch and the variation was measured and allowed for in making the hydraulic computations.

TEST PROCEDURE

The quantities of discharge giving the velocities of 2 to 14 feet per second were approximately 0.4 to 2.8 cubic feet per second. During the progress of each test continuous measurements were taken of the head on the weir, and the mean value was used in computing the mean velocity for the test.

Velocity traverses and pressure determinations were made on the bend at the beginning and end points and at each intermediate 22½° point; on the approach tangent at distances 0.5, 1.0, 3, 5, 10, 15, and 20 feet from the beginning of the bend; and on the discharge tangent at distances 0.5, 1.0, 3, 5, 10, 15, 20, and 25 feet from the end of the bend. At each of these sections there were eight piezometer connections, except that on bend types N and W there were but four connections on each circumference.

Measurements of velocities were made at 25 points in each cross section of the bends and tangents. (See typical section, figs. 1 and following.) Three check readings were always taken at the center of the pipe in each cross section, and numerous checks were made at other points. Frequently the original and check traverses were made by different men with different pitot tubes. It is believed that velocity readings obtained in the tangents are fairly accurate, but it is realized that those in the bends may be appreciably in error. Even though the velocity orifice of the pitot tube was held normal to the cross section, in the bend, turbulent flow and secondary currents acted on the pressure orifices in such manner that differential pressures greater or less than the true values might be shown. The velocity readings show that sometimes such errors actually occurred. They undoubtedly are one reason why points on the total-energy gradients, particularly on the bends, are so inconsistent at some cross sections.

In each test, readings were taken on all piezometers, and all these readings were referred to a common datum. Great care was taken to see that all air was excluded from the hose lines connecting the piezometer tubes with the nipples on the water pipes, and that all connections were tight. The water in the piezometer tubes oscillated considerably, as much as 0.10 foot or more during the higher discharges. These oscillations, caused by turbulent flow, made correct reading of the pressures somewhat difficult, but probably the errors in these readings seldom exceeded 0.01 or 0.02 foot, and then only for the larger discharges. Numerous check readings were taken to eliminate apparent inconsistencies or to assure that these inconsistencies continued throughout the test.

A complete test for a single quantity of flow involved the recording of some 230 piezometer readings and of the maximum velocity at from 500 to 1,000 different points, depending upon the amount of curvature of the bend, and required seven men for about 8 hours. Check measurements were taken on the diameters of the bends and pipe at various

sections before and after each test, to determine the amount of any change in diameter of the celluloid pipe. Levels on the tangents and the bends were taken daily during the tests to check the elevations of the piezometers.

The obstruction used to create nonuniform velocity distribution in the approach tangent consisted of a metal cylinder in which were placed rows of no. 9 wires, staggered one-half inch apart. The obstruction was 12 inches long, and was placed with the downstream end about 4 feet upstream from the beginning of the bend. This obstruction produced a velocity on one side of the pipe about four times that on the other side.

The pitot tubes used in measuring velocity (pl. 2, *C*) were of the combined type. They were made and calibrated at the laboratory especially for these tests. Each was so constructed that the area of contraction of flow was a minimum, and was constant regardless of the position of the orifice. The effect of the contraction was included in the calibration of the tube.

The quantities of flow were measured by 90° V-notch weir cut in the end of a steel tank 2½ feet wide, 2 feet deep, and 8 feet long. The weir was calibrated prior to the testing, by means of weighing tanks. The upper end of the tank was connected to the discharge end of the test pipe (pl. 1, *A*). By means of several baffles, the turbulence was eliminated before the water passed into the weir chamber.

VELOCITY CHANGES IN THE BEND

The velocity-distribution data obtained are shown by contours in figures 1 to 63, except for omission of the most distant sections on the tangents and of some intermediate sections on the longer bends. Sections on the bends are designated by their locations in degrees of curvature from the beginning of the bend. Sections on the tangents are designated by their distances in feet from the nearer end of the bend, preceded by a minus sign (—) or plus sign (+) to indicate respectively approach or discharge tangent. On the miter bend the ends are designated as sections 0° and 90°, and the intermediate sections are designated by distance from the intersection of tangents, measured on the inner side of the bend. The sections are shown as viewed when looking downstream.

It should be noted that the contour interval is not uniform throughout the series of graphs, but care has been taken to show the maximum, minimum, and peripheral velocities in each section within 0.5 foot per second.

The graphs are arranged in sets, seven for each bend, in the following order: 45°, standard 90°, 180° continuous curvature, 180° reversed curvature, 270°, type M, type N, type W, and miter bend. The graphs in each set show, in order, conditions obtaining with uniform velocity distribution in the approach tangent and mean velocities of 5, 8, and 12 feet per second, and with four nonuniform approach-velocity distributions and a mean velocity of 8 feet per second.

WITH UNIFORM VELOCITY DISTRIBUTION IN APPROACH PIPE

As the water approaches the bend, the filaments of flow along the inner side of the bend are accelerated. It has been generally observed that for a given discharge the velocity along the inner side of the bend

increases as the radius of curvature decreases. Except in the case of certain special-shape bends, the thread of maximum velocity in the bend gradually moves to the outer side as the water travels around the bend.

For the 5-foot velocity with uniform or normal velocity distribution in the approach pipe, see figures 1, 8, 15, 22, 29, 36, 43, 50, and 57. The velocity distributions at sections $-0.5'$ and $-1'$ for the different bends are fairly uniform, the greatest variations being for the special-shape bends and the miter bend. At station 0°, the beginning of the bend, there is a real decrease in velocity toward the outer side, not very noticeable for the 45° bend but very apparent for the others. At section 22½° there is a marked difference in velocity between the inner and outer sides of the bends, the differences being practically the same for the standard, the two 180°, and the 270° bends. For the special-shape bends the differences in velocity are not consistent with those for the other bends, showing that the shape of the bend has a real effect on the velocity distribution within it. For the 45° bend, the difference is not so great.

At section 45° there is a marked similarity in the velocity contours for the standard, the two 180°, and the 270° bends. For the special-shape bends, as would be expected, the velocity contours are not similar, but there is still a marked difference between the inner and outer sides of the bend. Even at section 67½° there is a similarity in velocity distribution for the standard and the 180° continuous-curvature bends.

Similar velocity-distribution characteristics with the 8- and 12-foot velocities are shown by the different bends, in figures 2 and 3, 9 and 10, etc.

With uniform velocity distribution in the approach tangent the velocity distribution became nearly normal again in 3 to 5 feet downstream from the end of the bend, as shown by the graphs.

WITH NONUNIFORM VELOCITY DISTRIBUTION IN APPROACH PIPE

The studies with nonuniform velocity distribution in the approach pipe were made primarily to determine the effects that such distribution might have on the velocity conditions in bends. In a pipe layout there may be two bends separated by a short tangent, so that the disturbance of velocity distribution caused by the first may persist to the second. The bends may be so situated that the loss of head in the second may be either less or more than in the first, even though the same quantity of water is flowing through both and the bends are of identical shape.

In most if not all tests reported in engineering literature on the flow of water through bends, uniform velocity distribution prevailed in the approach tangent. So far as the writer knows, no prior tests have been conducted in which nonuniform velocity distribution approaching the bend was created in order to study its effects.

With uniform velocity distribution in the approach tangent, the water next the inner side of the bend normally speeds up. When the approach velocity along the inner side is greater than normal, because of this added energy the filaments of water along the inner side flow around the bend even faster than normally, while the filaments along the outer side flow more slowly than normally. Hence the difference in velocity between the inner and outer sides of the bend is much greater than normal. This increased difference in velocity

causes a greater difference in pressure between the inner and outer sides of the bend, and a greater loss of head in the bend, than would occur with uniform approach flow.

Comparison of sections 0° in figures 2 and 4 shows the difference in velocity distribution in the 45° bend between uniform and nonuniform approach-velocity conditions. The difference is even more marked at section 22½°. At section 45° (fig. 4), the velocity along the inner side of the bend is still high even though the end of the bend is reached. The velocities at these same sections in the 90° bend show greater differences (figs. 9 and 11). In the 180° bend of continuous curvature, the differences are still greater (figs. 16 and 18). The flow in the special-shape bends shows similar characteristics, as may be seen by comparing figure 37 with figure 39, 44 with 46, and 51 with 53. In the 180° reverse-curve bend (figs. 23 and 25) and in the 270° bend (figs. 30 and 32) there were no marked differences in velocity distribution beyond about section 90°.

When initial high velocity prevailed toward the outer side of the bend, the velocity conditions in the bends became very different. This change of approach velocity also had a marked effect on both the velocity distributions and the pressures in the bends. Comparisons may be made between figures 2 and 5, 9 and 12, 16 and 19, 23 and 26, 30 and 33, 37 and 40, 44 and 47, 51 and 54, and 58 and 61.

When initial high velocity existed at the top of the approach pipe, abnormal velocity distribution prevailed throughout the bend. Comparison of the velocity distribution at section 0° in figure 6 with normal distribution at the same section (fig. 2), shows much greater variation with the nonuniform approach velocity. A marked difference prevailed throughout the bend and even beyond. Figures 9 and 13 show similar differences, and so do the velocity diagrams for the other bends.

With initial high velocity at the bottom of the approach tangent, the flow in the bends showed departures from the flow with uniform approach velocity generally similar to the departures shown when the initial high velocity was at the top of the pipe.

PRESSURE CHANGES IN THE BEND

Transverse profiles of the peripheral pressures at the different sections, as measured from a common datum, are shown above the velocity cross sections in figures 1 to 63. The piezometer readings are shown by circles and squares, circles for the top and side pressures and squares for the bottom pressures where those were different from the top readings.

WITH UNIFORM VELOCITY DISTRIBUTION IN APPROACH PIPE

Figures 1 to 63 show that, as the water moves through the bend, the pressure is greatest near the outer side and is much less along the inner side. Neglecting loss in friction, the total energy in any filament of flow is constant; therefore, the greater the increase in velocity along the inner side of the bend, the lower will the pressure drop there. This is evident in a comparison of the first three graphs shown for each bend.

For the same bend, the greater the difference in velocity, the greater the radial difference in pressure, as may be seen by comparing

figures 1, 2, and 3; 8, 9, and 10; 15, 16, and 17; etc. Also, the greater the velocity of flow through a given bend, the greater the possible variation in pressures against the top and bottom of the bend. Figures 3, 10, and 17 have considerably more squares, showing bottom pressures different from top pressures, than do figures 1, 8, and 15.

The variations in pressure along the inner and outer sides of the bends, at the horizontal diameter, are shown for representative velocities in figures 64 to 81. So far as practicable these graphs show pressures for tests other than those shown in figures 1 to 63, but such diagrams can be constructed from the data given in those figures.

Figures 64 to 72 show that the differences in transverse pressure were greater for the higher than for the lower velocities in the same bend, and that for the same velocity of flow there was a very close agreement between the differences for all the bends except types M, N, and W. The maximum differences in the three special-shape bends were less than those in the other bends, but the differences in the miter bend were twice those in the standard bend.

With a given velocity, the difference in pressure at section 22½° was the same for the standard bend, the two 180° bends, and the 270° bend. The differences at this section for the 45° bend were not quite so great, probably because this bend was much shorter. The pressure differences at section 45° in the four bends, 90° to 270°, were practically the same as at section 22½°. Beyond section 45°, this similarity in pressure differences does not continue because of length and direction of curvature.

The pressure differences were maximum at sections 22½° and 45° in the standard and 180° continuous-curvature bends. In both bends of reversed curvature the maximum difference was at section 135°, being slightly greater than the difference at section 45° which in the 270° bend was practically the same as that at section 225°.

For most bends, with velocities greater than 5 feet per second the pressures along the inner side of the bend were less than at either end of the bend. This drop in pressure was less, however, for the special-shape than for the standard bend. The rise in pressure along the outer sides of types M and W was somewhat greater than in the standard bend. In the hyperbolic type M bend the pressure on the inner side was greater midway of the bend than at either end (fig. 69). This condition was true with all velocities greater than 5 feet per second, and with velocities greater than 12 feet per second the pressure on the inner side became a foot or more greater than at either end. Knowledge of this fact may be useful where it is desired to obtain a greater pressure on the inner side of the bend than will exist at either end.

For bends of uniform cross section, with uniform radius of curvature and uniform approach velocity, it appears that in general the difference between the pressures on the inner and the outer sides is substantially the same throughout the length of the bend except near the ends and, in the case of reverse-curvature bends, near the points of reversal. The amount of the difference varied with the velocity. In the bends with cross section increased at midlength the pressure was raised throughout the cross section by an amount corresponding to the reduction in velocity head (figs. 69 and 71). When the radius of curvature of the bend was decreased, the difference between the two wall pressures was correspondingly increased.

WITH NONUNIFORM VELOCITY DISTRIBUTION IN APPROACH PIPE

In the 45° bend (fig. 73) the drop in pressure along the inner side was greatest when the approach velocity was high on that side, and was least when the approach velocity was high on the outer side, even less than obtained with uniform velocity distribution in the approach pipe. High velocity at the top and high velocity at the bottom of the approach pipe gave pressure distributions in the bend that were very much alike, although the high bottom velocity usually gave slightly greater pressure differences between the inner and outer sides. As before stated, this condition may be related to the secondary currents set up within the bend. Comparison of the pressure differences for the 90° and 180° continuous-curvature bends shows similar characteristics, as do also the first 90° of both reverse-curvature bends. The pressure relations in the miter bend appear generally similar, but the fluctuations and differences were about double those in the standard bend.

The pressure differences for the special-shape bends are unusually interesting, and worthy of considerable study. These few tests seem to show that it would be possible to design a bend in which the pressures along the inner side would have, at least for any particular velocity, a definite relation to the pressures at the beginning and end of the bend.

SECONDARY CURRENTS

Secondary currents are caused in a bend by the differences in centrifugal force of the filaments having different velocities, which induce transverse flow in addition to the forward motion of the fluid. These transverse currents usually become apparent first next to the top and bottom of the pipe and increase in strength as the water moves around the bend.

Tests on bends in rectangular channels[7] showed that the type of secondary current that prevails in a bend depends on the velocity distribution in the approach tangent. When there was a high velocity at the top and a low velocity at the bottom of the approach channel, in a conduit bending to the right the secondary current was counterclockwise as viewed looking downstream; when the high velocity was at the bottom in the approach channel, the direction of the secondary current was clockwise. When uniform velocity distribution existed in the approach tangent, two secondary currents were set up in the bend, one clockwise in the upper portion of the cross section and the other counterclockwise in the lower portion. It is believed that the same condition holds true in round pipes.

The same tests showed that with high velocity toward the outer side either one or two secondary currents might be set up within the bend, depending upon its length and radius of curvature. When high velocity existed toward the inner side, the flow was so disturbed that definite secondary currents were difficult to detect. This condition of flow, however, gives definitely the greatest loss of head in pipe bends (figs. 91 to 99). Secondary currents exist also in open-channel bends, but usually there is only one, even with approximately uniform velocity distribution in the channel approaching the bend.

The strength of the secondary currents in bends is greater in wide channels than in narrow channels. Therefore the use of blade turns

[7] See footnote 2.

in 90° elbows and guide vanes in quarter-turn draft tubes increases the efficiency of those bends, by reducing the magnitude of the secondary currents. In general, the greater the velocity of flow, the more pronounced are the secondary currents, and any means that will reduce these currents and create a greater effective area of forward flow will reduce the energy loss, and hence improve the efficiency of the conduit.

LOSS OF HEAD

The loss of head in a pipe bend results mostly from two causes: (1) Skin friction of the forward flowing water against the pipe walls, as in straight pipe; and (2) internal friction of the induced or secondary currents within and downstream from the bend. The nature of the secondary currents and the energy loss resulting from them are influenced appreciably by the distribution of velocities in the approach pipe to the bend. The loss of energy caused by the bend, more than required for straight flow for an equal distance, is really the energy required to bring the disorderly condition of flow back to normal streamline motion.

The loss of energy or head due to a bend may be expressed as—

$$H_b = K \frac{\text{width of channel}}{\text{inner radius}} \frac{V^2}{2g} \tag{1}$$

Because the tests included special-shape bends having variable radii, the losses due to the bends as determined by these experiments have been expressed simply, as—

$$H_b = K' \frac{V^2}{2g} \tag{2}$$

in which the effects of size of pipe and radius of curvature of the bend are incorporated in the coefficient K'.

The friction loss in 50.5 feet of straight 6-inch celluloid pipe was determined for a wide range of velocities, and the friction loss per foot of straight pipe was found to be

$$h_f = 0.0302 \frac{V^2}{2g} \tag{3}$$

From the velocity measurements taken on the two tangents and the bends at three quantities of flow, those giving mean velocities of 5, 8, and 12.1 feet per second, the losses of head due to the bend were computed by the following method:

The total energy was computed at various sections upstream from the bend, and these values were then reduced to an equivalent of that at the beginning of the bend. For example, the total energy at the section $-0.5'$ was determined from velocity and pressure measurements at that section, and the friction loss for 0.5 foot of straight pipe was deducted, to compute the total energy at section 0°. By the same method, the total energy at section 0° was calculated from measurements made at sections $-1'$, $-3'$, $-5'$, and $-10'$. When these computations had been made, errors in measurement at any section were easily seen, and radically discordant values could be discarded. The same method was followed below the bend, the total energy for sections $+10'$, $+15'$, and $+20'$ being reduced to equivalents of that at section $+25'$. The averages of these determinations for section 0°

and for section +25′ were then obtained, and the difference between them was the total energy loss between sections 0° and +25′. The net loss caused by the bend, exclusive of wall friction, was obtained by deducting from this difference the friction for a length of straight pipe equal to the distance from section 0° to section +25′ measured along the center line of the pipe.

In the foregoing calculations the velocity head for each section was not computed directly from the total quantity flowing in the pipe, but was computed as the average of determinations for parts weighted according to quantity of flow. The cross section was divided into unit areas, each of which was multiplied by its mean velocity to obtain the unit quantity of flow. Then the sum of the unit quantities multiplied by their respective velocity heads (Σhq) was divided by the sum of the quantities (Σq) to obtain the mean velocity head that was used for the section. The result, however, was not much different from the head computed from the mean velocity for the section, except in the bends.

Loss of head was computed also from the tests in which measurements were made only of the peripheral pressures, these tests comprising velocities ranging from 2 to 14 feet per second. The methods of computation were the same as for the experiments in which velocities were measured, except that the mean velocity head for each section necessarily was calculated directly from the mean velocity for the whole section.

Thus the actual loss of head due to the bend exclusive of friction was determined for all the tests on each bend for each quantity of flow. These losses then were plotted as abscissas against velocities as ordinates, on logarithmic paper, and an equation for the loss in each bend was determined.

The equations are as follows:

45° bend	$H_b=0.11\frac{V^2}{2g}$	(4)
Standard bend	$H_b=0.15\frac{V^2}{2g}$	(5)
180° bend, continuous curvature	$H_b=0.19\frac{V^2}{2g}$	(6)
180° bend, reverse curvature	$H_b=0.31\frac{V^2}{2g}$	(7)
270° bend	$H_b=0.40\frac{V^2}{2g}$	(8)
Type M bend	$H_b=0.15\frac{V^2}{2g}$	(9)
Type N bend	$H_b=0.13\frac{V^2}{2g}$	(10)
Type W bend	$H_b=0.17\frac{V^2}{2g}$	(11)
Miter bend	$H_b=1.17\frac{V^2}{2g}$	(12)

In comparing the standard and the special-shape bends with respect to loss of head as shown by the above formulas, it should be remembered that the mean radius of the standard bend was only 8¼ inches whereas that of the type M bend on its center line was approximately

12 inches, that of the type N bend was 15 inches, and that of the type W bend varied from 8.8 inches to infinity. If a 90° bend with a mean radius of 15 inches could have been tested, its formula might have had a lower coefficient than obtained for any of the special-shape bends.

Formulas for loss of head under conditions of nonuniform velocity distribution at the beginning of the bend were not developed, because the variability of the ratio of high to low velocity in practice is too great for such formulas to have any real use or value.

In order to make readily apparent the loss of head caused by a bend, and the distance downstream through which it accumulates, the data are presented graphically in figures 82 to 90 for uniform distribution of velocity in the approach tangent and in figures 91 to 99 for nonuniform approach velocity. The total energy gradient is shown from section $-1.0'$ to the end of the discharge tangent, $+25'$. The energy gradient for straight pipe is shown for comparison, by extending the gradient line determined from the measurements at all the sections on the approach tangent. The vertical distance between the two gradient lines gives the total accumulated loss to that section.

With a uniform distribution of velocity in the approach tangent (figs. 82 to 90), the loss of head caused by the bend increased for about 5 feet downstream from the bend. The end of this zone of increase is the section at which the energy gradient for the bend becomes parallel to the energy gradient for straight pipe.

This graphic method of determining the loss of head due to bends is especially useful in studying the effects of unequal velocity distribution in the approach pipe (figs. 91 to 99). The tests on the 45° bend (fig. 91) show the loss of head with high velocity toward the inner side of the bend as nearly 2.5 times that obtained with uniform velocity distribution in the approach pipe, whereas with the high velocity toward the outer side, the loss was only about three-fourths that obtained with uniform velocity distribution. When high velocity existed at either the top or the bottom of the pipe, the loss of head was from two to three times that obtained with uniform velocity distribution. For the standard bend (fig. 92) the high velocity toward the inner side caused a loss more than three times that obtained with uniform velocity, high velocity toward the outer side gave slightly greater loss than did the uniform velocity, and high velocity at the top and at the bottom gave losses 80 to 100 percent greater. These differences were obtained with a nonuniform velocity distribution having high and low velocities at section 0° of about 12 and 4 feet per second, respectively; with greater ratios of nonuniformity, the differences in losses probably would be greater.

It appears that for some bends the length of the downstream tangent, 25 feet, was not quite sufficient for measuring the total loss of head. This is shown in figures 94, 95, and 96 for the 180° reverse-curvature, the 270°, and the type-M bends, particularly with high velocity at either the top or the bottom of the approach pipe. For those bends and such velocity distribution, a longer downstream tangent would have been desirable.

PIPE BENDS AS FLOW METERS[8]

It would seem that in many installations a pipe bend could be used as a flow meter by measuring the difference in pressure between the

[8] See also the following publication: LANSFORD, W. M. THE USE OF AN ELBOW IN A PIPE LINE FOR DETERMINING THE RATE OF FLOW IN THE PIPE. Ill., Engin. Expt. Sta. Bull. 289, 36 pp., illus. 1936.

outer and inner sides. That difference may be as large as or even larger than that produced in a venturi meter or pitot tube, and, as in those other measuring devices, it varies with the second power of the velocity. The experiments indicate that the errors likely to be involved in using the bend for this purpose are no greater than those experienced with the other devices named. Where great accuracy is desired, however, each bend should be calibrated individually in place.

Theoretically, the difference in pressures between the two sides of bend is—

$$(h_o - h_i) = \frac{V^2 B}{gR} \tag{13}$$

in which h_o and h_i are the pressures at the outer and inner sides of the bend, V is the mean velocity at the section, B is the width of the section—the diameter, for round pipe—, g is the acceleration of gravity, and R is the mean radius of curvature. Then, introducing a coefficient to cover energy losses the mean velocity may be expressed as follows:

$$V = C\sqrt{h_o - h_i}\sqrt{\frac{gR}{B}} \tag{14}$$

in which C is a coefficient depending upon the kind of pipe bend. From equation (14) a simple formula for a single pipe bend may be written as—

$$Q = c'\sqrt{h_o - h_i} \tag{15}$$

in which Q is the discharge in cubic feet per second and c' is a constant depending upon the dimensions and condition of the bend.

Formula (15) would be convenient to use, because the pressure difference can be quickly determined and the discharge then be obtained by a simple calculation or be taken from an easily prepared table. For the celluloid bends with mean curvature radius of 8¼ inches, differences in pressure at section 22½° have been plotted against discharges (fig. 100). Those graphs show the same value of c' for four of the bends, and a value but slightly different for the 45° bend. For pressure differences at section 45°, the coefficients for the 90° to 270° bends differed but little (fig. 101). The equations obtained for the special-shape bends are shown in figure 102. For those bends the coefficients differed considerably, for pressure differences measured at either section 22½° or section 45°.

Pressure differences were measured on the 90° cast-iron bend nearest the weir tank in the pipe connecting the celluloid pipe to the weir tank (pl. 1, *A*). This bend closely approximated the standard bend in dimensions. The measurements were of necessity made at points 21½° and 38½° from the beginning of this bend. The pressure differences plotted against discharges are shown in figure 103, and it will be noted that the coefficient c' for section 21½° has the same value as was obtained for section 22½° on the standard bend (fig. 76).

The study of bends as flow meters did not include experiments with nonuniform velocity distribution in the approach tangent.

CONCLUSIONS

The results of the experiments on flow through pipe bends reported in the foregoing pages seem to warrant the following conclusions:

1. All bends act as obstructions to flow, causing greater loss of head than an equal length of straight pipe.

2. The velocities of the filaments along the inner side of the bend are increased and those along the outer side are decreased from their velocities in the tangent approaching the bend.

3. The loss of head increases with increase in length of the bend, for pipe of equal size, equal radius of curvature, and like material and condition, and is greatest for a bend in which the tangents are joined without an intervening curved section. The ratios of the loss in head caused by the other round-pipe bends to that caused by the 90° standard bend were approximately, for the 45° bend, 0.75; for the 180° continuous-curvature bend, 1.25; for the 180° reverse-curvature bend, 2.1; for the 270° bend, 2.7; for the miter bend, 7.8.

4. For a given pipe bend and given quantity of flow, the head lost in the bend is influenced greatly by the velocity distribution in the approach tangent. With velocity in the approach tangent high toward the inner side, the losses of head shown by all the bends ranged from about 1.5 to 4 times that obtained when uniform velocity prevailed in the approach tangent. With the approach velocity high toward the outer side, some bends showed slightly less and some slightly greater losses than obtained with uniform velocity of approach. With high velocity at the top of the approach tangent the loss for each bend was between 1.25 and 2 times that obtained with uniform approach velocity, and with approach velocity high at the bottom the loss was between 1.3 and 3 times that obtained with uniform velocity. These ratios were obtained with a high velocity along one side of the approach tangent about three times the low velocity along the other side.

5. From the difference between the pressures on the inner and outer sides of a bend at the point of maximum differences, and having the size of pipe and the radius of curvature of the bend, it is possible to compute the mean velocity and therefore the quantity of flow. When a pipe bend has been calibrated it may be used as a flow meter with which the discharge can be determined by measuring merely the difference in pressure.

6. The losses in the pipe bends experimented upon appear to vary as the square of the velocity, and not as the 2.25 power as suggested by some writers.

PRACTICAL APPLICATIONS OF TEST OBSERVATIONS AND DATA

Observations during the tests showed that a single piezometer on a bend or close to the bend on a tangent may not give the correct average pressure in the conduit at the cross section. Hence it is highly important that, in such work as making efficiency tests on pumps, the piezometer determinations be made at several points on any section.

The experiments showed considerable greater loss of head in bends of reverse curvature than in bends of continuous curvature. Therefore it is advantageous in water-piping installations to avoid, so far as practicable, reversal of direction of curvature by bends placed near together.

In most installations, at least one pipe bend can be calibrated as a flow meter, and a manometer constructed by which discharge can be read directly.

From the information obtained on loss of head resulting from non-uniform velocity distribution in the approach tangent, it is apparent that in planning pipe lay-outs if two bends on the same line curve in the same direction, the second will cause less loss of head than the first if the bends can be placed near together.

Cast-iron bends doubtless cause greater loss of head than the celluloid bends tested, because of greater roughness of the interior walls which naturally causes secondary currents of greater intensity and magnitude. The tests with celluloid bends suggest, however, the relative effects of increased length and of change in direction of curvature upon loss of head in bends of equal pipe diameter and equal curvature radius.

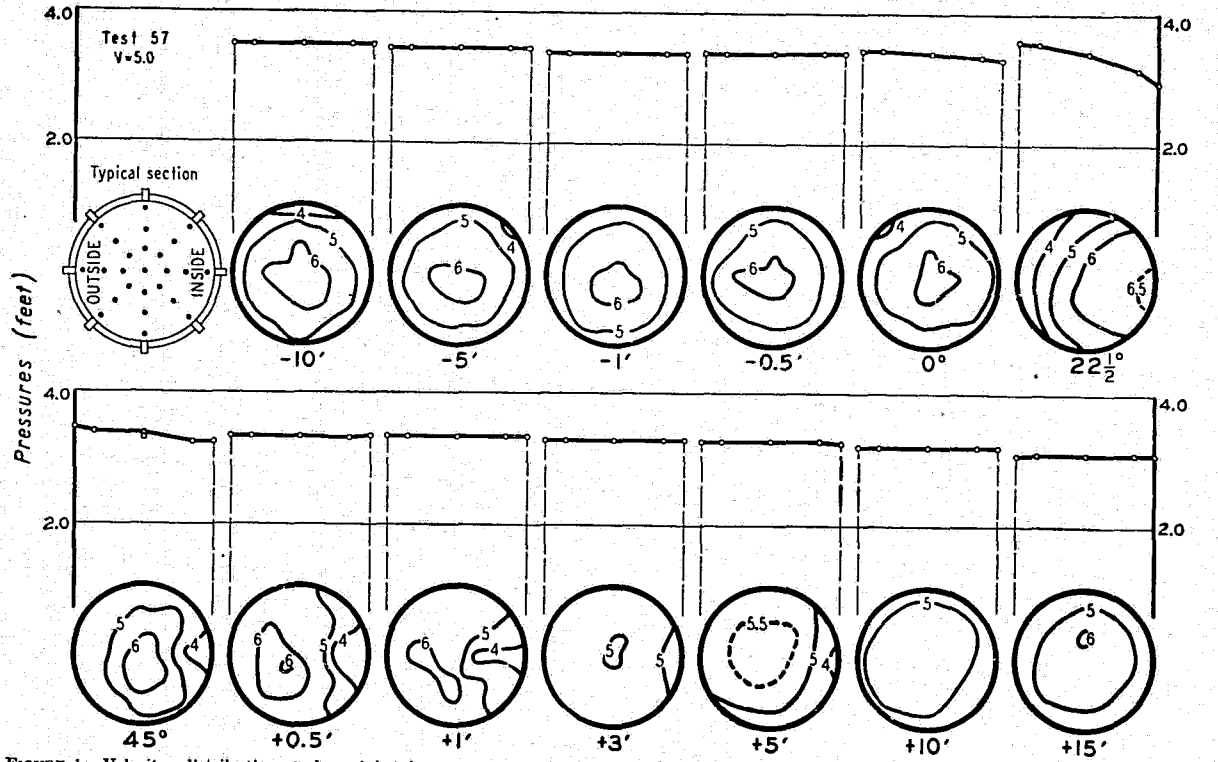

FIGURE 1.—Velocity distribution and peripheral pressures in 45° bend with approximately uniform velocity distribution in approach tangent; mean velocity, 5 feet per second.

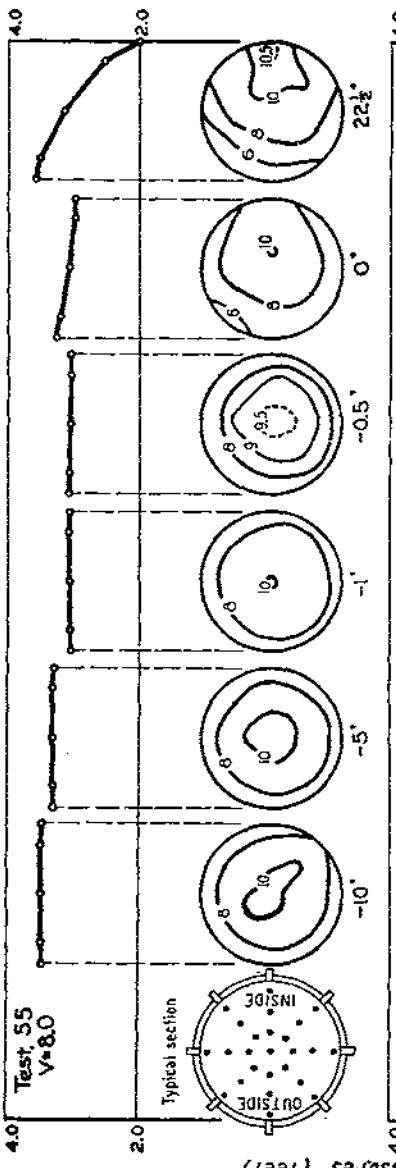

FIGURE 2.—Velocity distribution and peripheral pressures in 45° bend with approximately uniform velocity distribution in approach tangent; mean velocity, 8 feet per second.

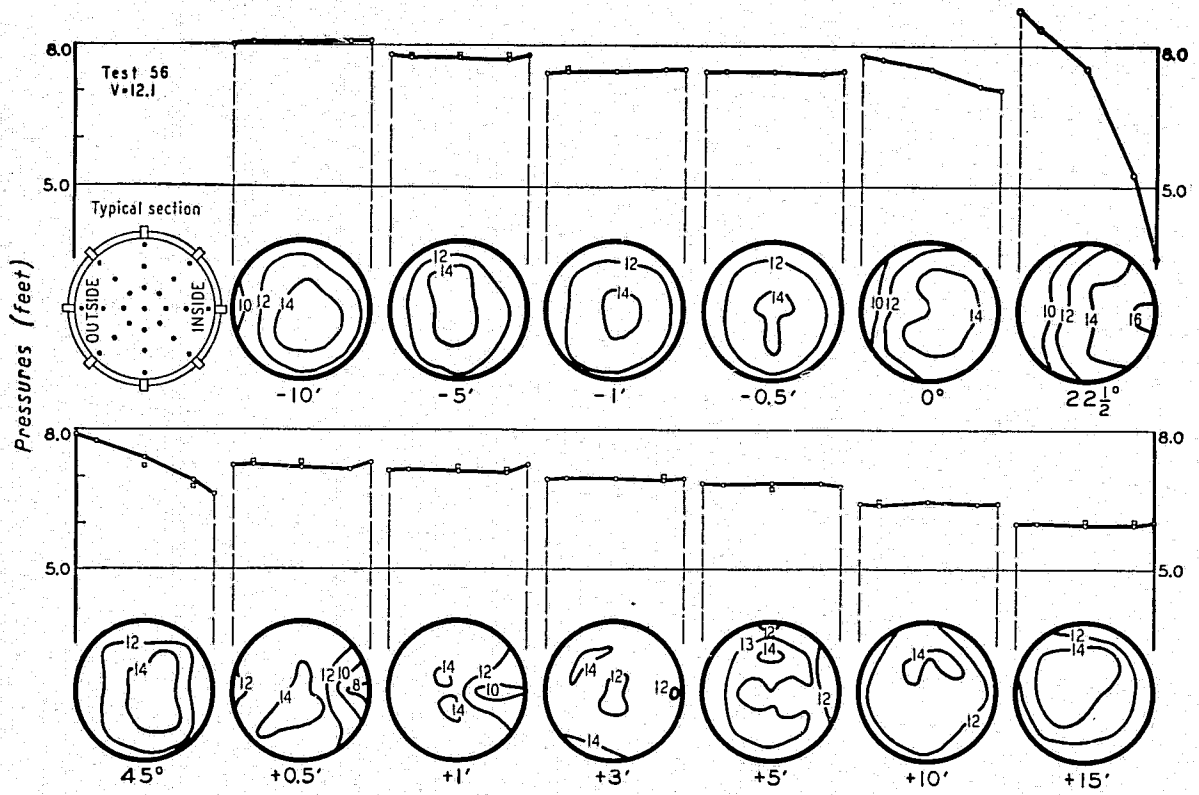

FIGURE 3.—Velocity distribution and peripheral pressures in 45° bend with approximately uniform velocity distribution in approach tangent; mean velocity, 12.1 feet per second.

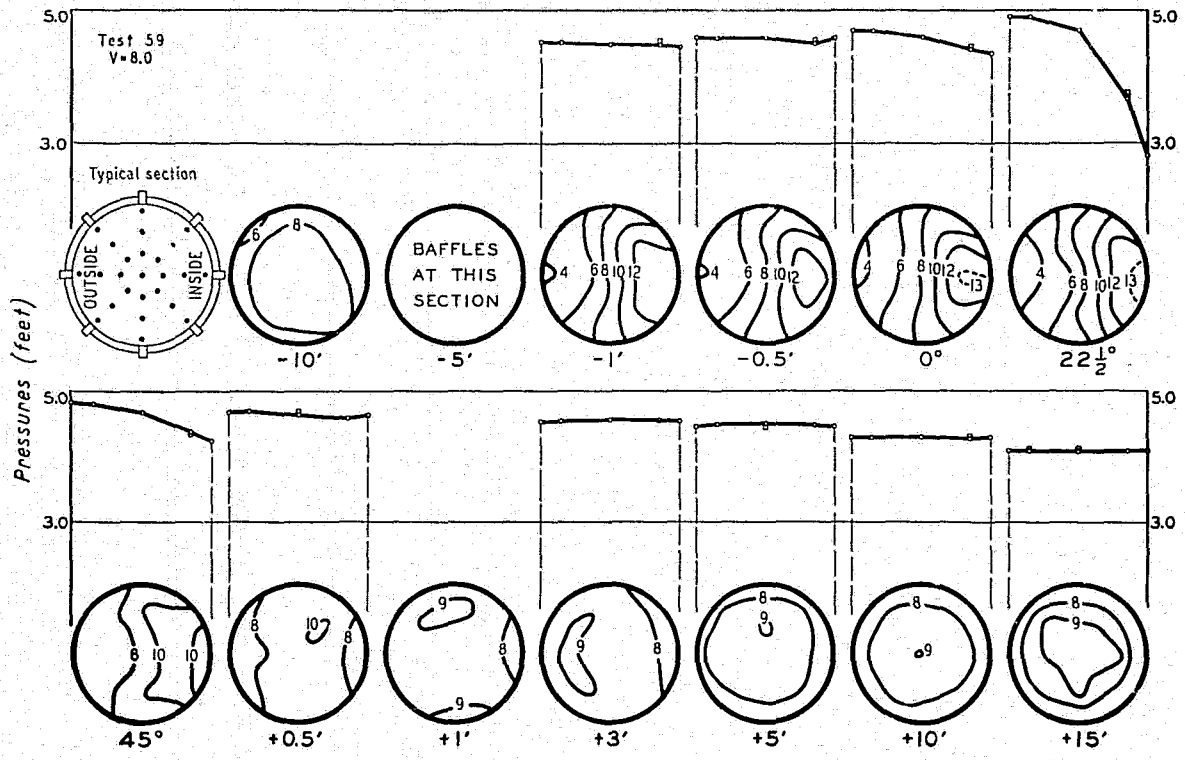

FIGURE 4.—Velocity distribution and peripheral pressures in 45° bend with velocity in approach tangent high toward inner side; mean velocity 8 feet per second.

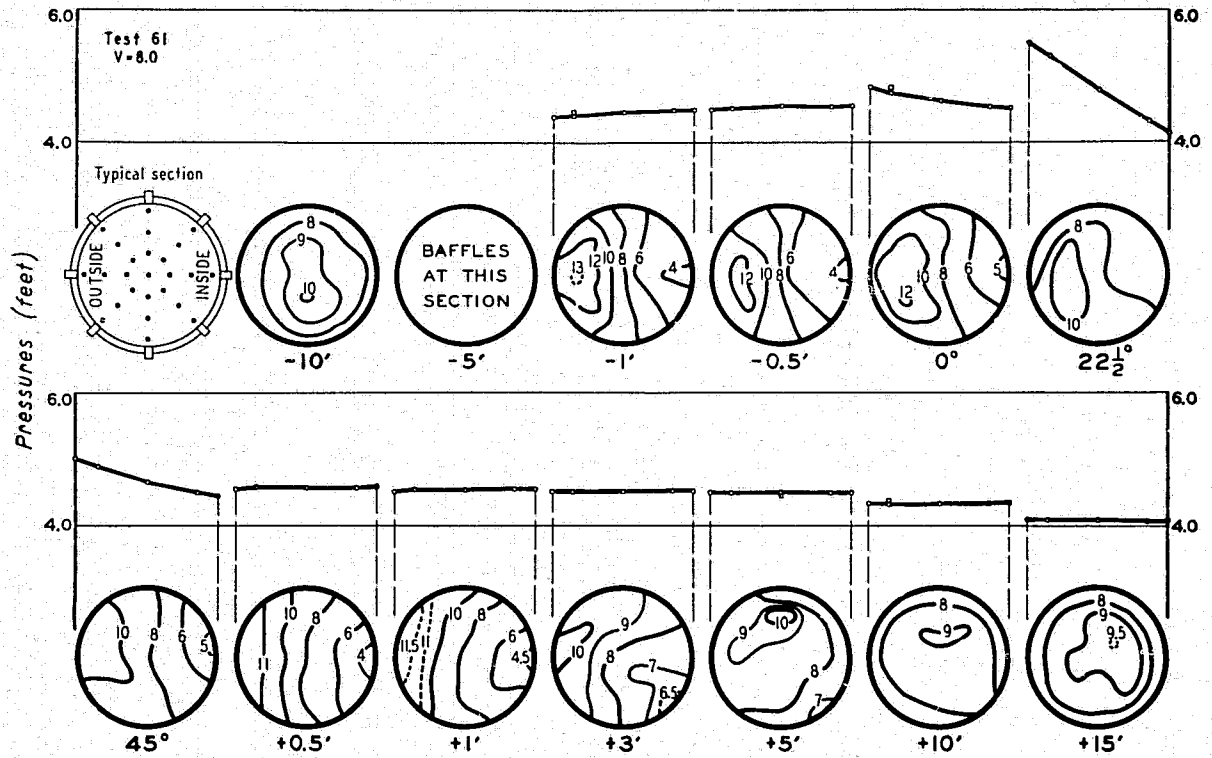

FIGURE 5.—Velocity distribution and peripheral pressures in 45° bend with velocity in approach tangent high toward outer side; mean velocity, 8 feet per second.

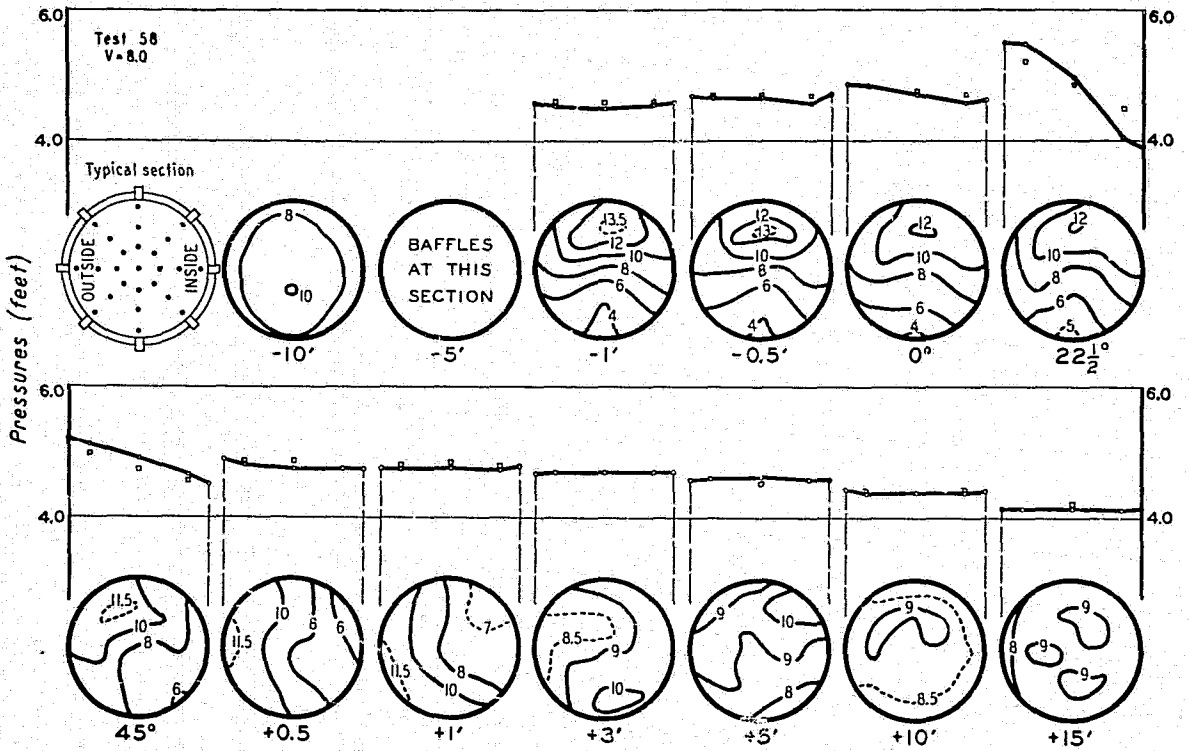

FIGURE 6.—Velocity distribution and peripheral pressures in 45° bend with velocity in approach tangent high at top; mean velocity, 8 feet per second.

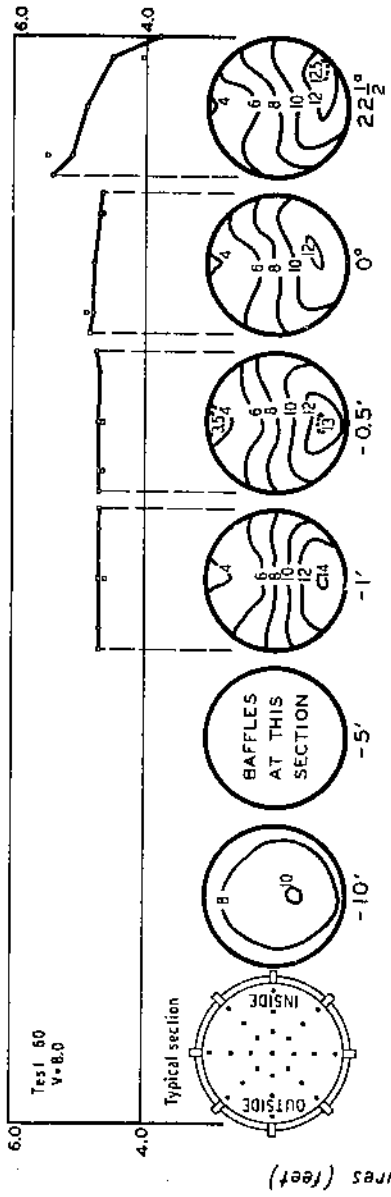

FIGURE 7.—Velocity distribution and peripheral pressures in 45° bend with velocity in approach tangent high at bottom; mean velocity, 8 feet per second.

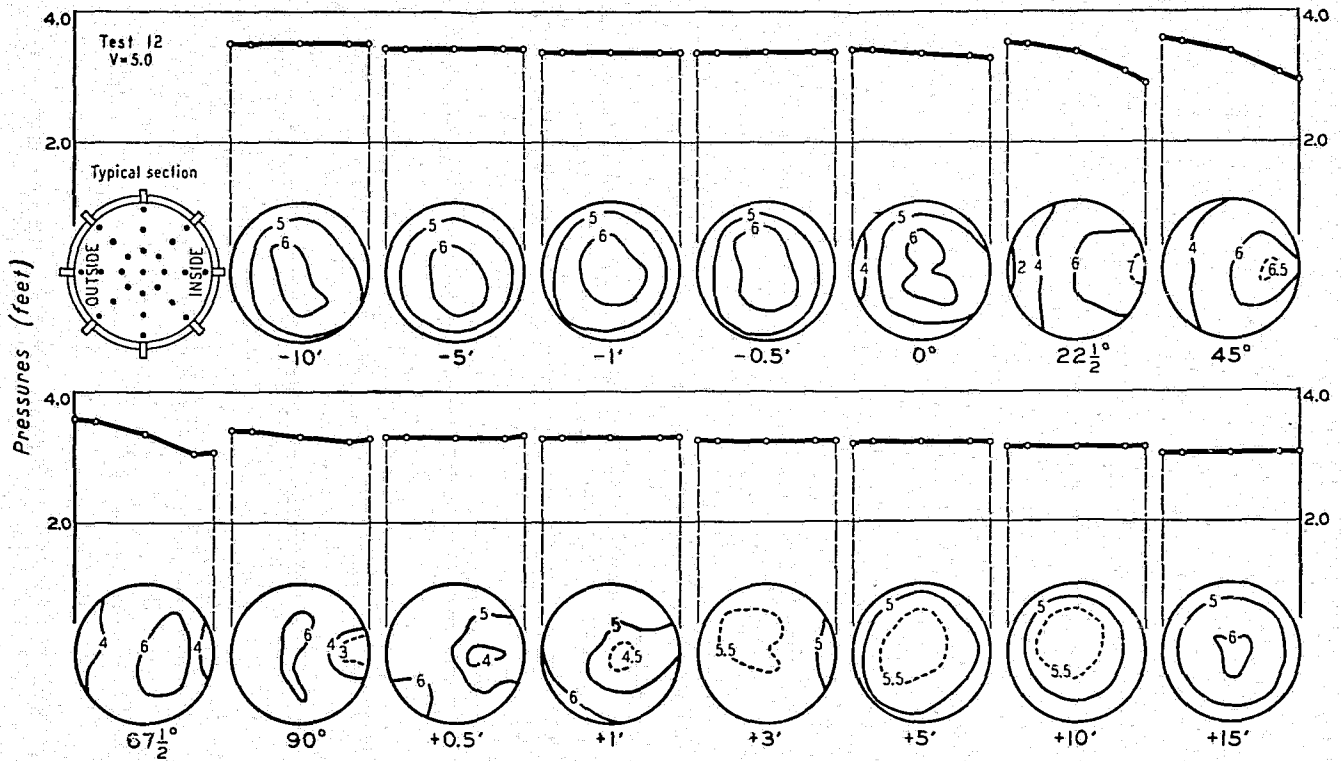

FIGURE 8.—Velocity distribution and peripheral pressures in standard bend with approximately uniform velocity distribution in approach tangent; mean velocity, 5 feet per second.

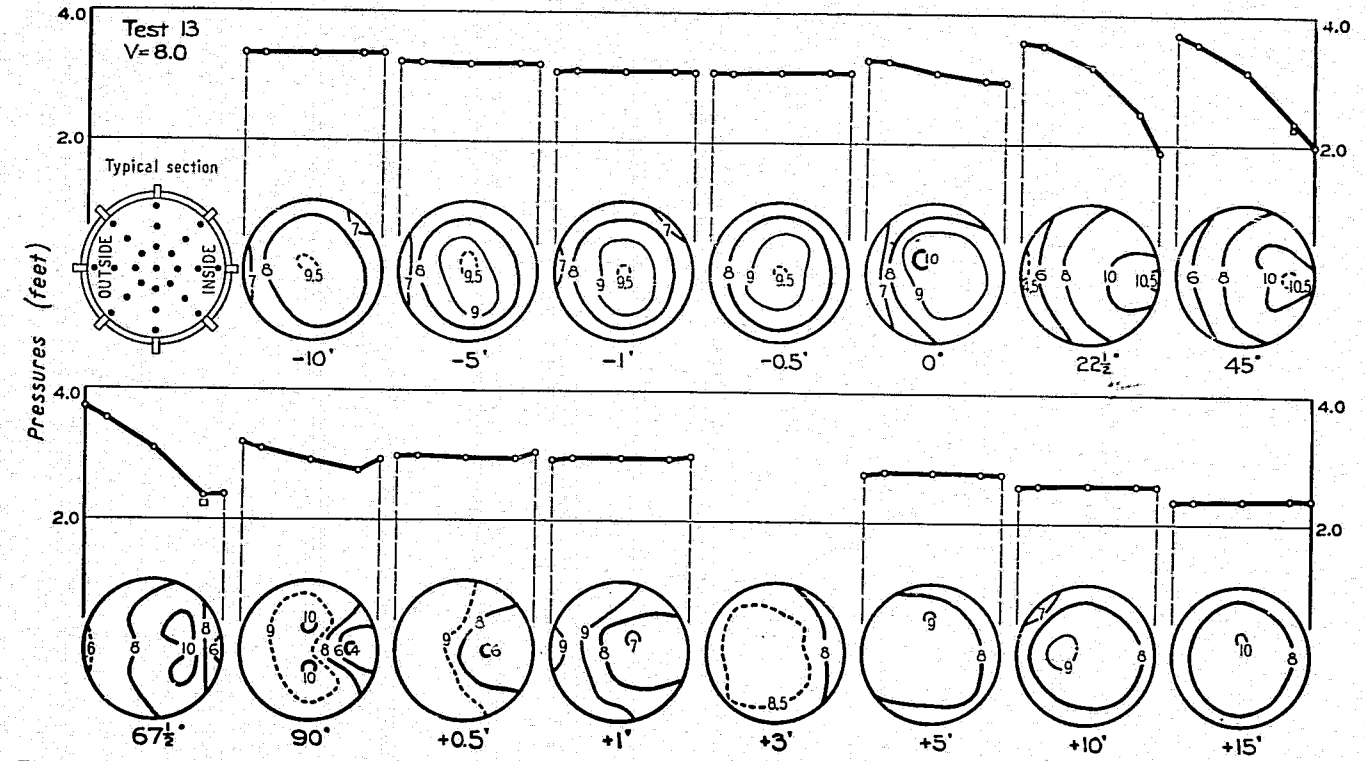

FIGURE 9.—Velocity distribution and peripheral pressures in standard bend with approximately uniform velocity distribution in approach tangent; mean velocity, 8 feet per second.

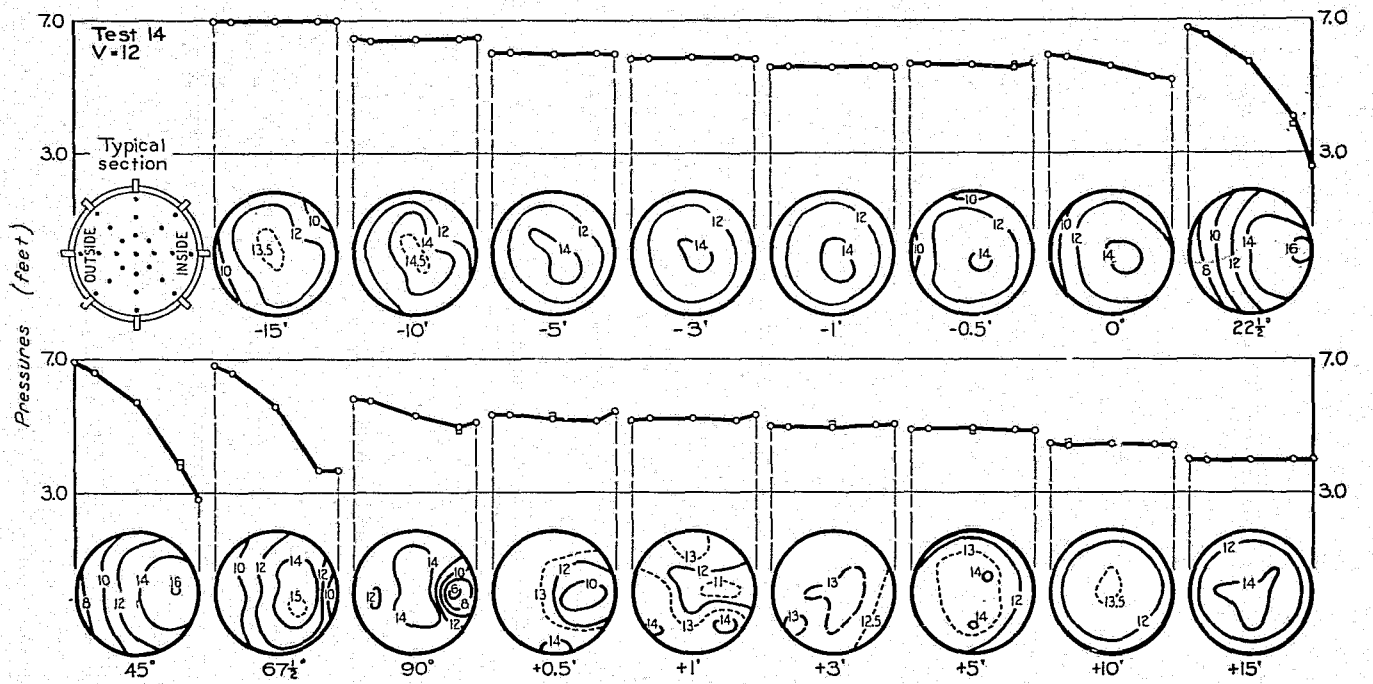

FIGURE 10.—Velocity distribution and peripheral pressures in standard bend with approximately uniform velocity distribution in approach tangent; mean velocity, 12. feet per second.

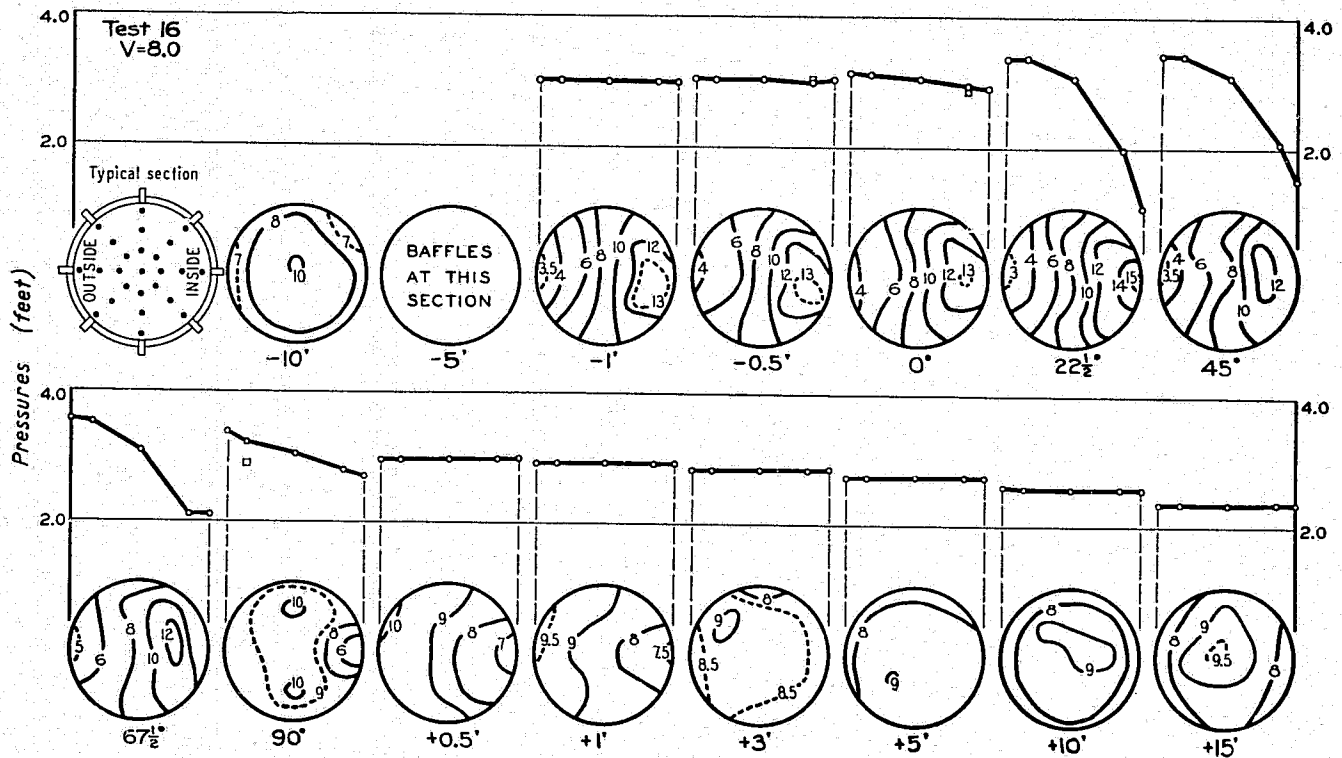

FIGURE 11.—Velocity distribution and peripheral pressures in standard bend with velocity in approach tangent high toward inner side; mean velocity, 8 feet per second.

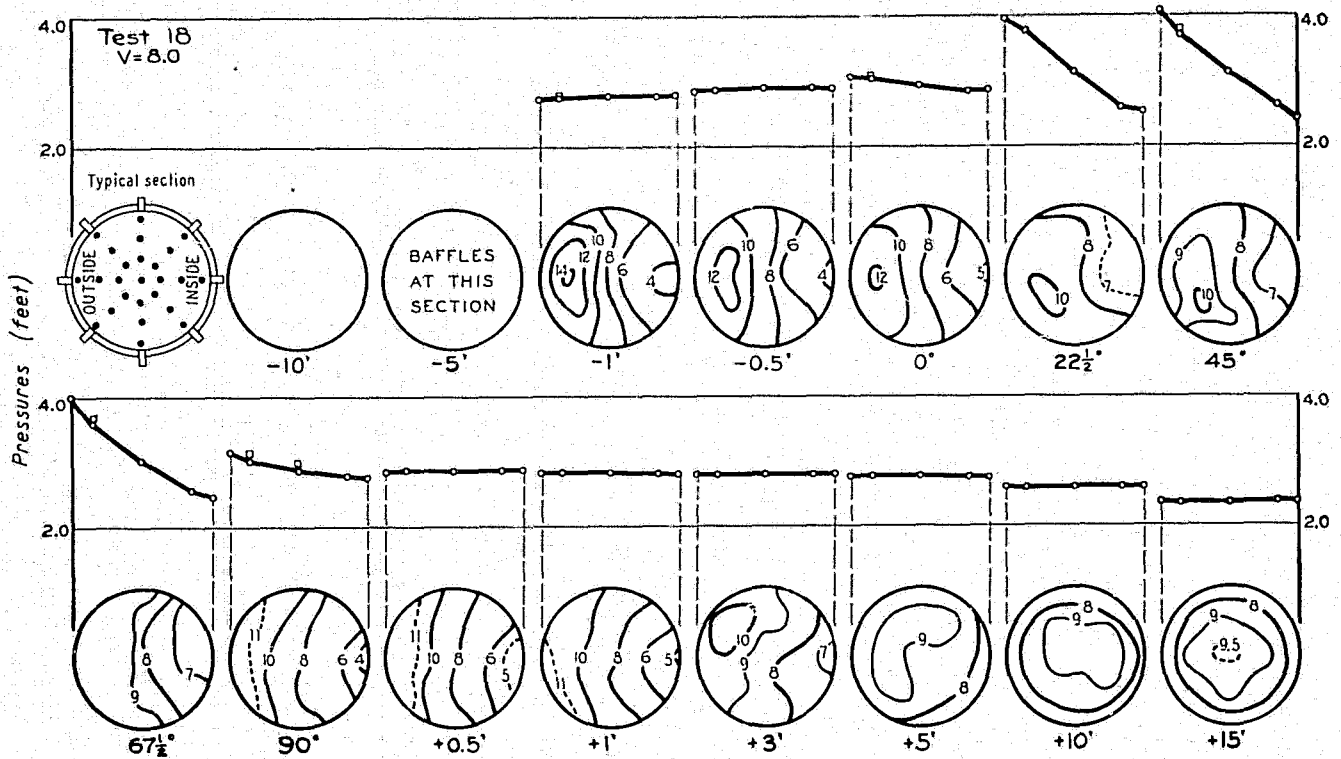

FIGURE 12.—Velocity distribution and peripheral pressures in standard bend with velocity in approach tangent high toward outer side; mean velocity, 8 feet per second.

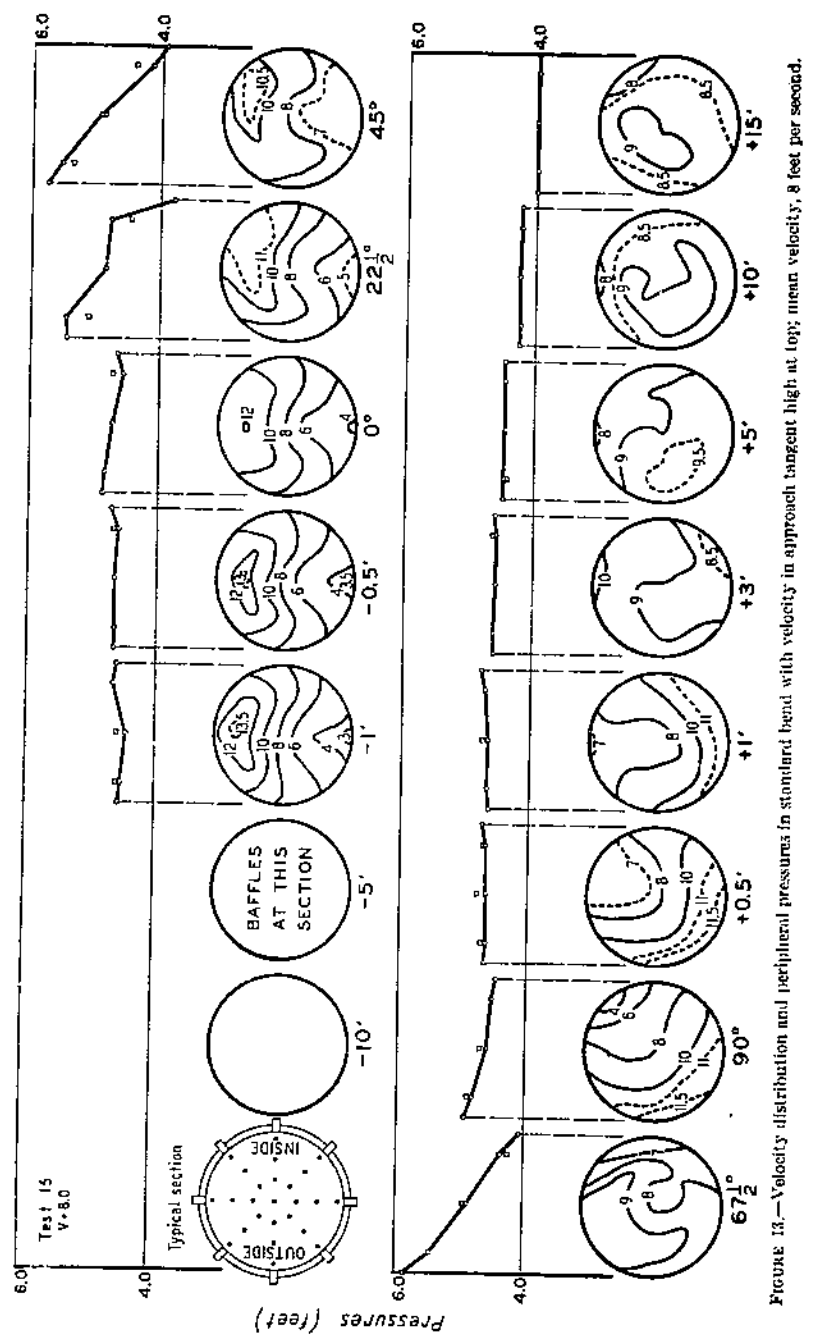

FIGURE 13.—Velocity distribution and peripheral pressures in standard bend with velocity in approach tangent high at top; mean velocity, 8 feet per second.

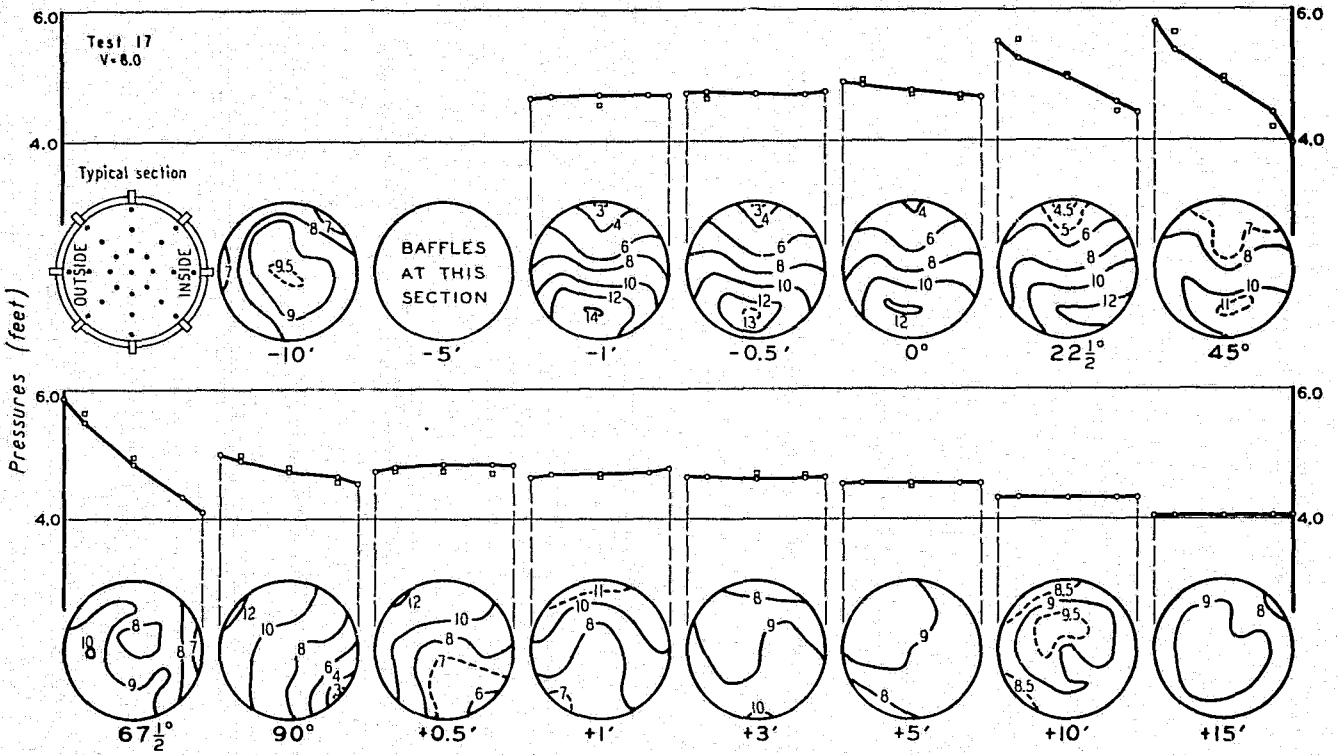

FIGURE 14.—Velocity distribution and peripheral pressures in standard bend with velocity in approach tangent high at bottom; mean velocity, 8 feet per second.

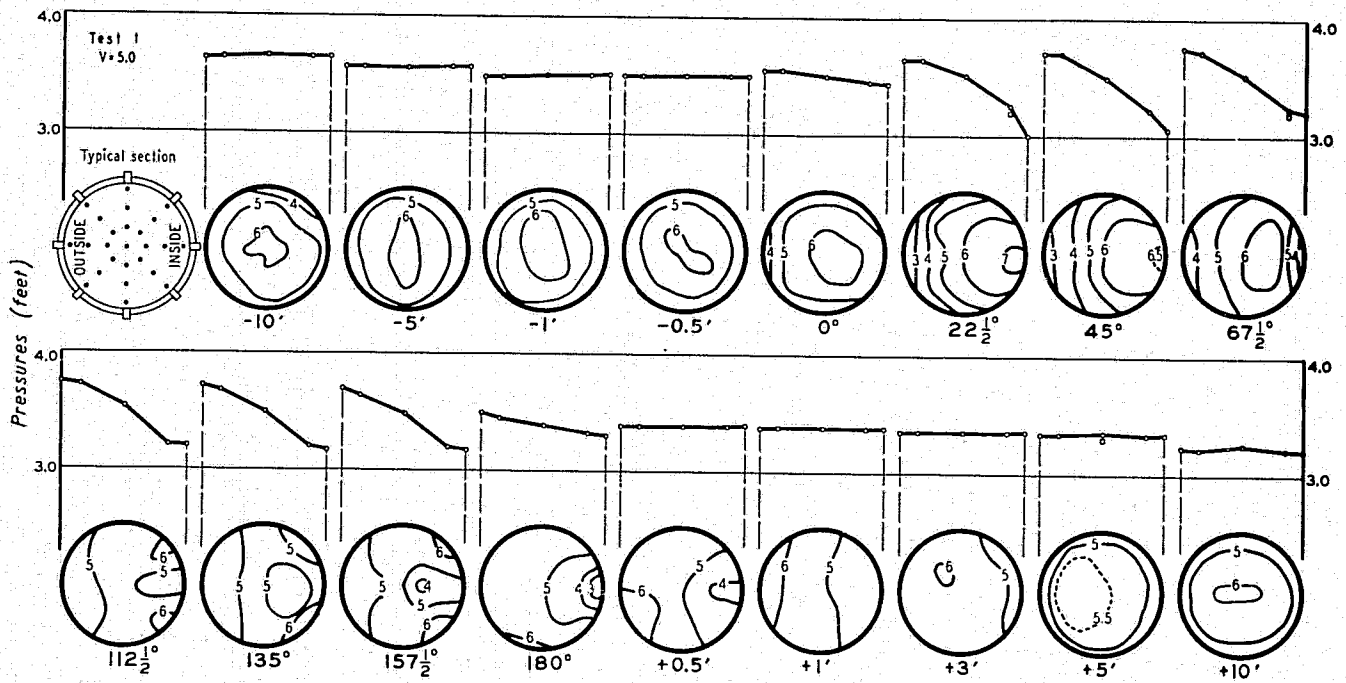

FIGURE 15.—Velocity distribution and peripheral pressures in 180° bend of continuous curvature with approximately uniform velocity distribution in approach tangent; mean velocity 5 feet per second.

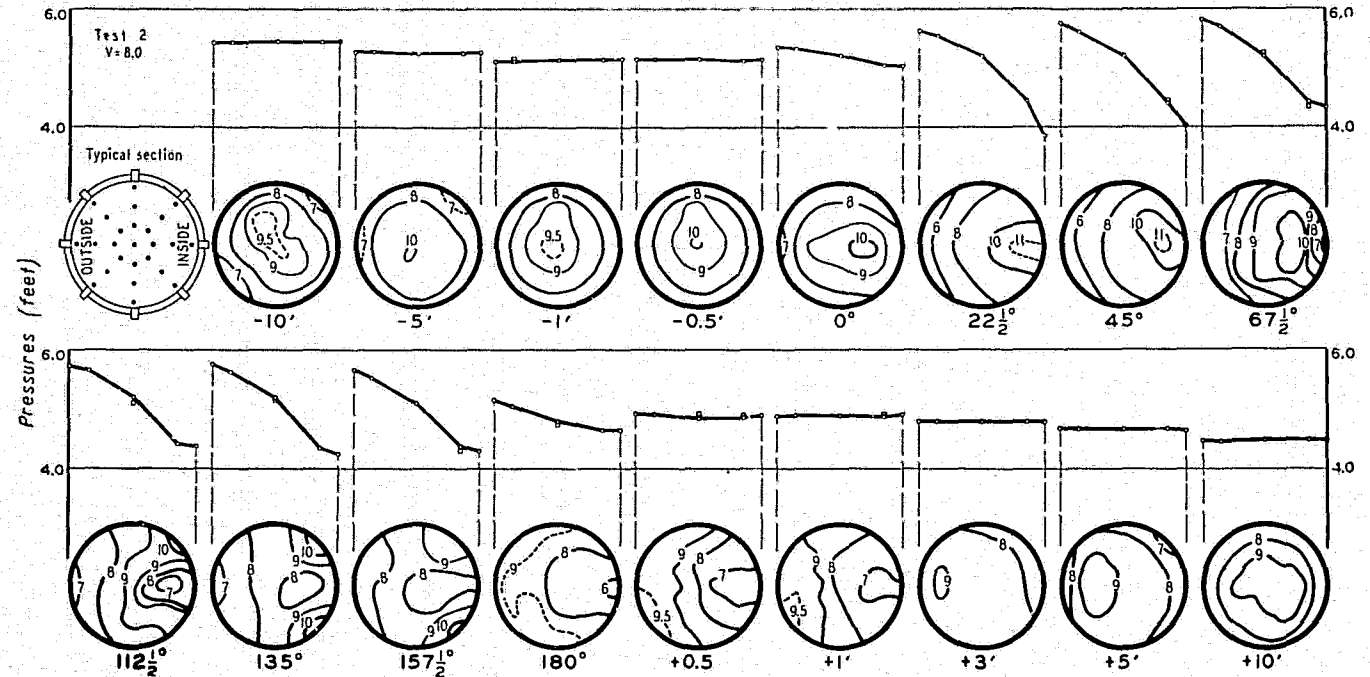

FIGURE 16.—Velocity distribution and peripheral pressures in 180° bend of continuous curvature with approximately uniform velocity distribution in approach tangent; mean velocity 8 feet per second.

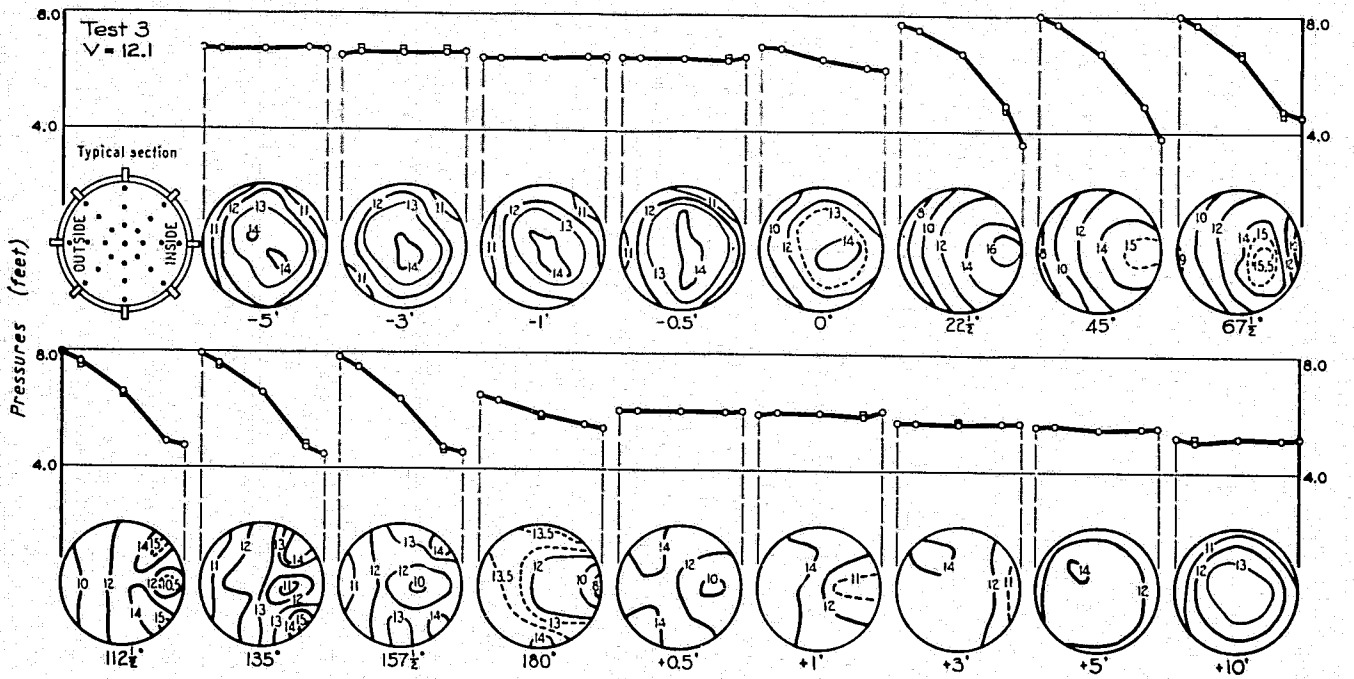

FIGURE 17.—Velocity distribution and peripheral pressures in 180° bend of continuous curvature with approximately uniform velocity distribution in approach tangent; mean velocity 12.1 feet per second.

151350°—37——3

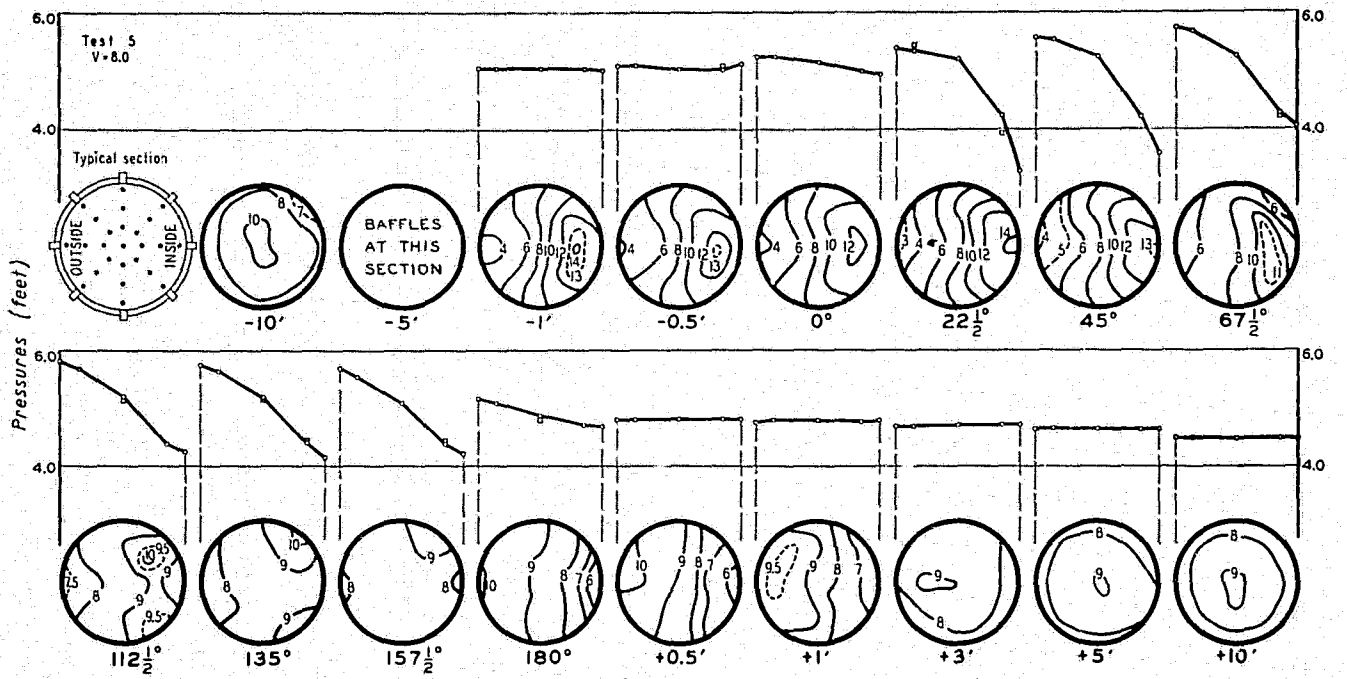

FIGURE 18.—Velocity distribution and peripheral pressures in 180° bend of continuous curvature with velocity in approach tangent high toward inner side; mean velocity 8 feet per second.

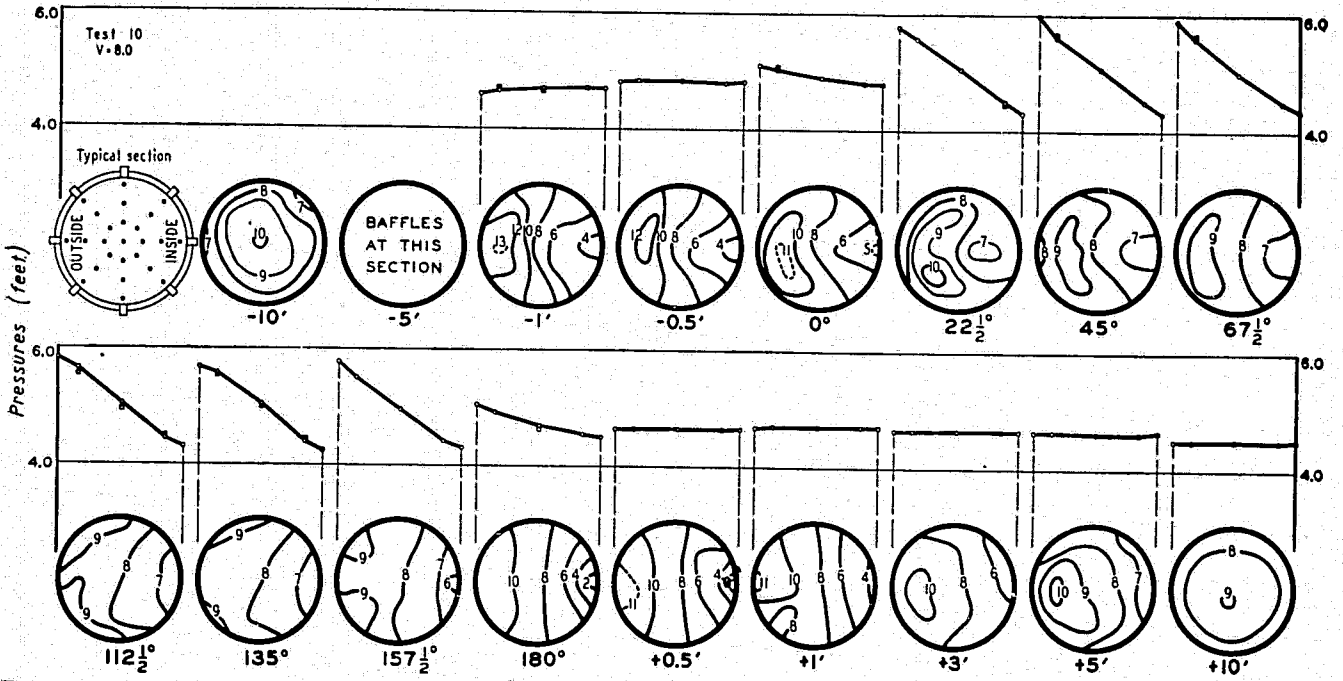

FIGURE 19.—Velocity distribution and peripheral pressures in 180° bend of continuous curvature with velocity in approach tangent high toward outer side; mean velocity 8 feet per second.

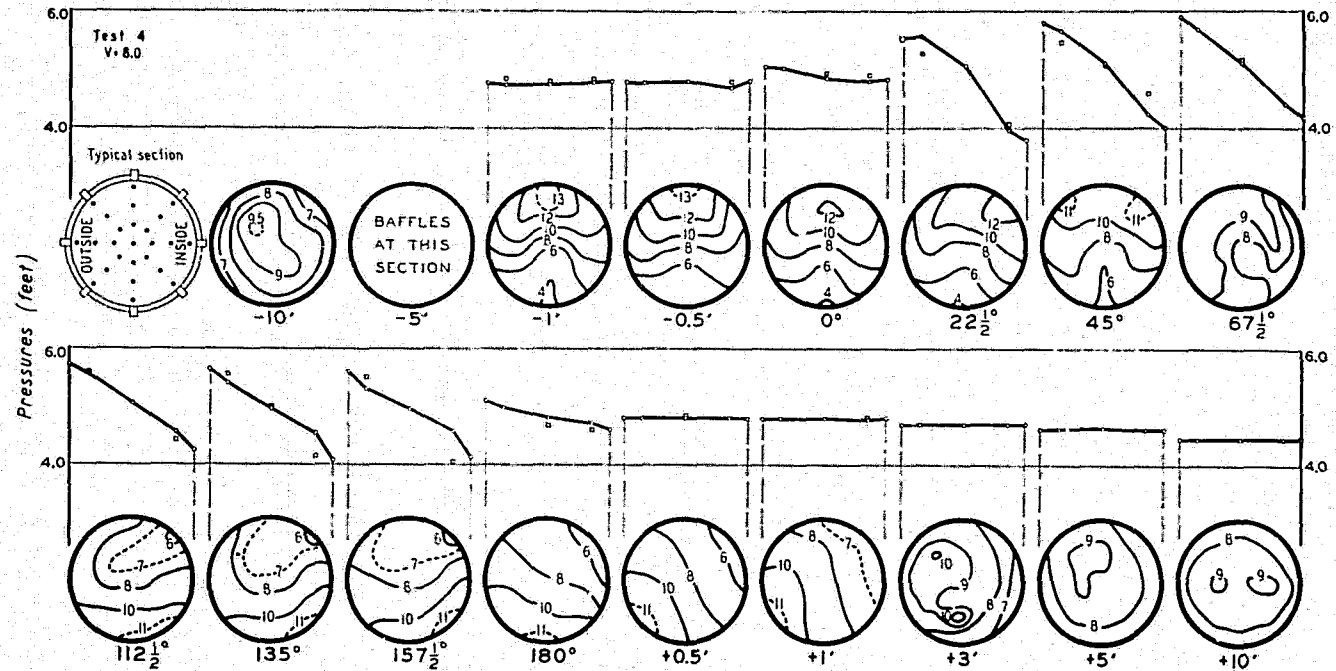

FIGURE 20.—Velocity distribution and peripheral pressures in 180° bend of continuous curvature with velocity in approach tangent high at top; mean velocity, 8 feet per second.

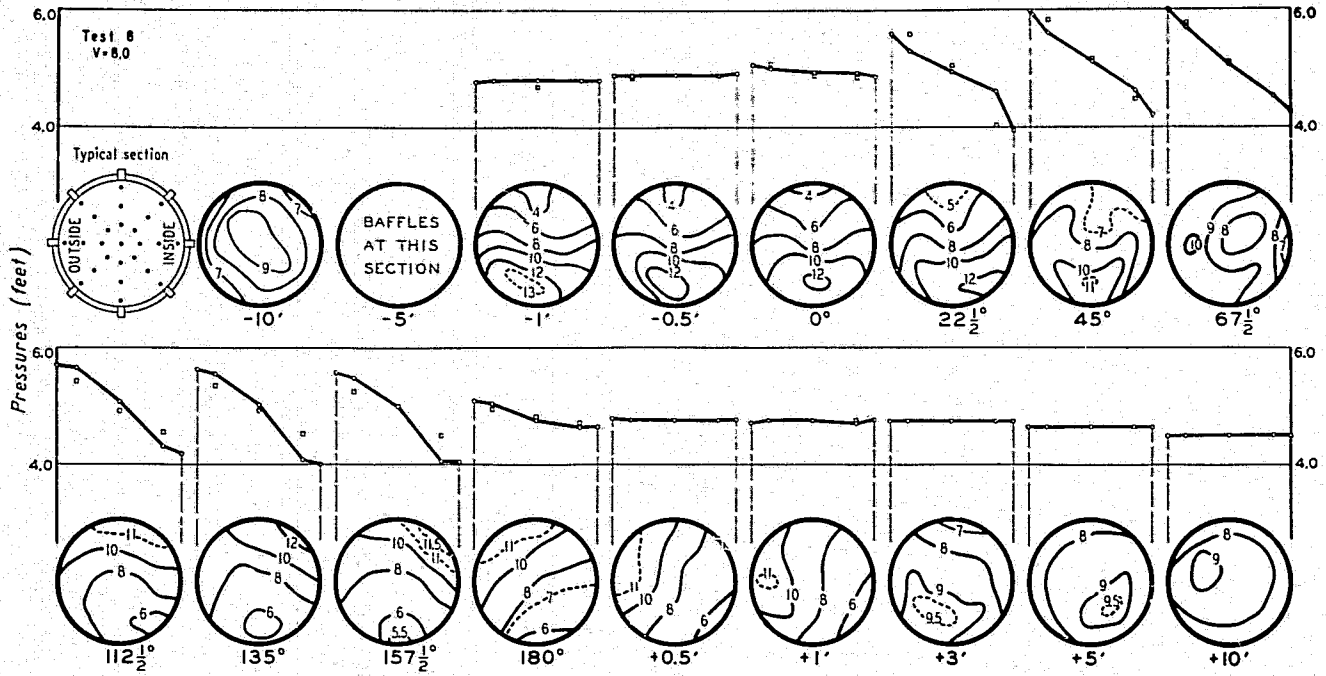

FIGURE 21.—Velocity distribution and peripheral pressures in 180° bend of continuous curvature with velocity in approach tangent high at bottom; mean velocity, 8 feet per second.

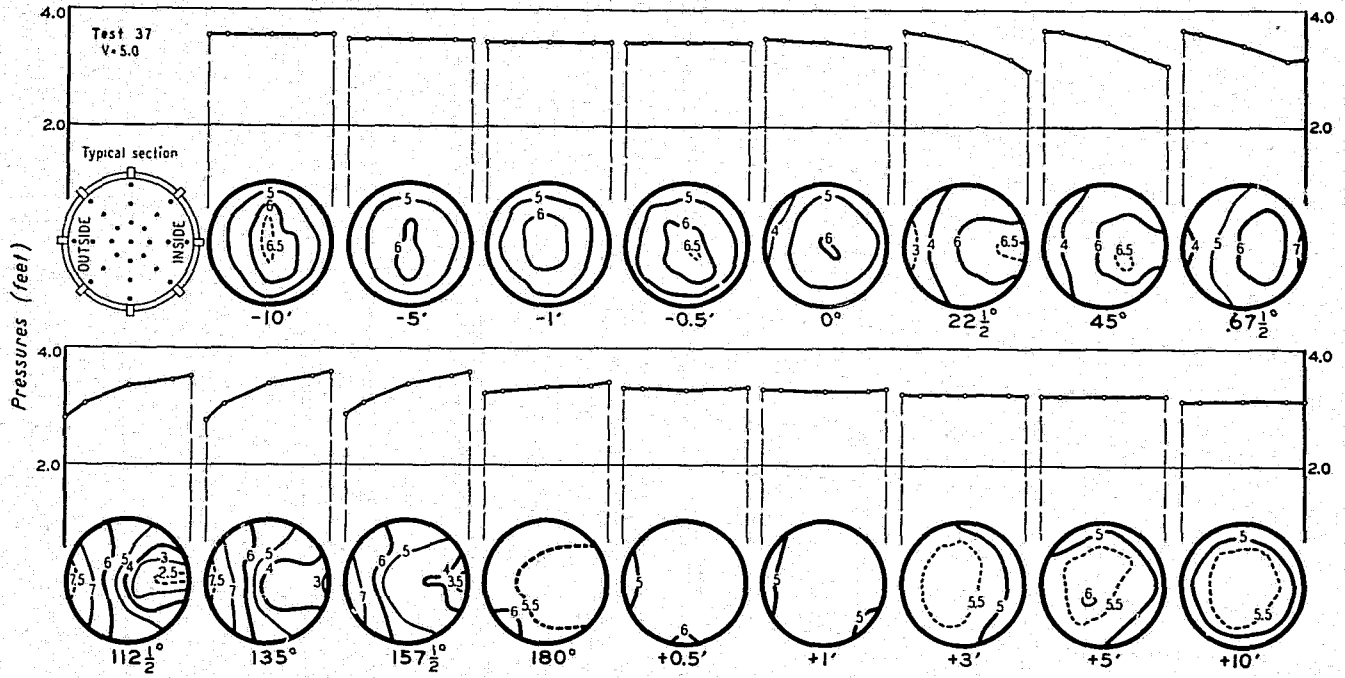

FIGURE 22.—Velocity distribution and peripheral pressures in 180° bend of reverse curvature with approximately uniform velocity distribution in approach tangent; mean velocity, 5 feet per second.

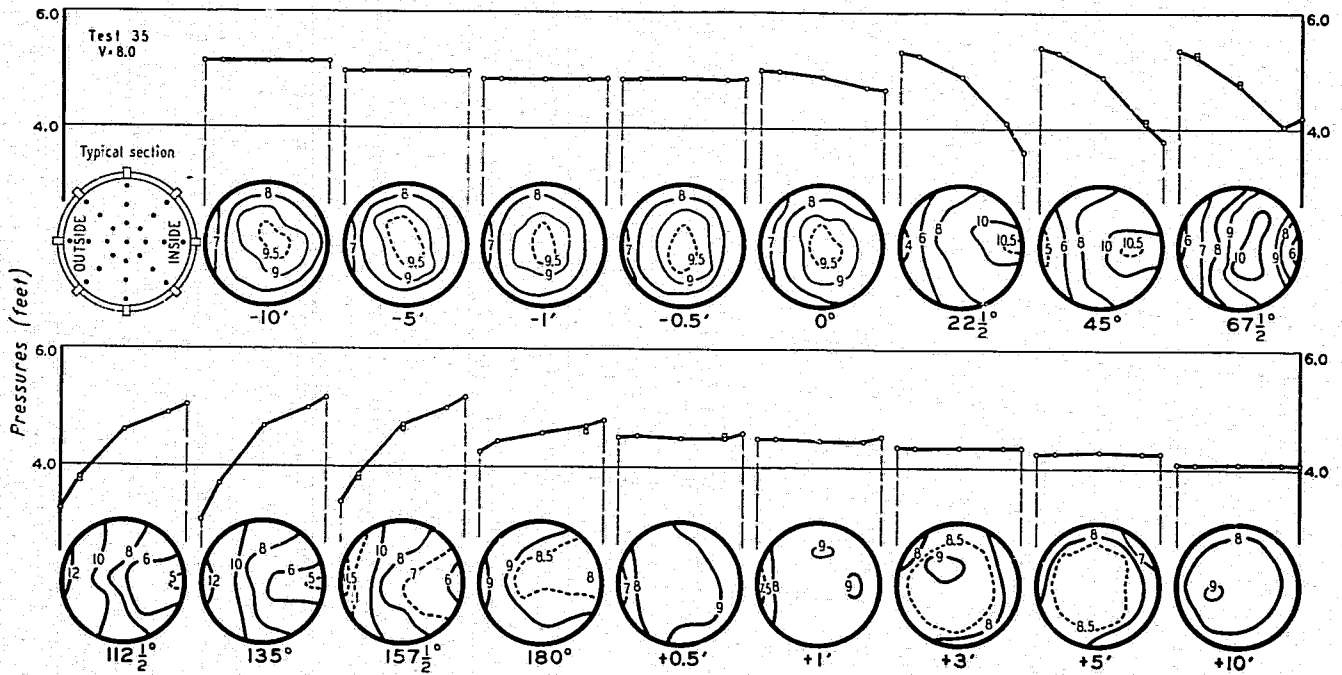

FIGURE 23.—Velocity distribution and peripheral pressures in 180° bend of reverse curvature with approximately uniform velocity distribution in approach tangent; mean velocity, 8 feet per second.

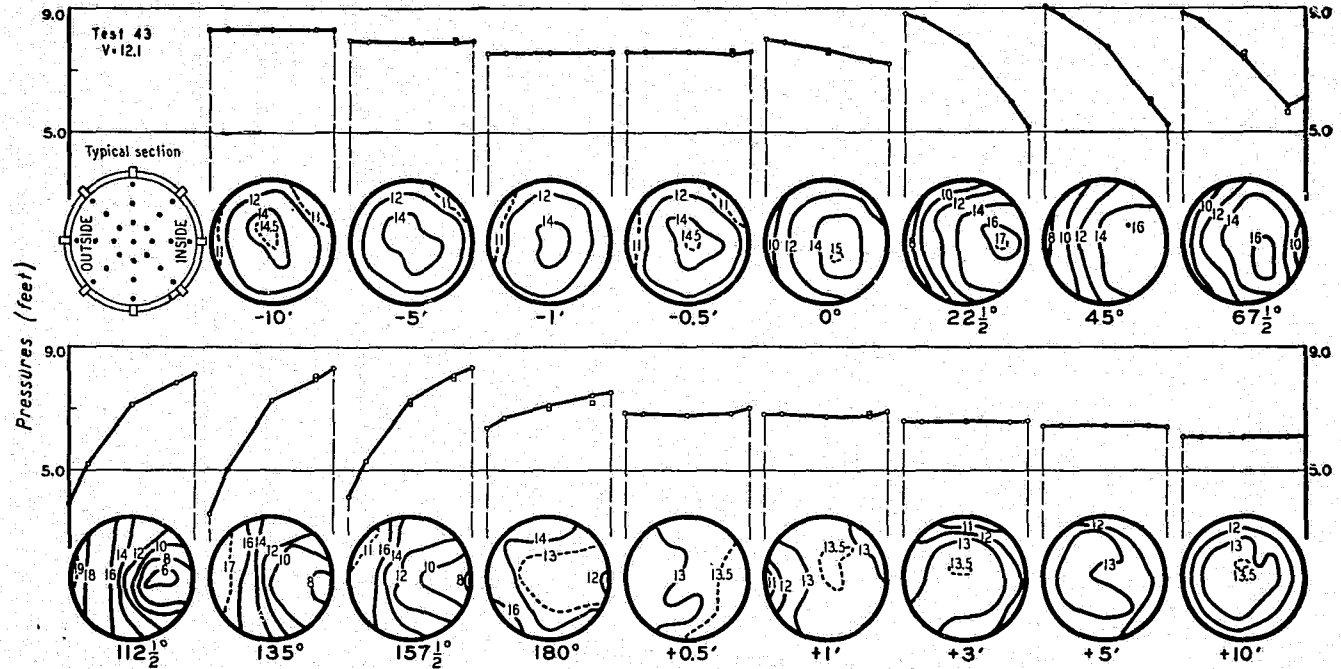

FIGURE 24.—Velocity distribution and peripheral pressures in 180° bend of reverse curvature with approximately uniform velocity distribution in approach tangent; mean velocity, 12.1 feet per second.

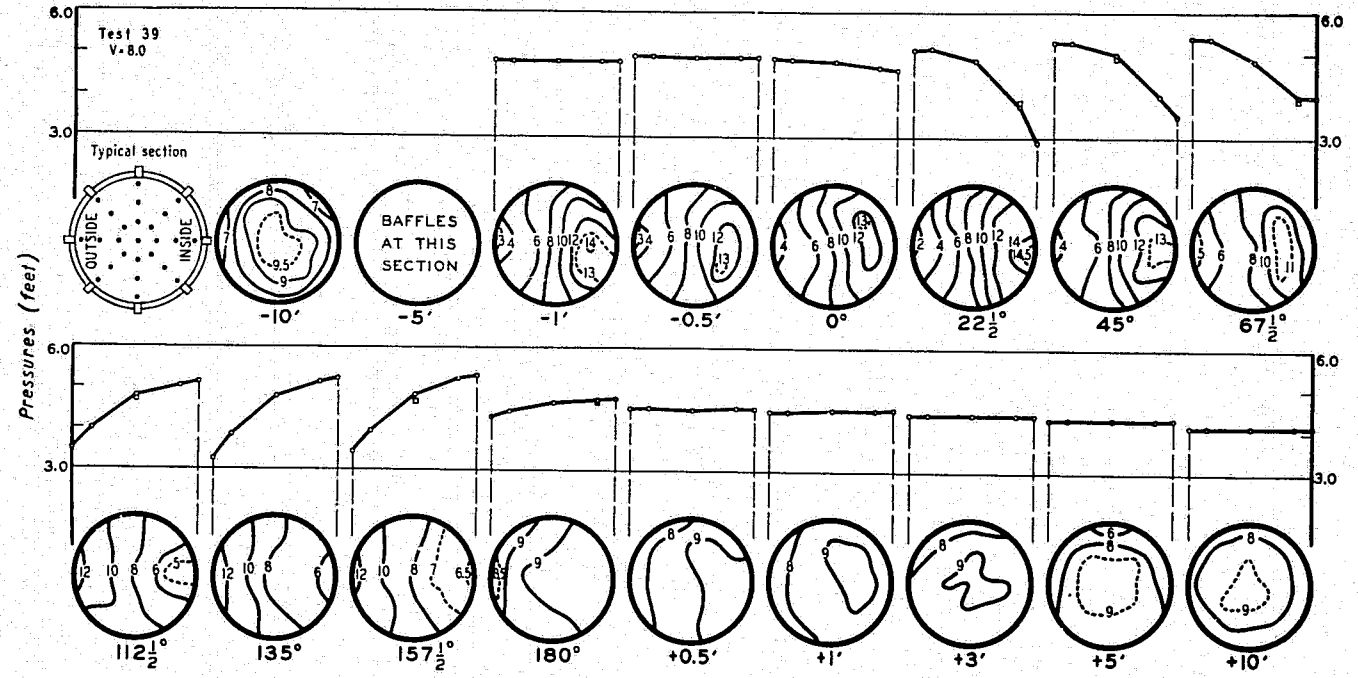

FIGURE 25.—Velocity distribution and peripheral pressures in 180° bend of reverse curvature with velocity in approach tangent high toward inner side; mean velocity, 8 feet per second.

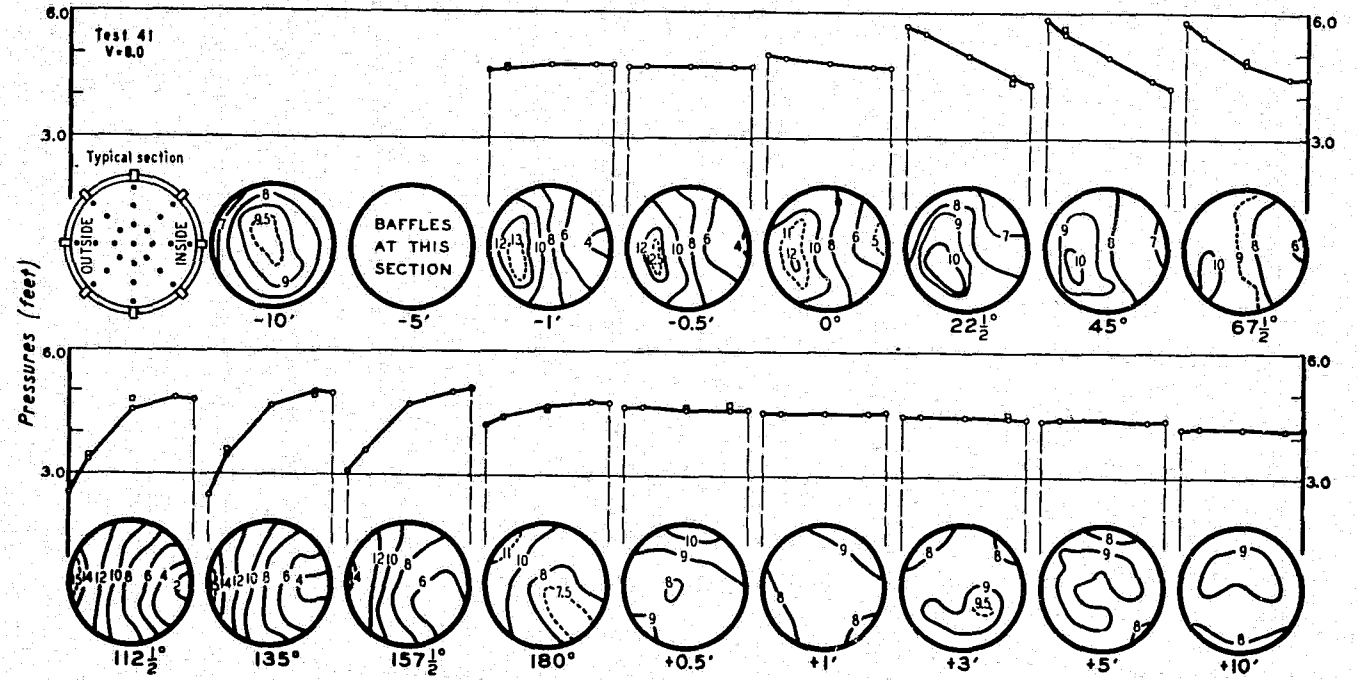

FIGURE 26.—Velocity distribution and peripheral pressures in 180° bend of reverse curvature with velocity in approach tangent high toward outer side; mean velocity, 8 feet per second.

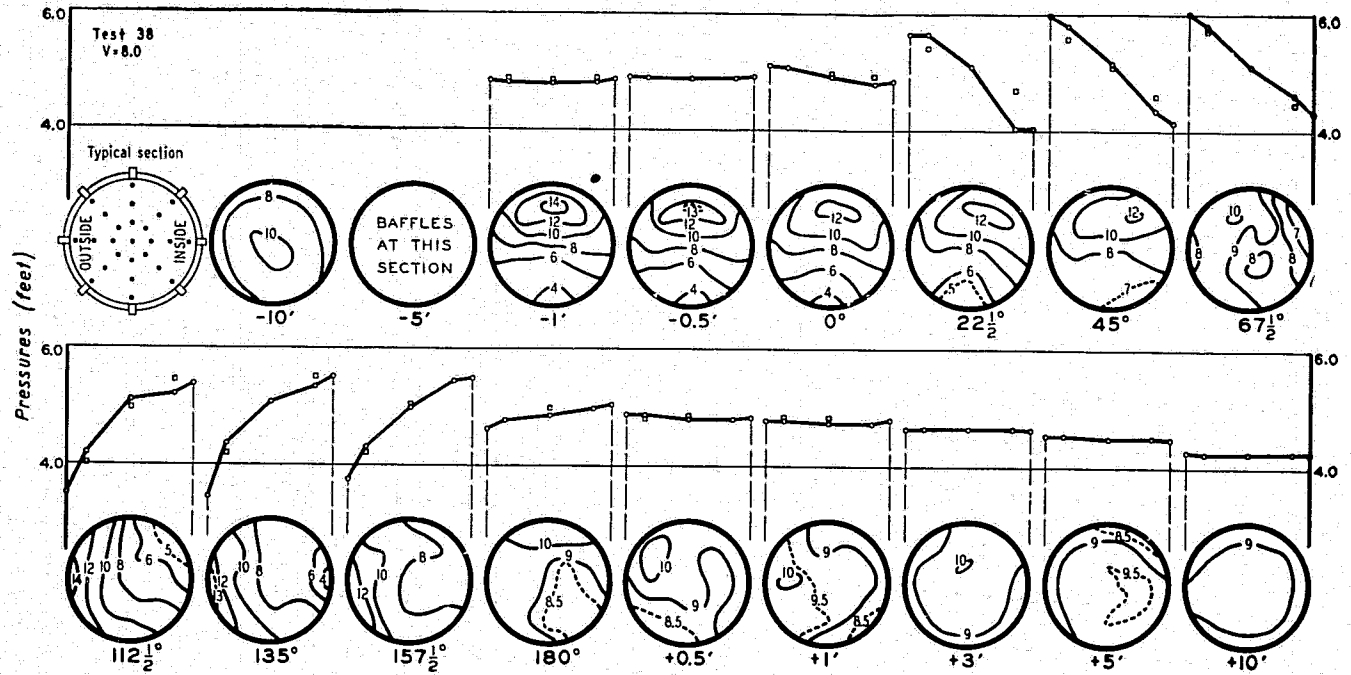

FIGURE 27.—Velocity distribution and peripheral pressures in 180° bend of reverse curvature with velocity in approach tangent high at top; mean velocity, 8 feet per second.

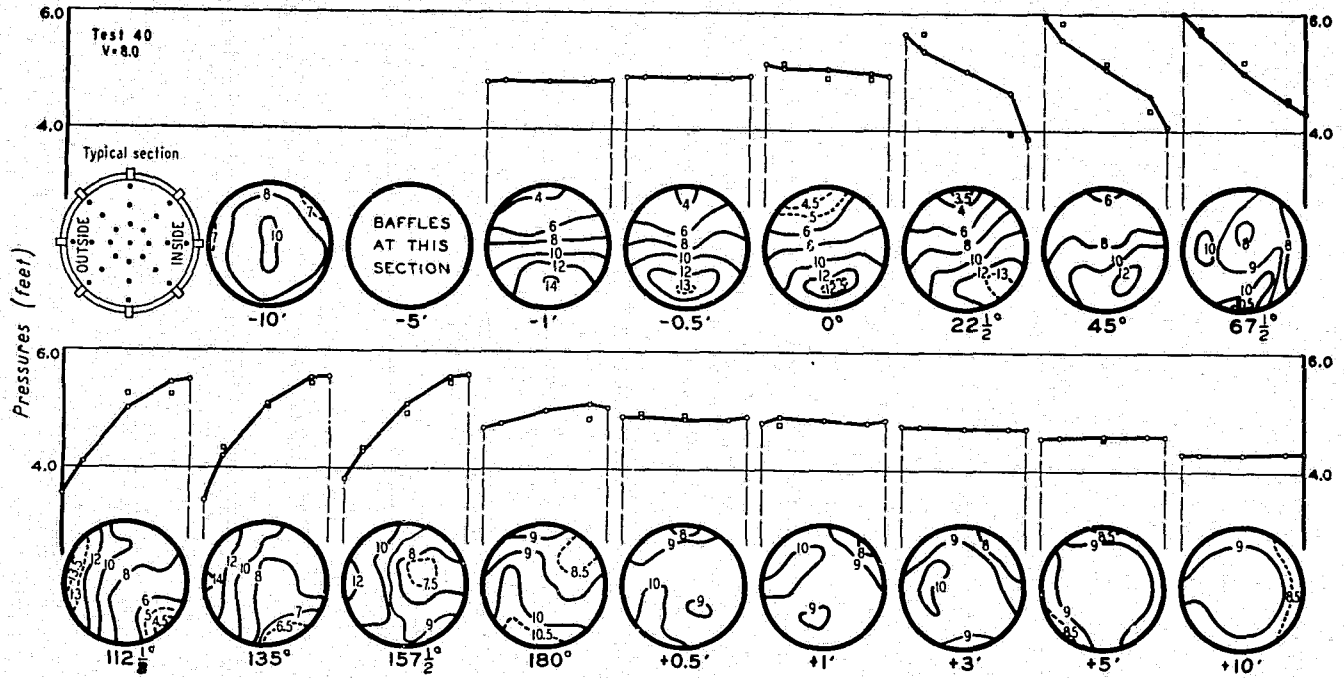

FIGURE 28.—Velocity distribution and peripheral pressures in 180° bend of reverse curvature with velocity in approach tangent high at bottom; mean velocity, 8 feet per second.

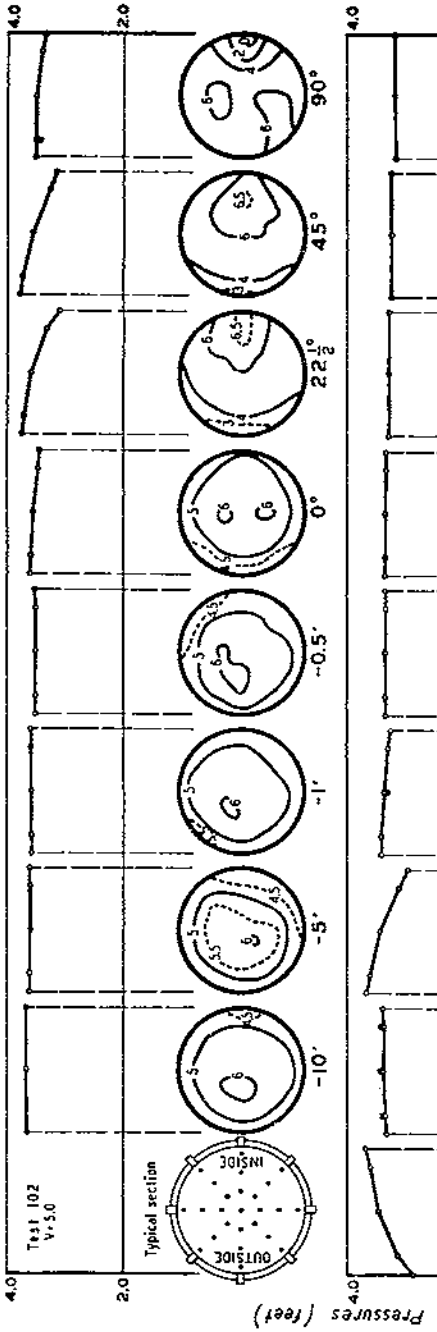

FIGURE 20.—Velocity distribution and peripheral pressures in 270° bend with approximately uniform velocity distribution in approach tangent; mean velocity, 5 feet per second.

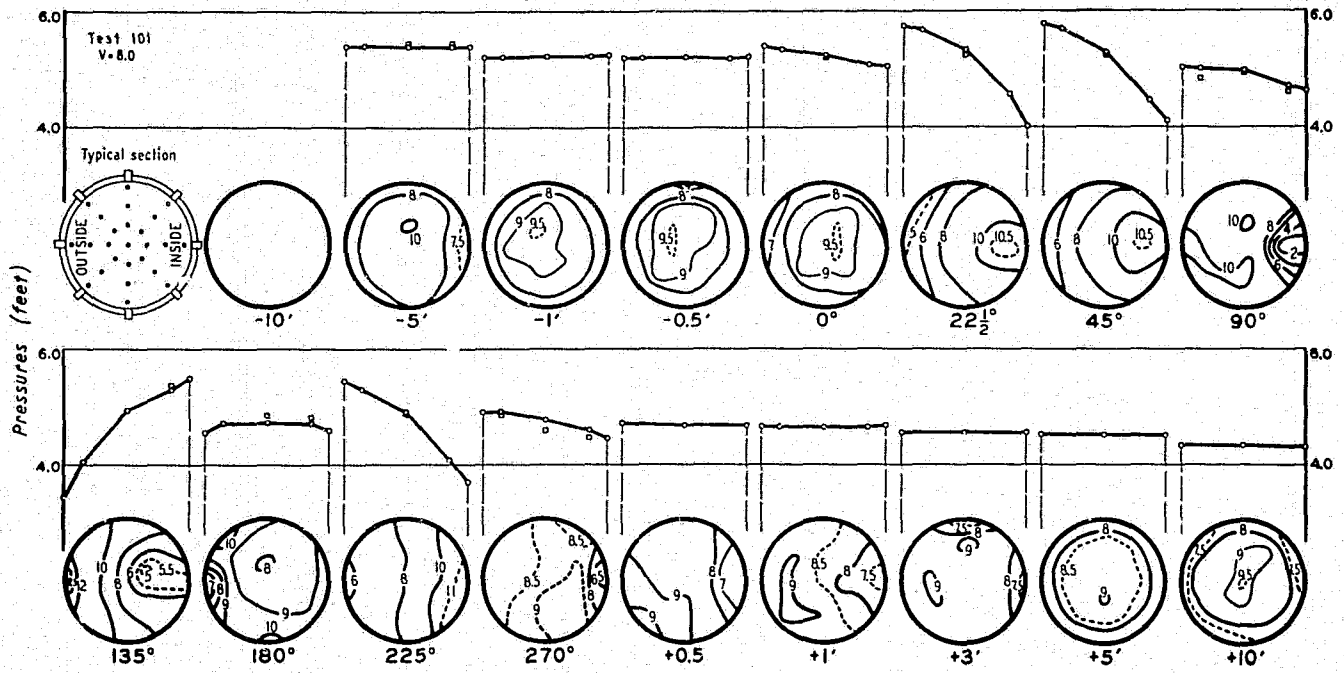

FIGURE 30.—Velocity distribution and peripheral pressures in 270° bend with approximately uniform velocity distribution in approach tangent; mean velocity, 8 feet per second.

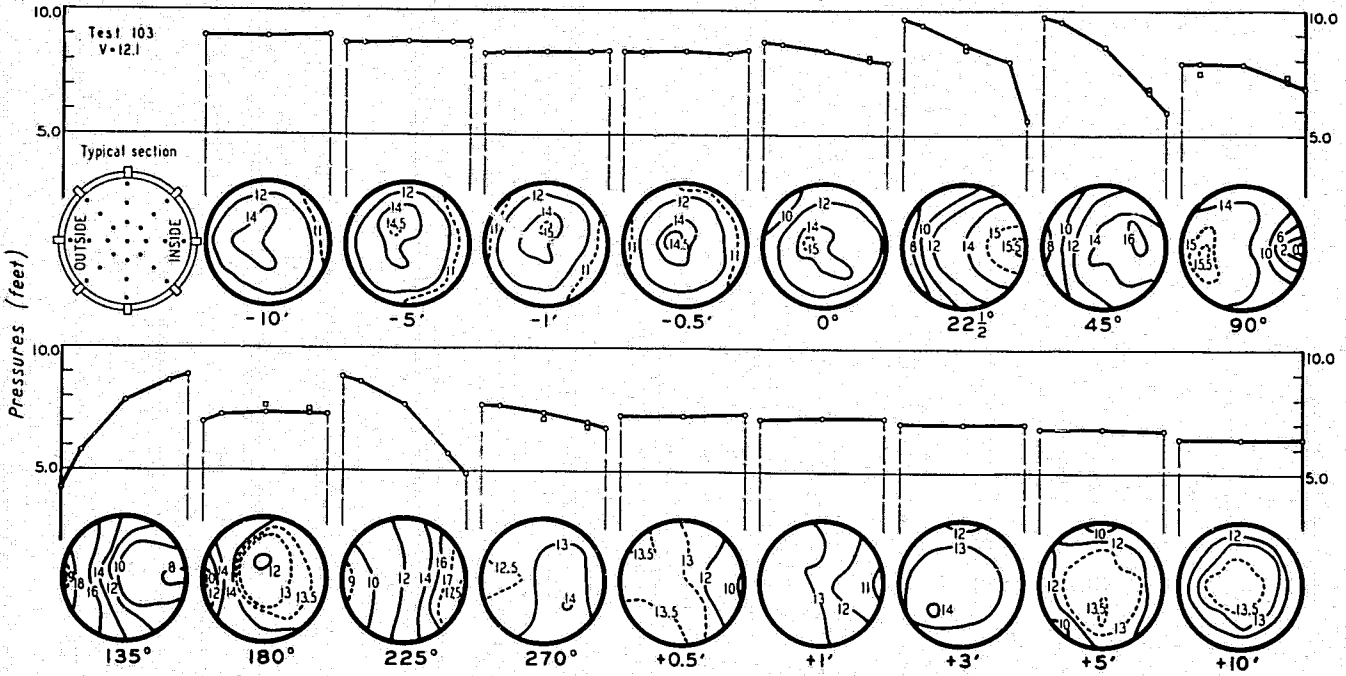

FIGURE 31.—Velocity distribution and peripheral pressures in 270° bend with approximately uniform velocity distribution in approach tangent; mean velocity, 12.1 feet per second.

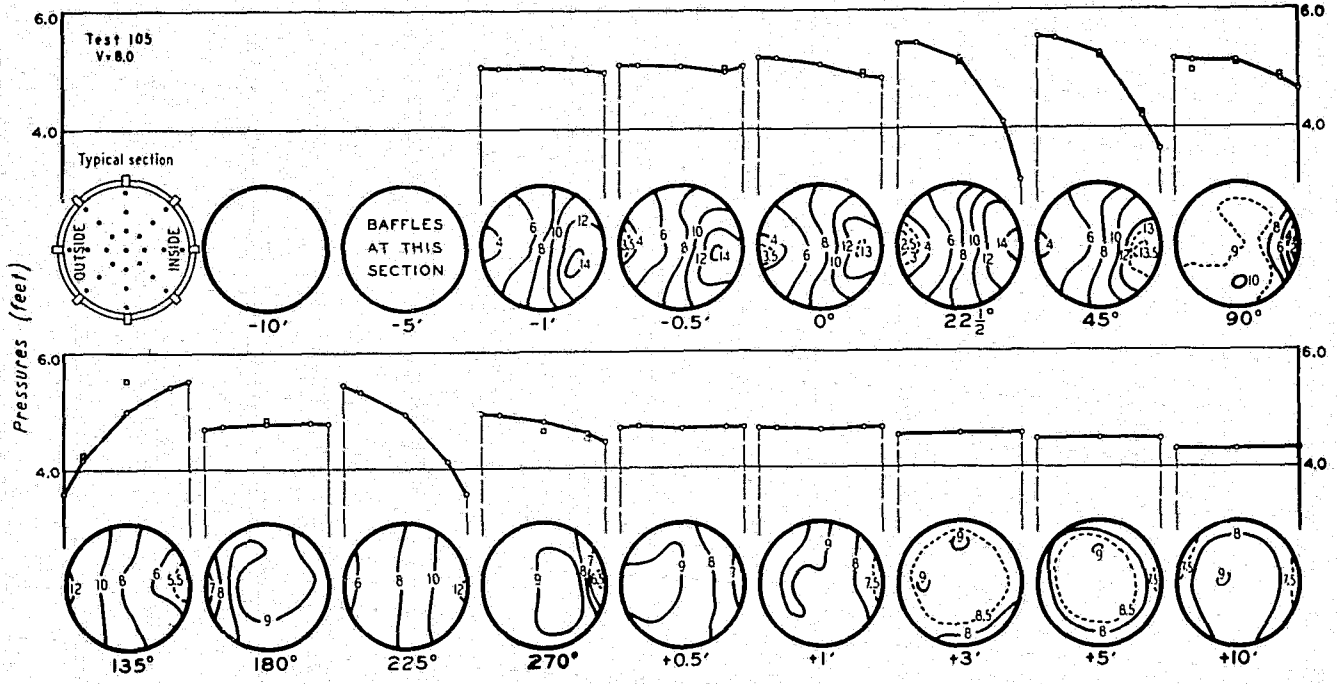

FIGURE 32.—Velocity distribution and peripheral pressures in 270° bend with velocity in approach tangent high toward inner side; mean velocity, 8 feet per second.

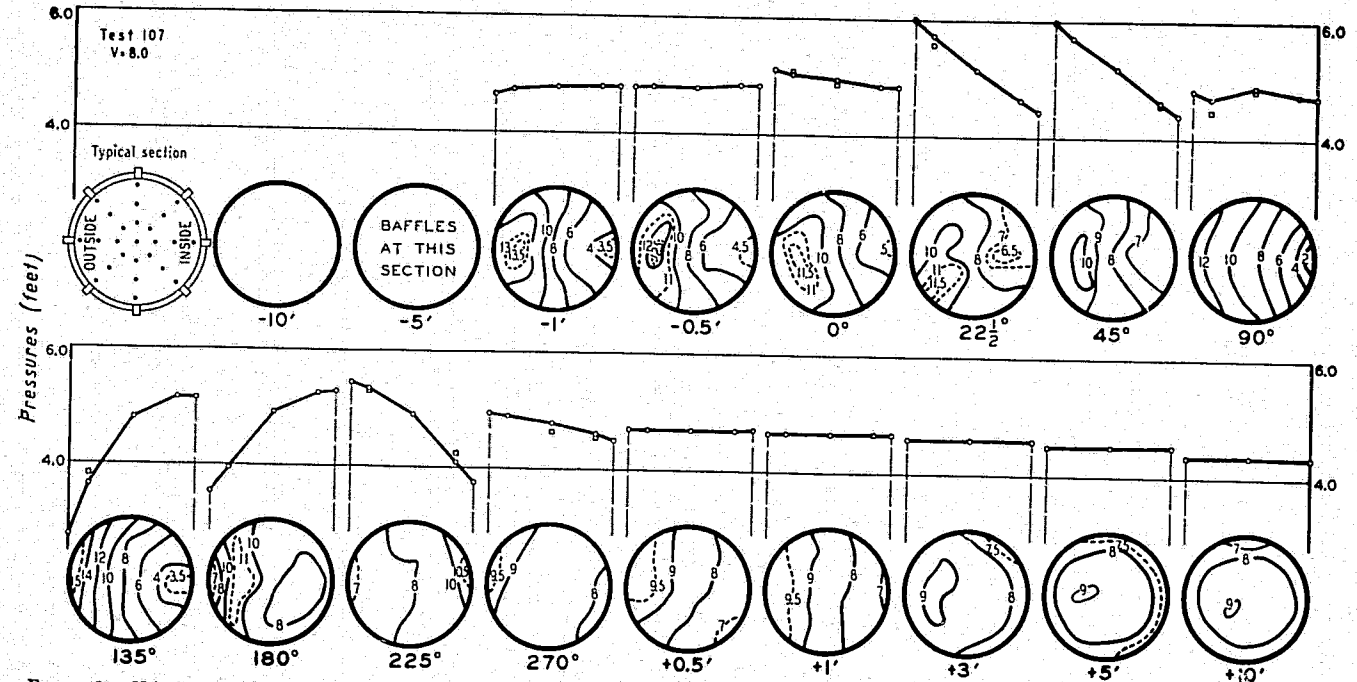

FIGURE 33.—Velocity distribution and peripheral pressures in 270° bend with velocity in approach tanget high toward outer side; mean velocity, 8 feet per second.

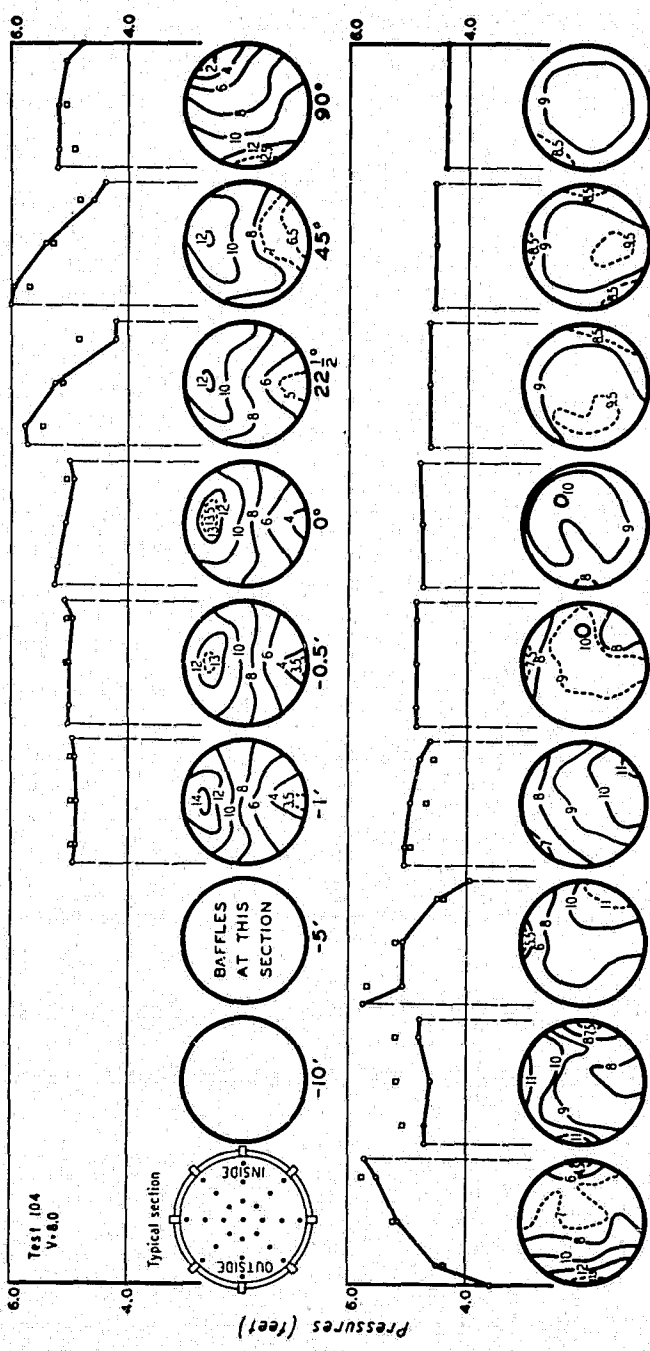

FIGURE 34.—Velocity distribution and peripheral pressures in 270° bend with velocity in approach tangent high at top; mean velocity, 8 feet per second.

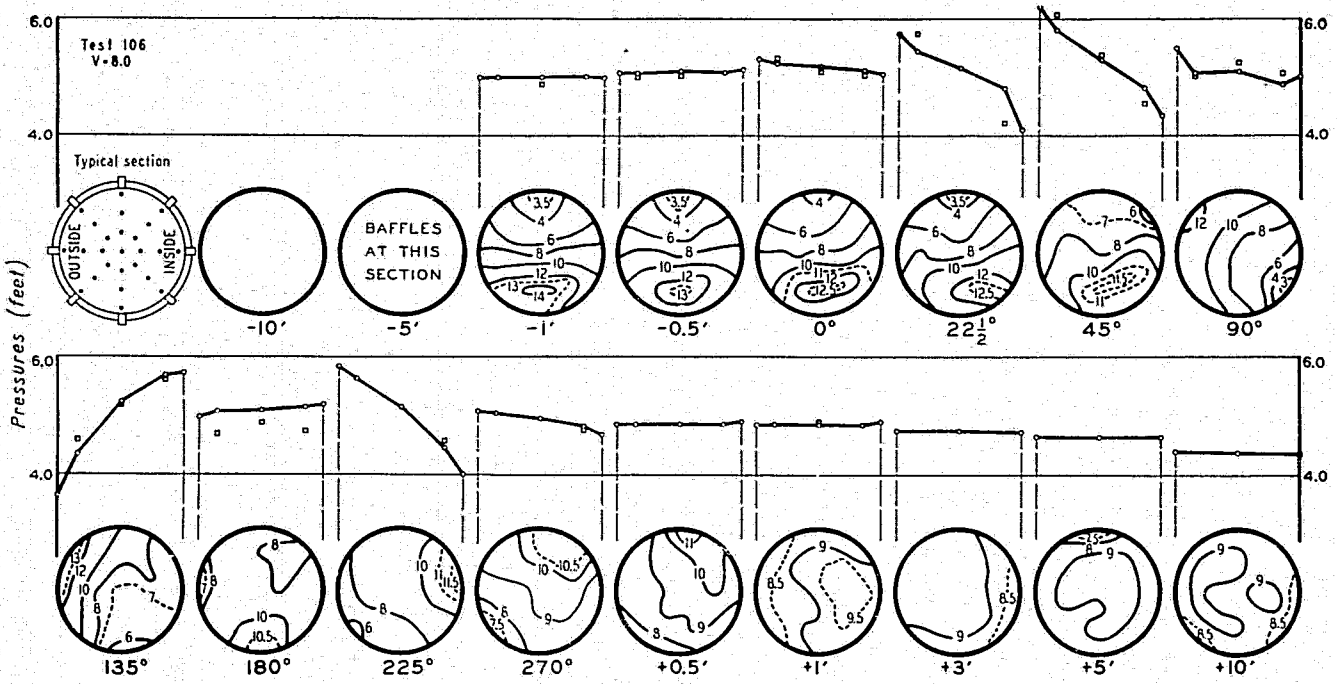

FIGURE 35.—Velocity distribution and peripheral pressures in 270° bend with velocity in approach tangent high at bottom; mean velocity, 8 feet per second.

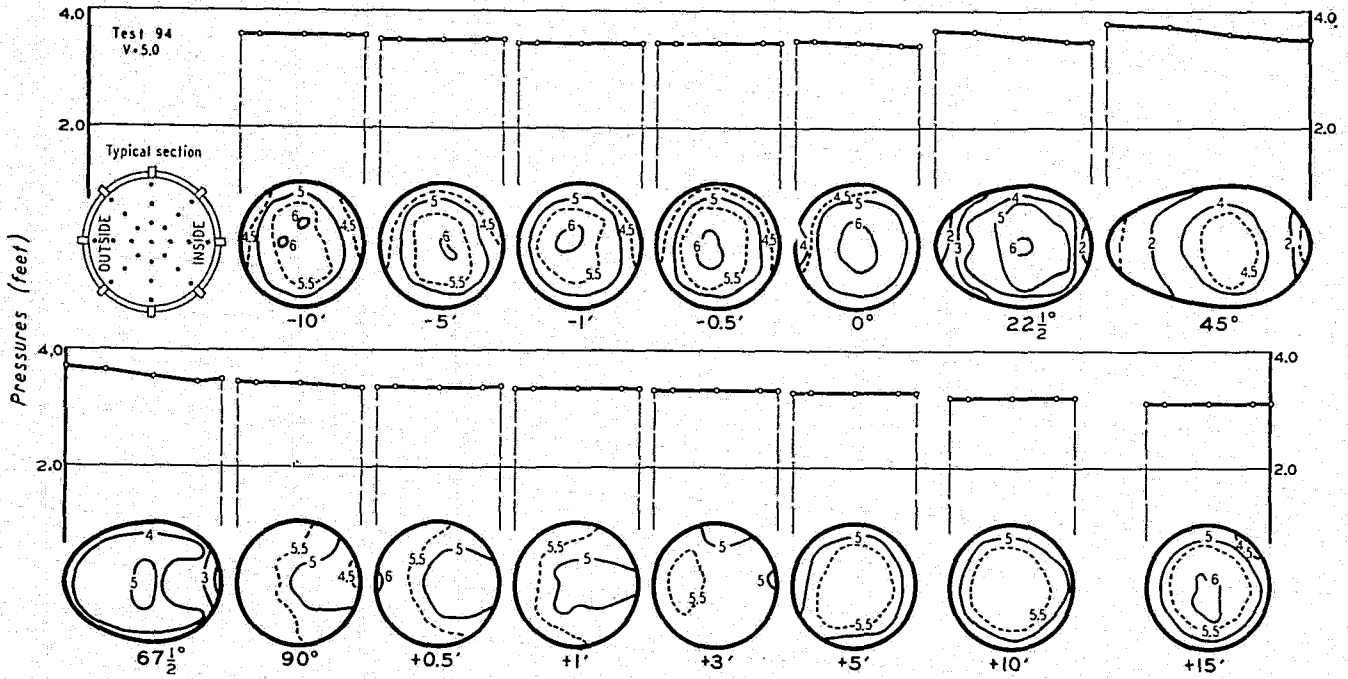

FIGURE 36.—Velocity distribution and peripheral pressures in type M bend with approximately uniform velocity distribution in approach tangent; mean velocity, 5 feet per second.

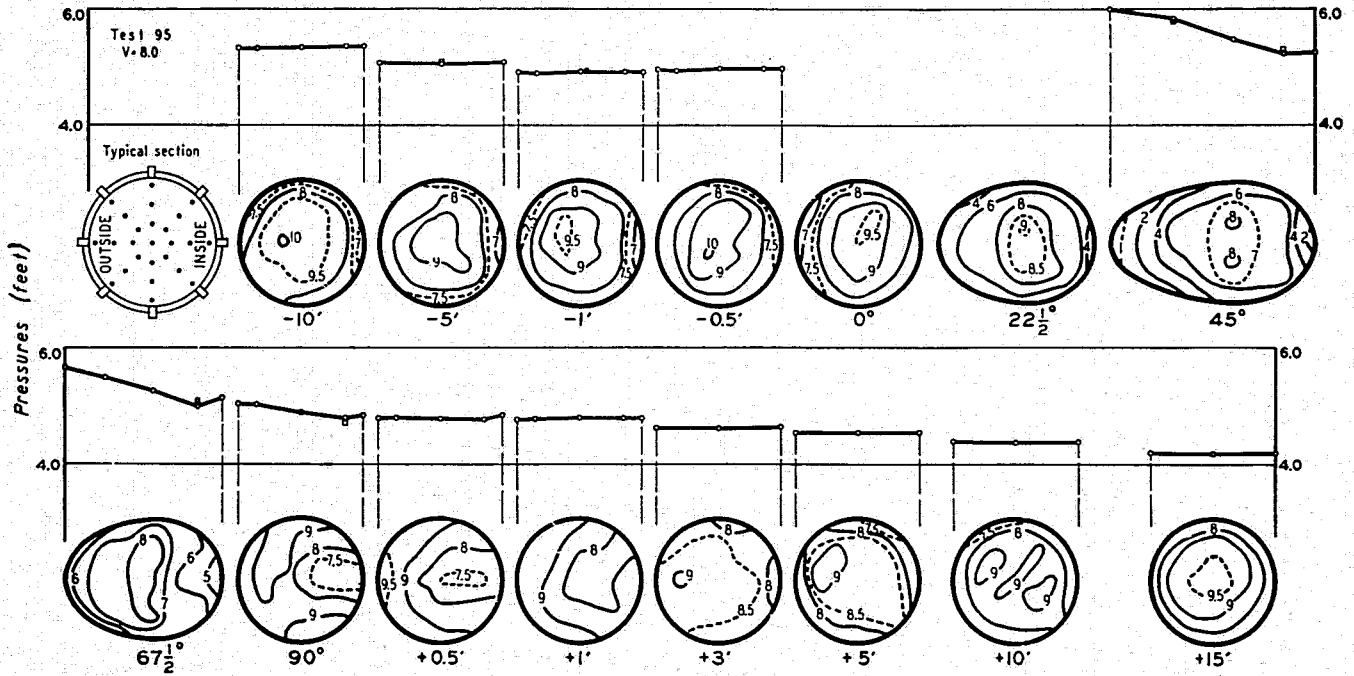

FIGURE 37.—Velocity distribution and peripheral pressures in type M bend with approximately uniform velocity distribution in approach tangent; mean velocity, 8 feet per second.

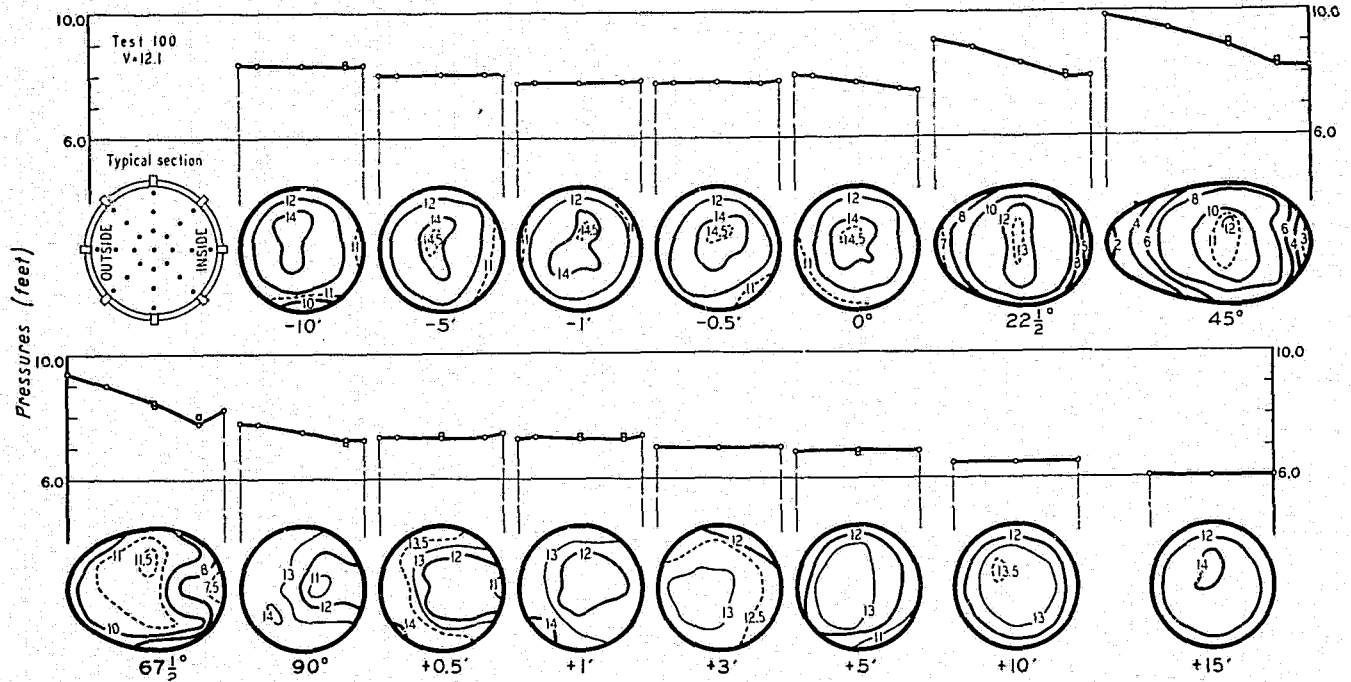

FIGURE 38.—Velocity distribution and peripheral pressures in type M bend with approximately uniform velocity distribution in approach tangent; mean velocity, 12.1 feet per second.

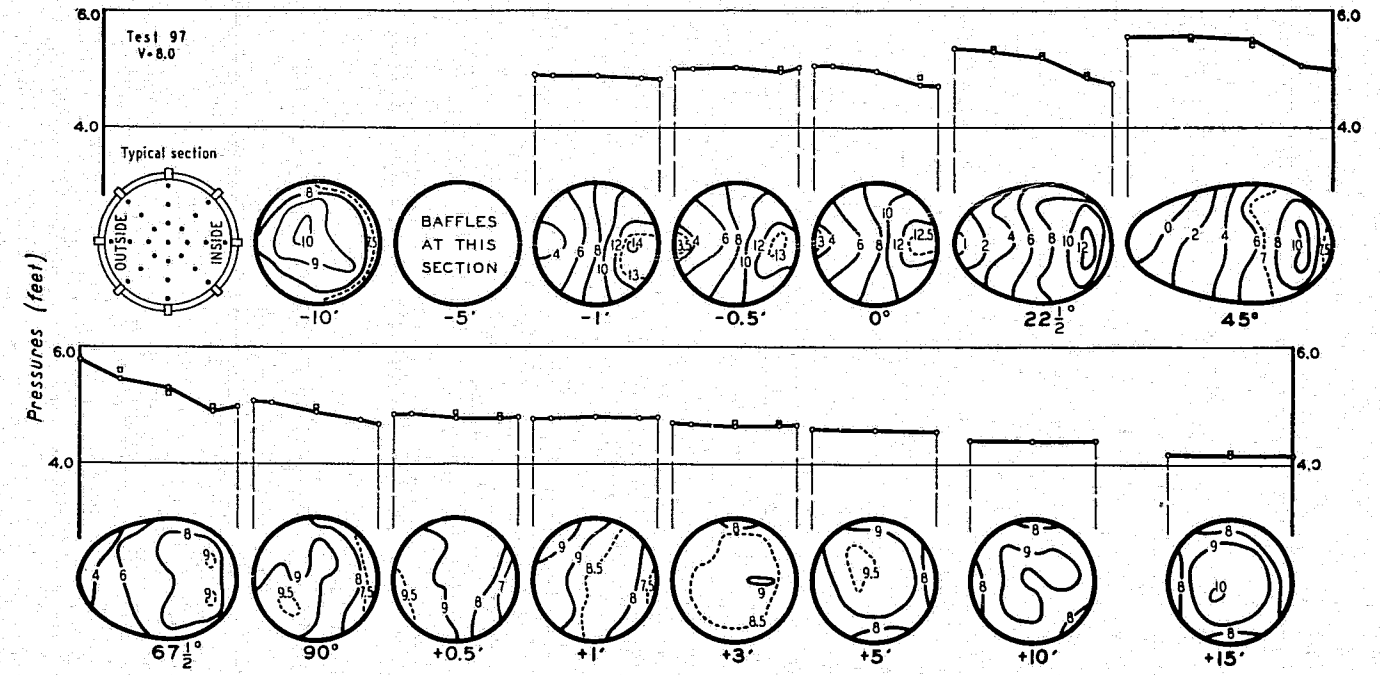

FIGURE 39.—Velocity distribution and peripheral pressures in type M bend with velocity in approach tangent high toward inner side; mean velocity, 8 feet per second.

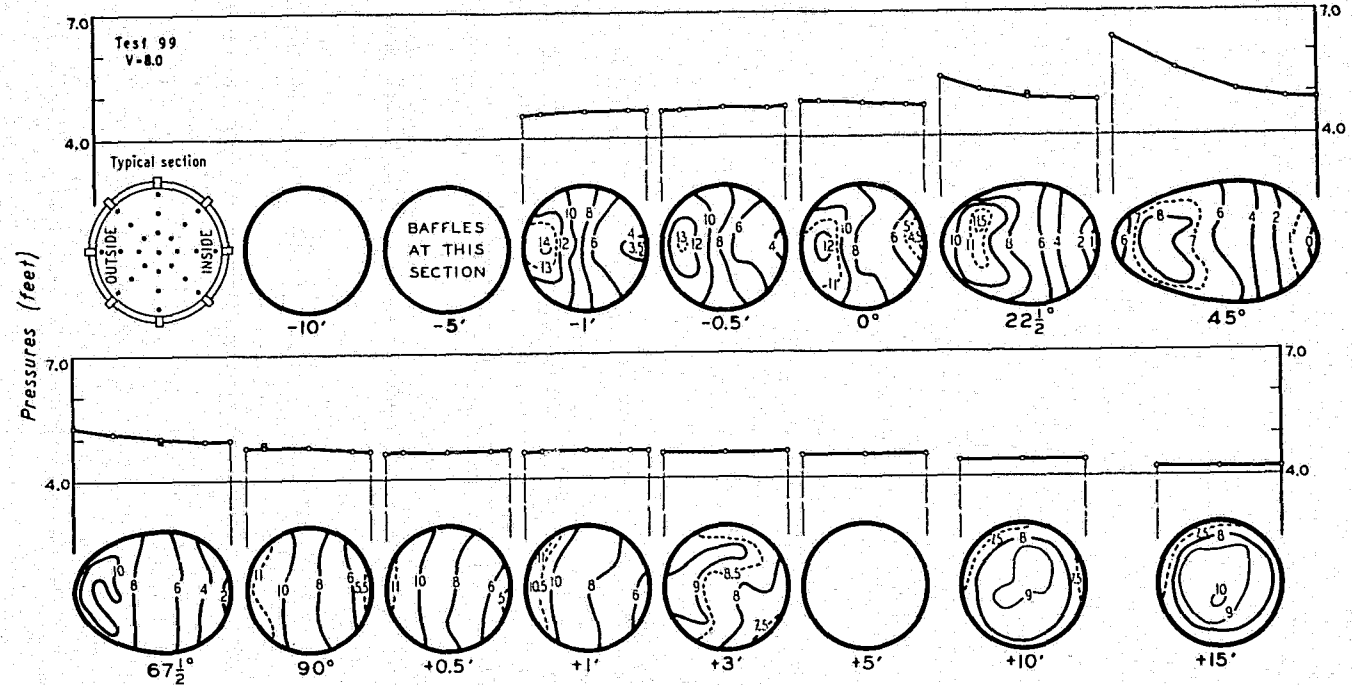

FIGURE 40.—Velocity distribution and peripheral pressures in type M bend with velocity in approach tangent high toward outer side; mean velocity, 8 feet per second.

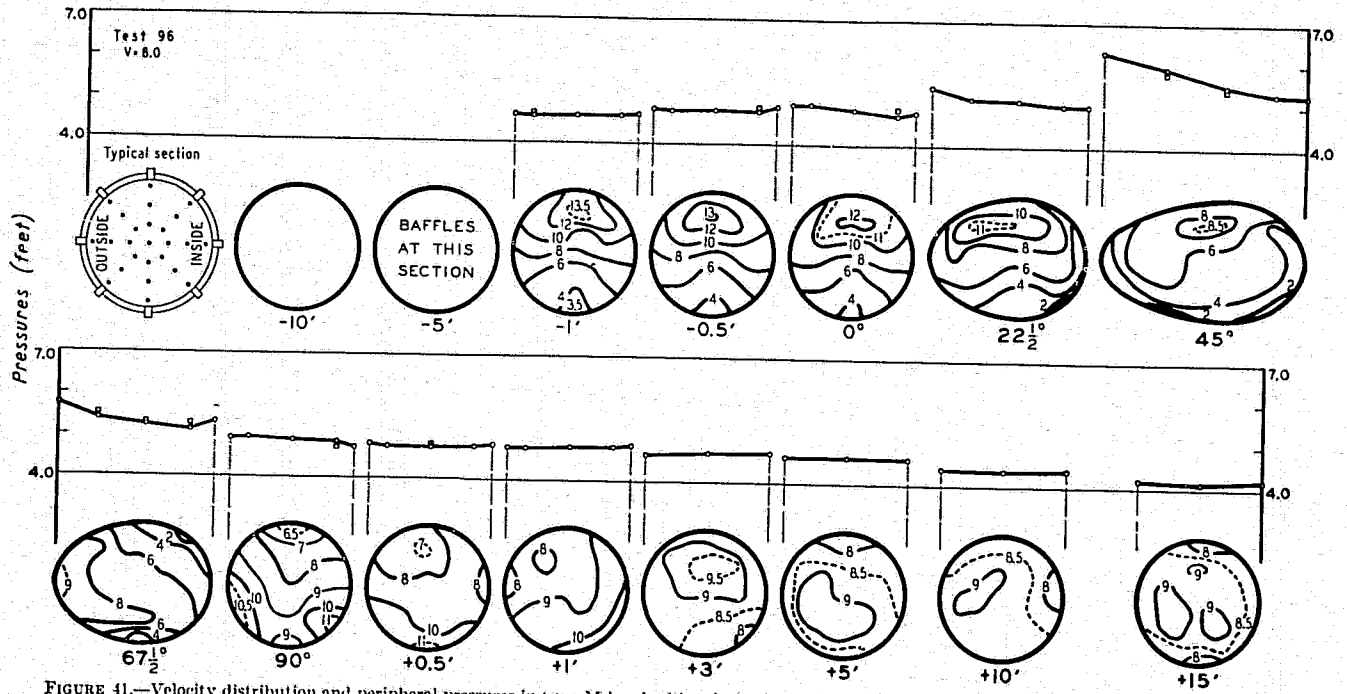

FIGURE 41.—Velocity distribution and peripheral pressures in type M bend with velocity in approach tangent high at top; mean velocity, 8 feet per second.

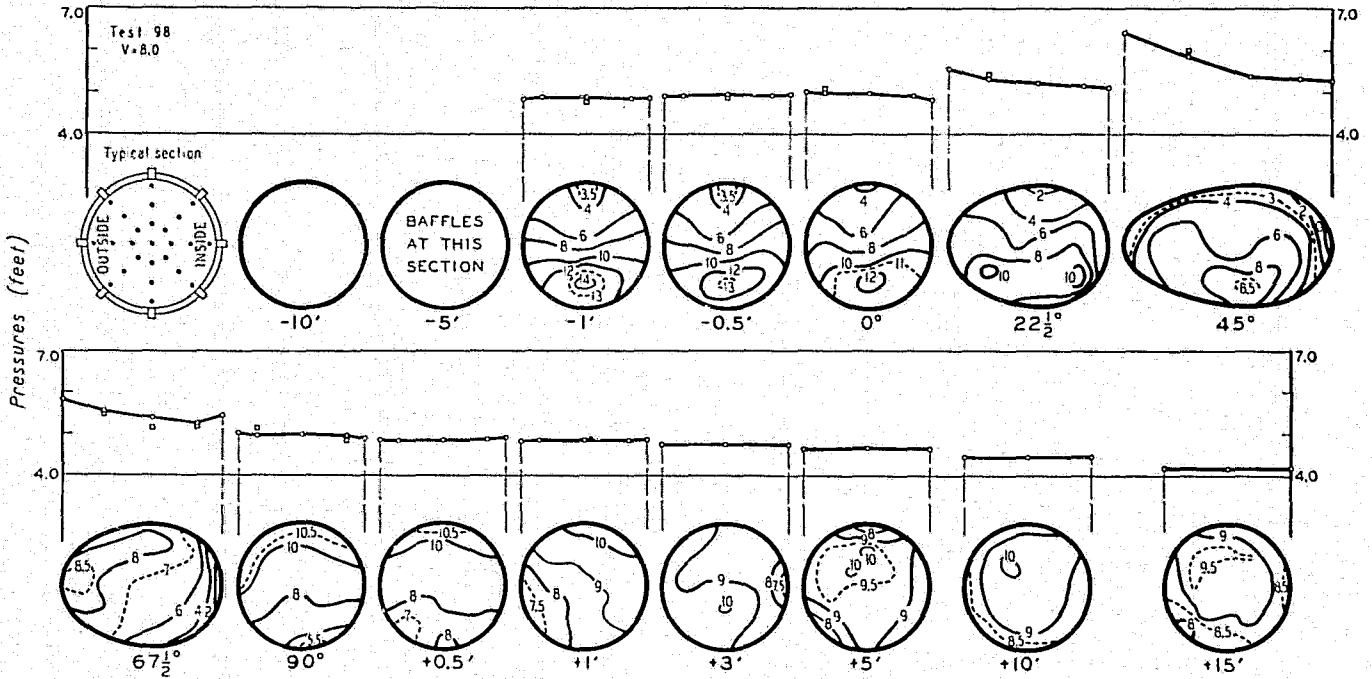

FIGURE 42.—Velocity distribution and peripheral pressures in type M bend with velocity in approach tangent high at bottom; mean velocity, 8 feet per second.

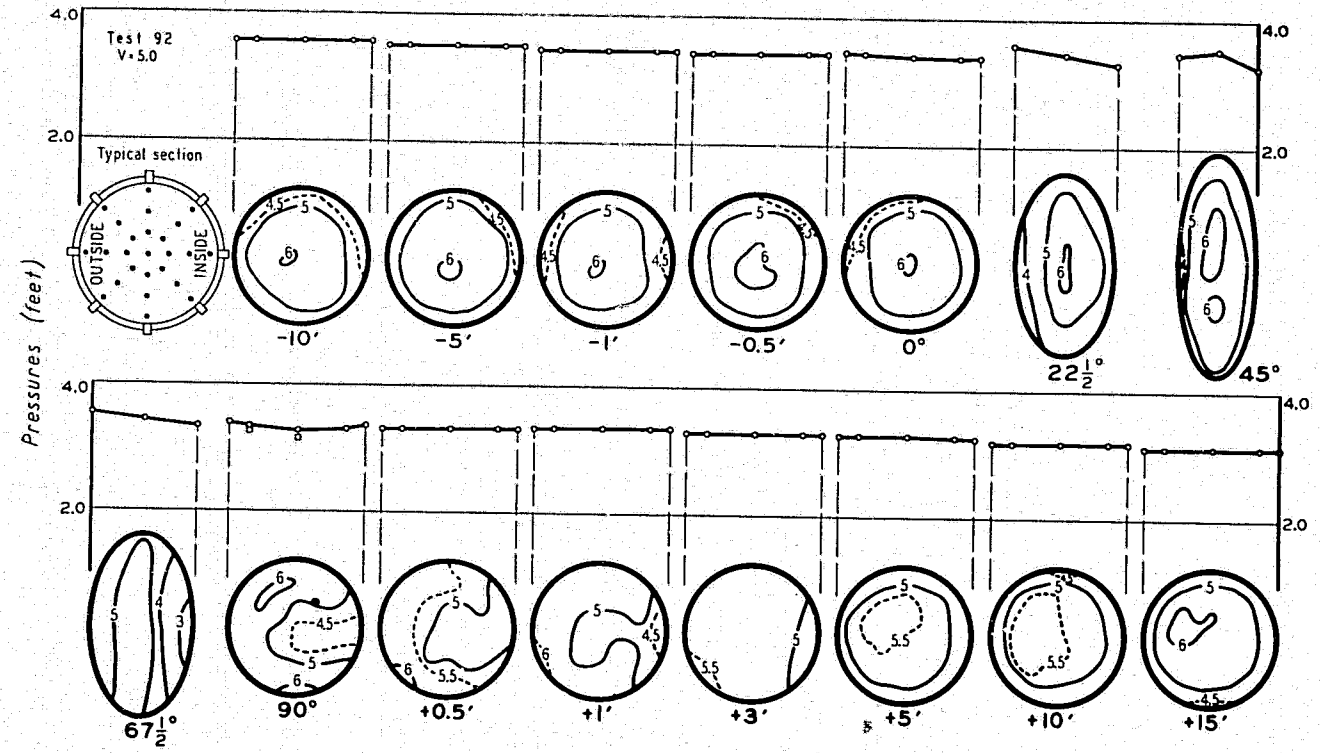

FIGURE 43.—Velocity distribution and peripheral pressures in type N bend with approximately uniform velocity distribution in approach tangent; mean velocity 5 feet per second.

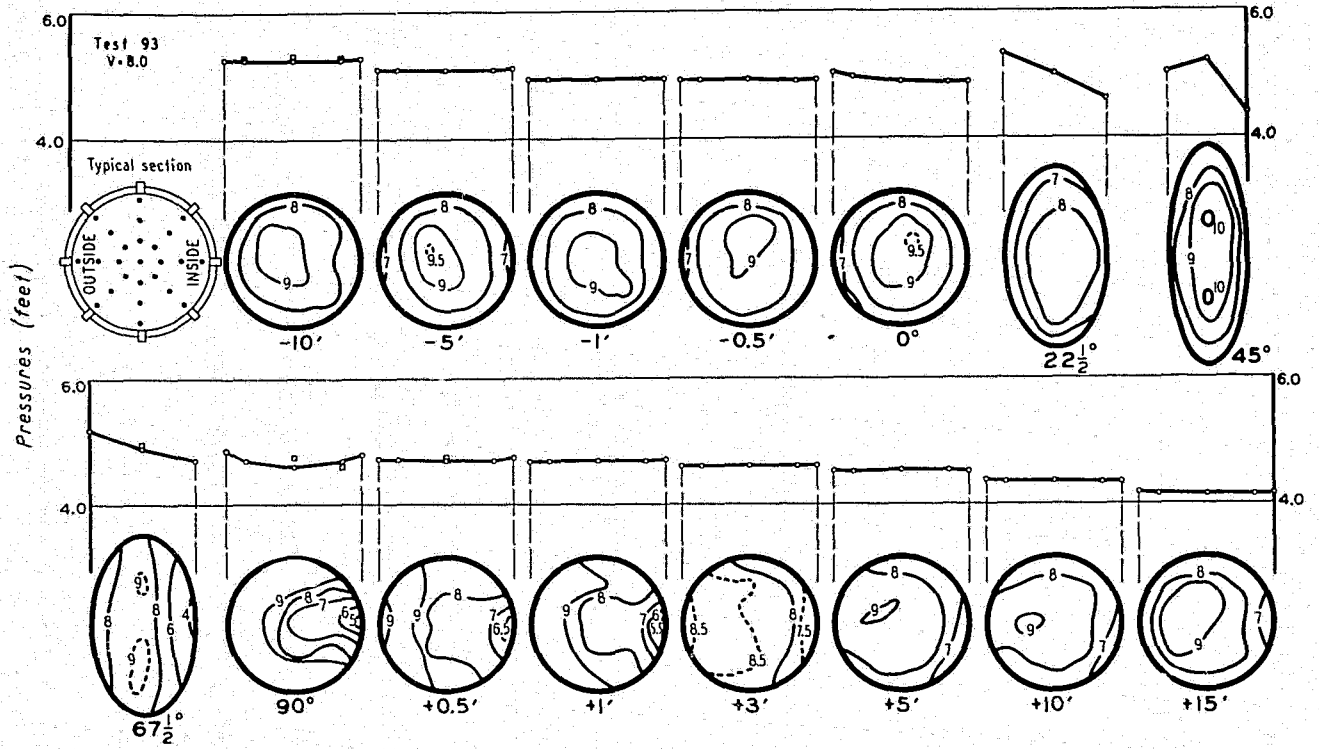

FIGURE 44.—Velocity distribution and peripheral pressures in type N bend with approximately uniform velocity distribution in approach tangent; mean velocity, 8 feet per second.

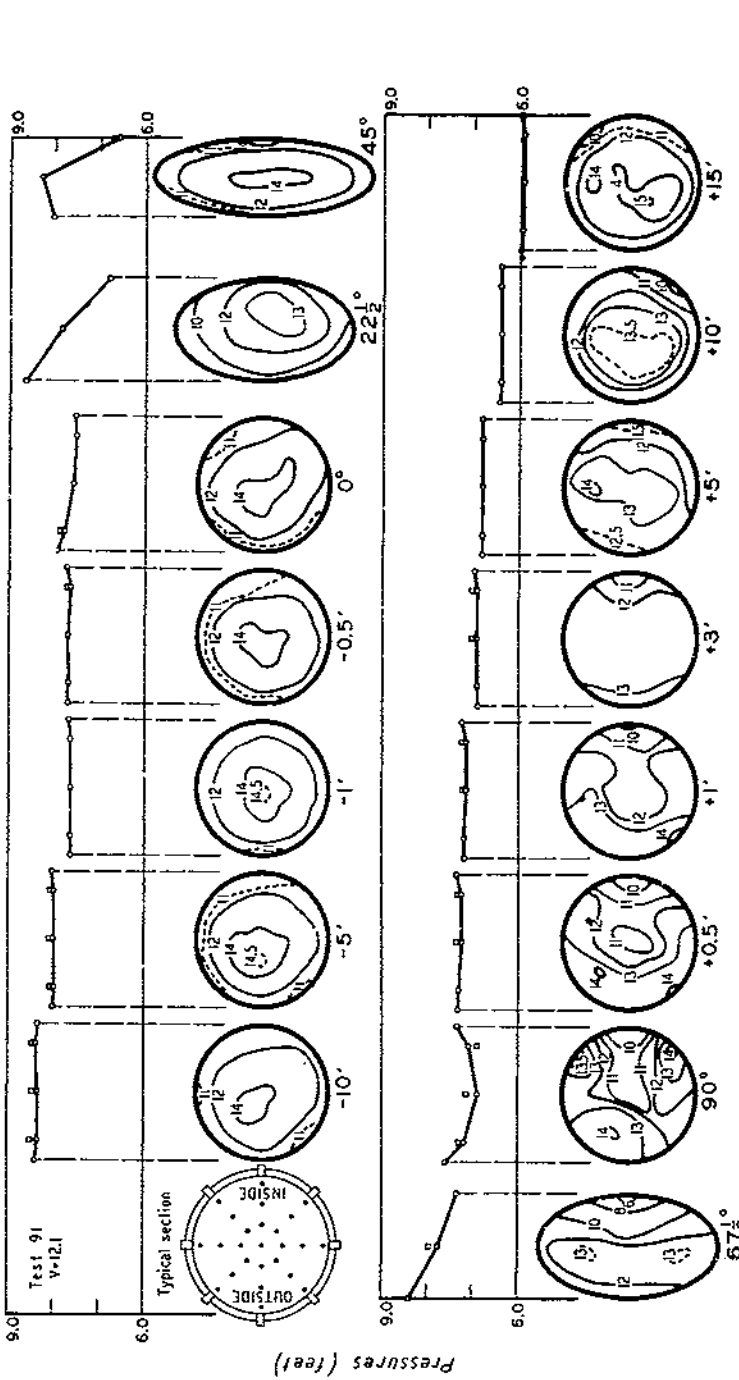

FIGURE 45.—Velocity distribution and peripheral pressures in type N bend with approximately uniform velocity distribution in approach tangent; mean velocity, 12.1 feet per second

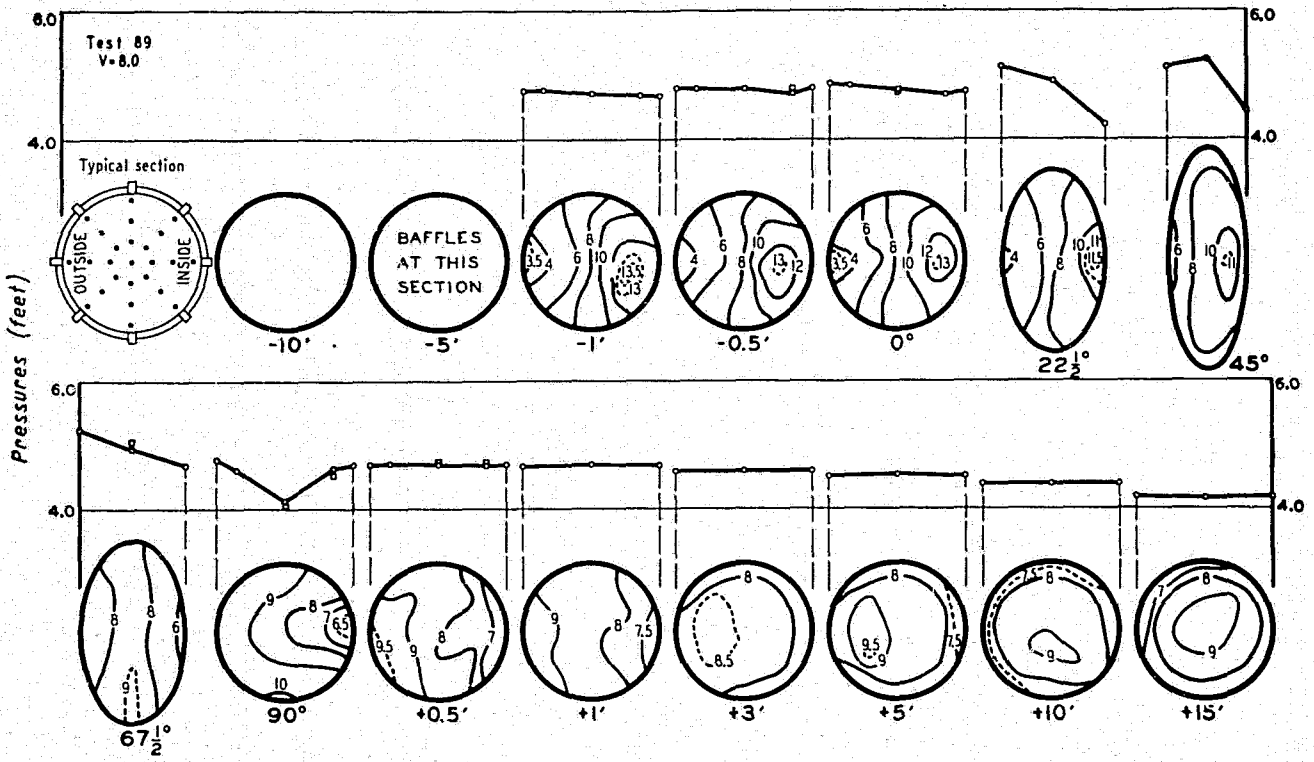

FIGURE 46.—Velocity distribution and peripheral pressures in type N bend with velocity distribution in approach tangent high toward inner side; mean velocity, 8 feet per second.

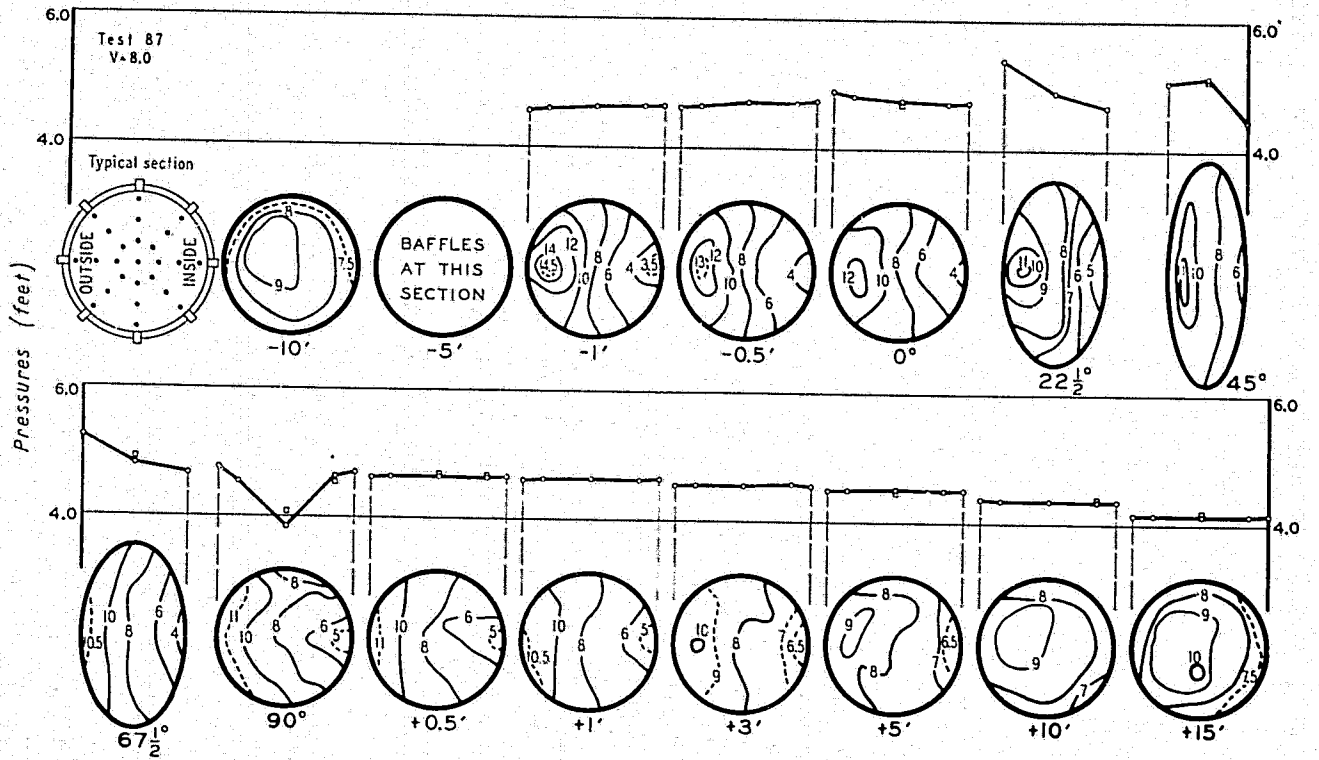

FIGURE 47.—Velocity distribution and peripheral pressures in type N bend with velocity distribution in approach tangent high toward outer side; mean velocity, 8 feet per second.

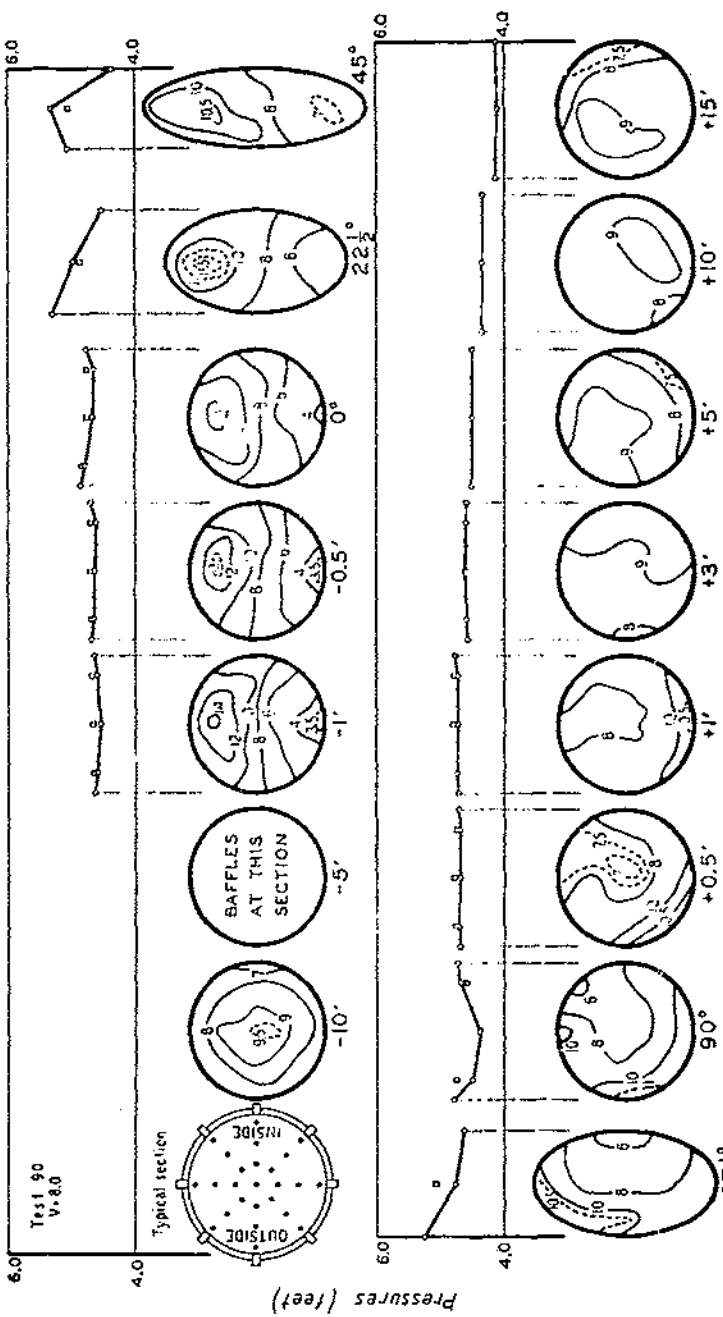

FIGURE 48. Velocity distribution and peripheral pressures in type N bend with velocity distribution in approach tangent high at top; mean velocity, 8 feet per second.

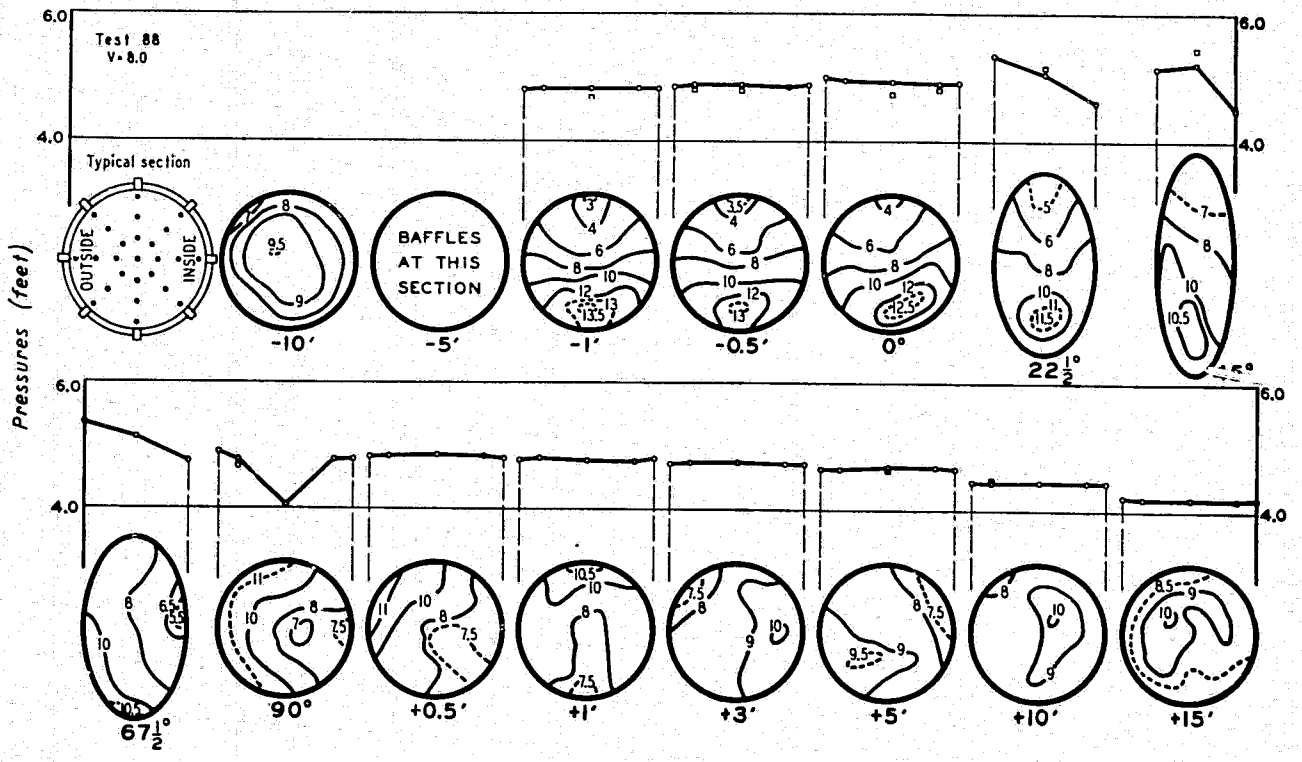

FIGURE 49.—Velocity distribution and peripheral pressures in type N bend with velocity distribution in approach tangent high at bottom; mean velocity, 8 feet per second.

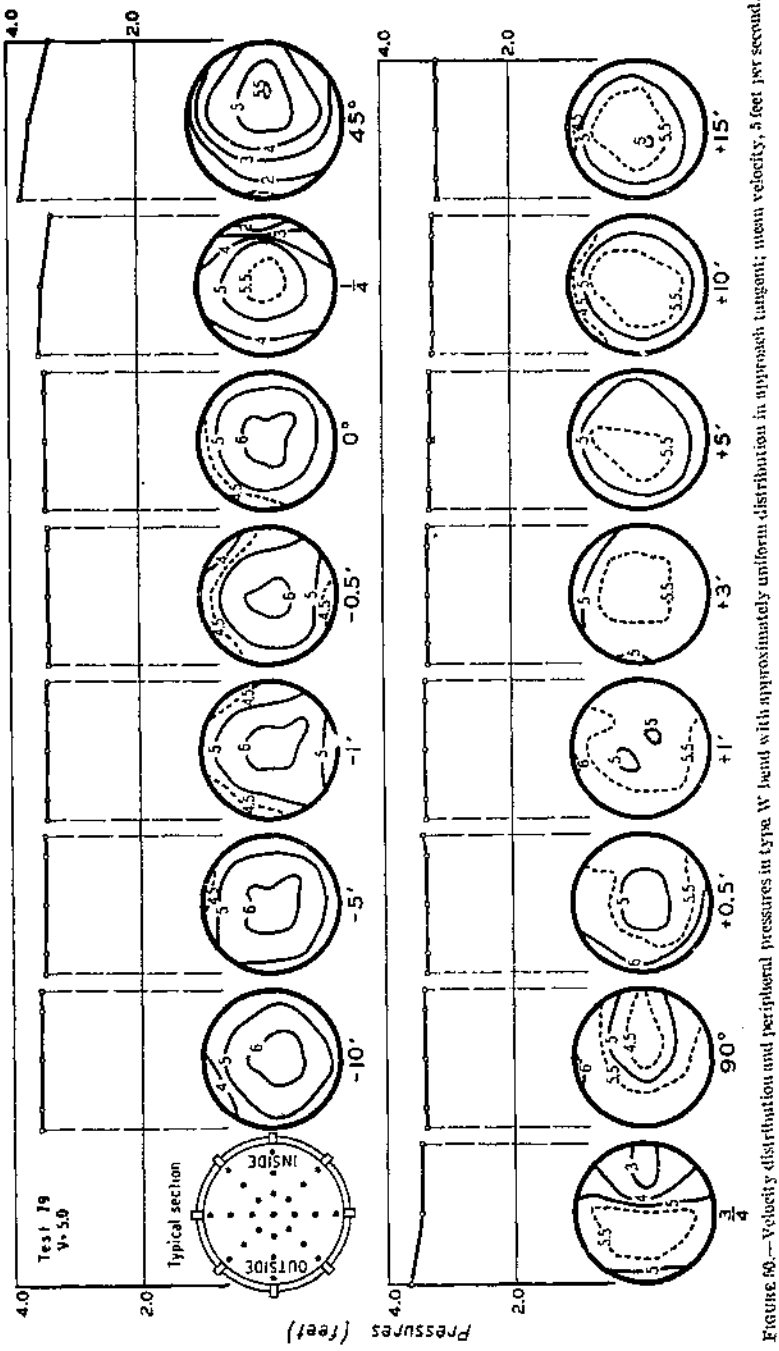

FIGURE 60.—Velocity distribution and peripheral pressures in type W bend with approximately uniform distribution in approach tangent; mean velocity, 5 feet per second.

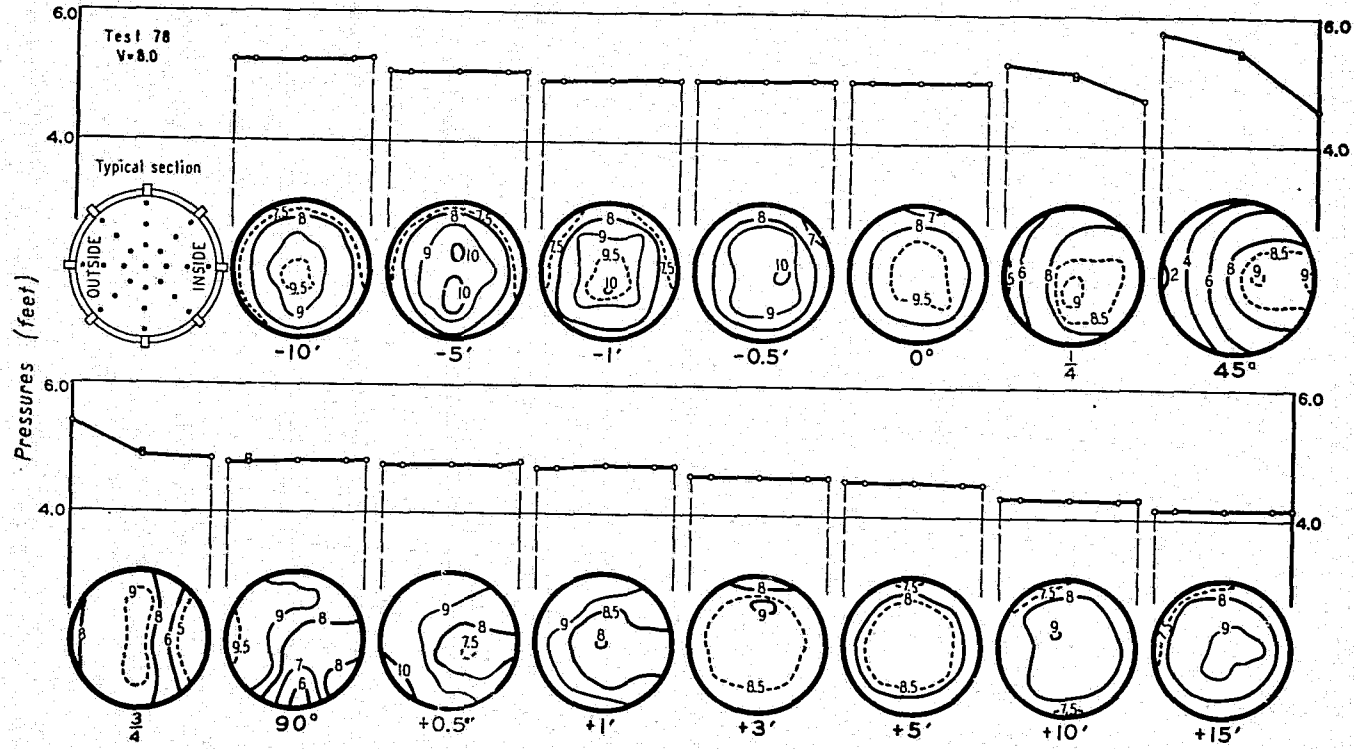

FIGURE 51.—Velocity distribution and peripheral pressures in type W bend with approximately uniform distribution in approach tangent; mean velocity, 8 feet per second.

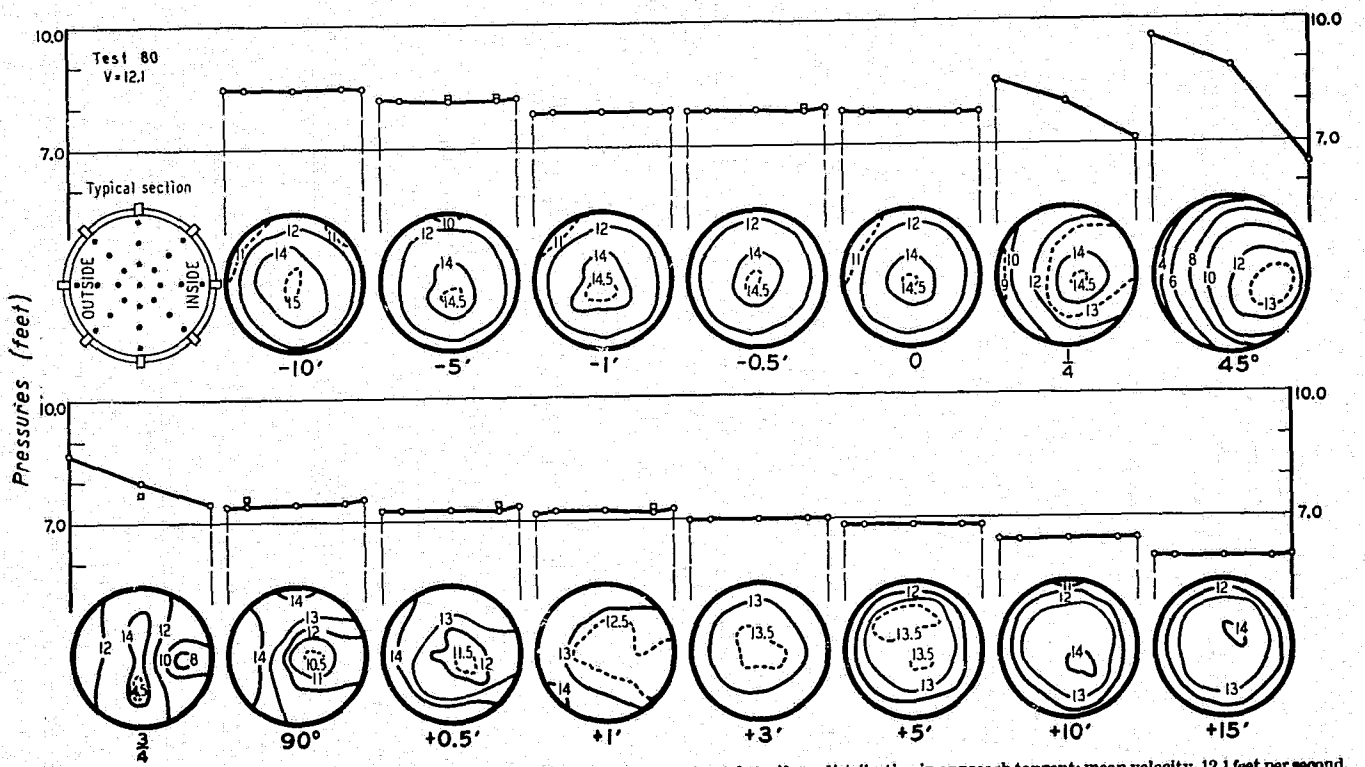

FIGURE 52.—Velocity distribution and peripheral pressures in type W bend with approximately uniform distribution in approach tangent; mean velocity, 12.1 feet per second.

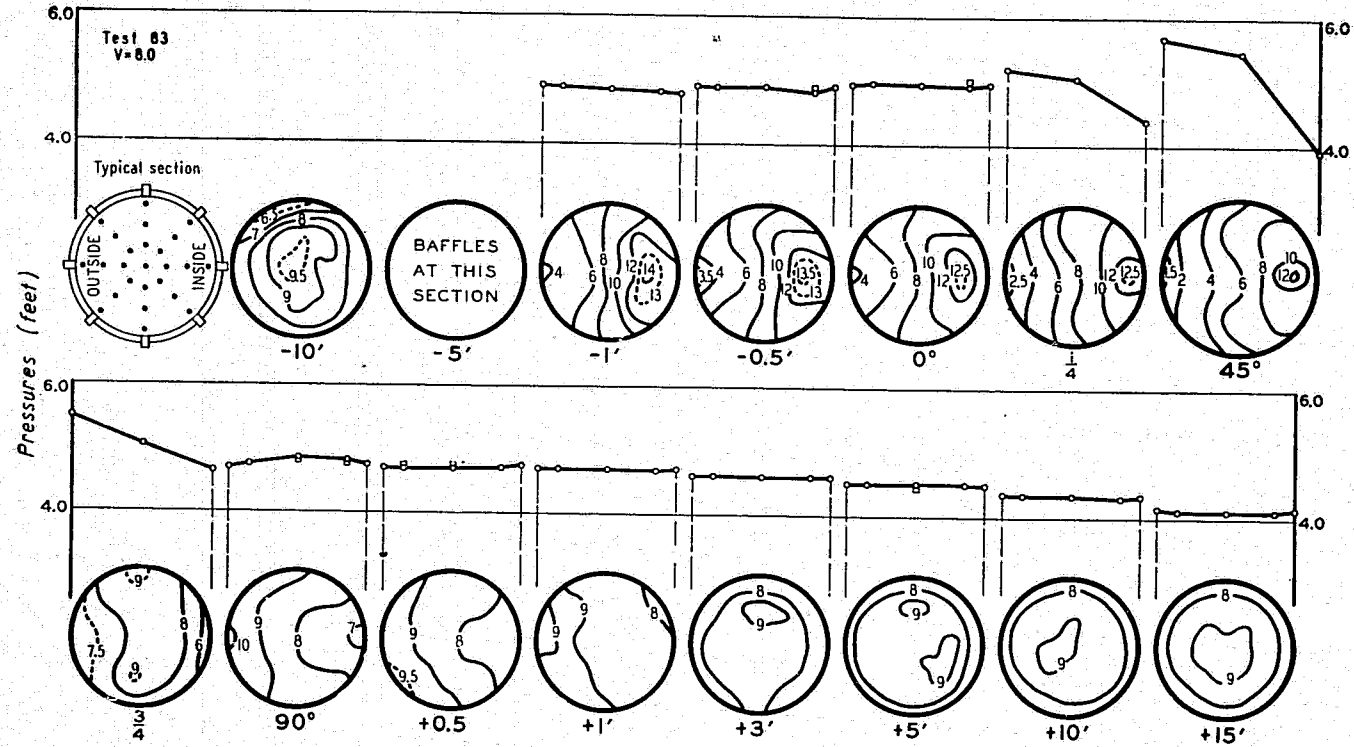

FIGURE 53.—Velocity distribution and peripheral pressures in type W bend with velocity in approach tangent high toward inner side; mean velocity, 8 feet per second.

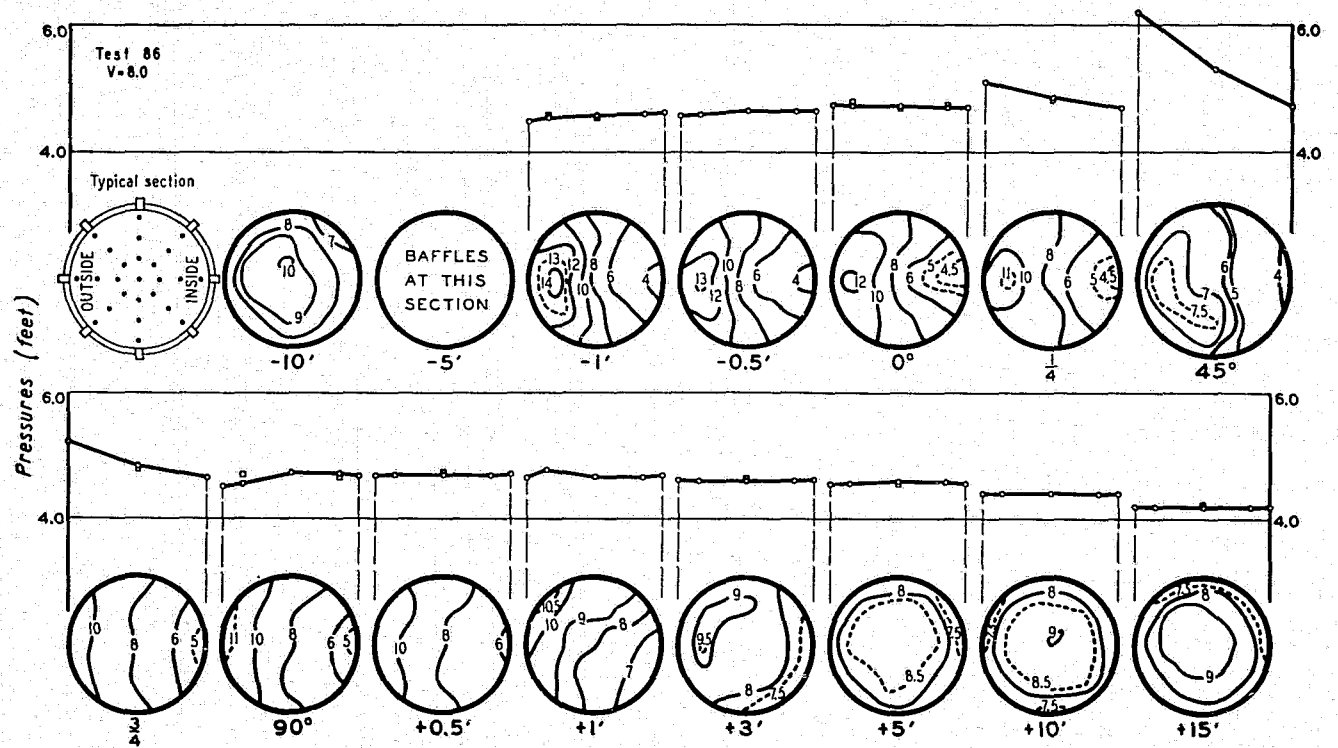

FIGURE 54.—Velocity distribution and peripheral pressures in type W bend with velocity in approach tangent high toward outer side; mean velocity, 8 feet per second.

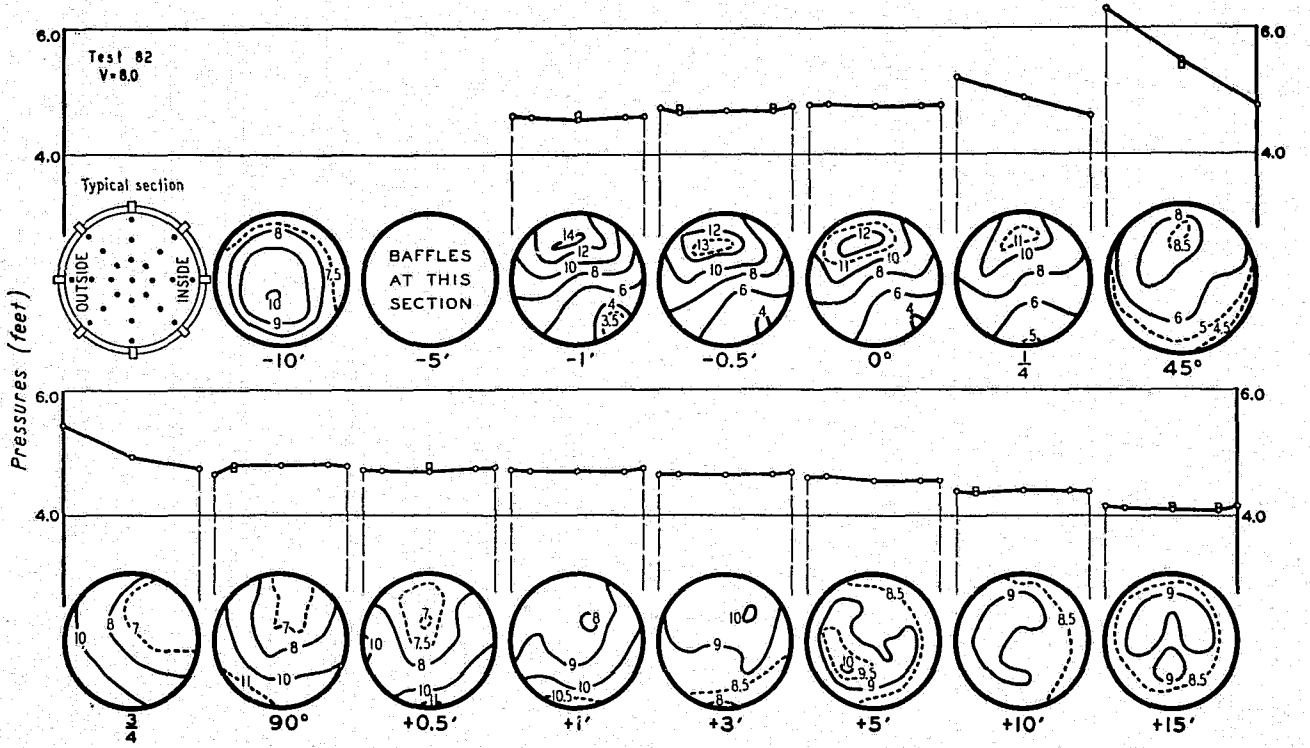

FIGURE 55.—Velocity distribution and peripheral pressures in type W bend with velocity in approach tangent high at top; mean velocity, 8 feet per second.

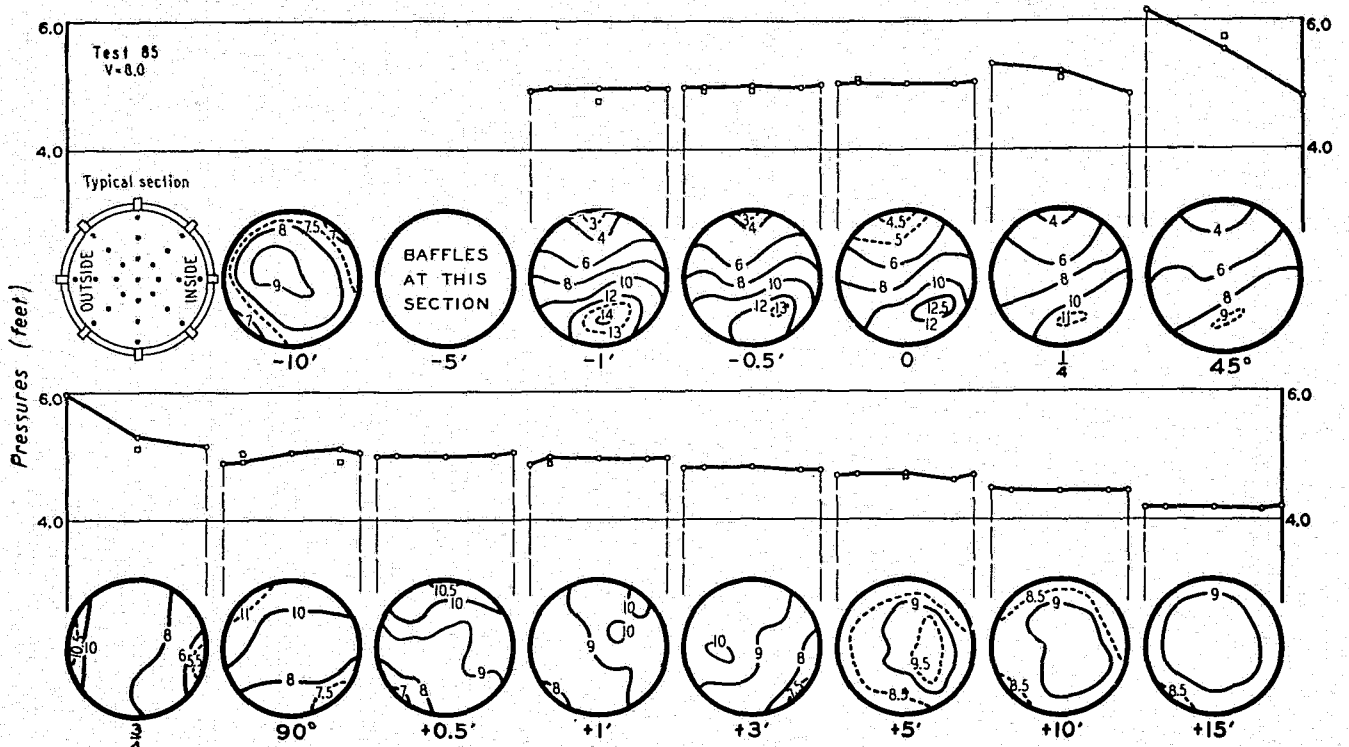

FIGURE 56.—Velocity distribution and peripheral pressures in type W bend with velocity in approach tangent high at bottom; mean velocity, 8 feet per second.

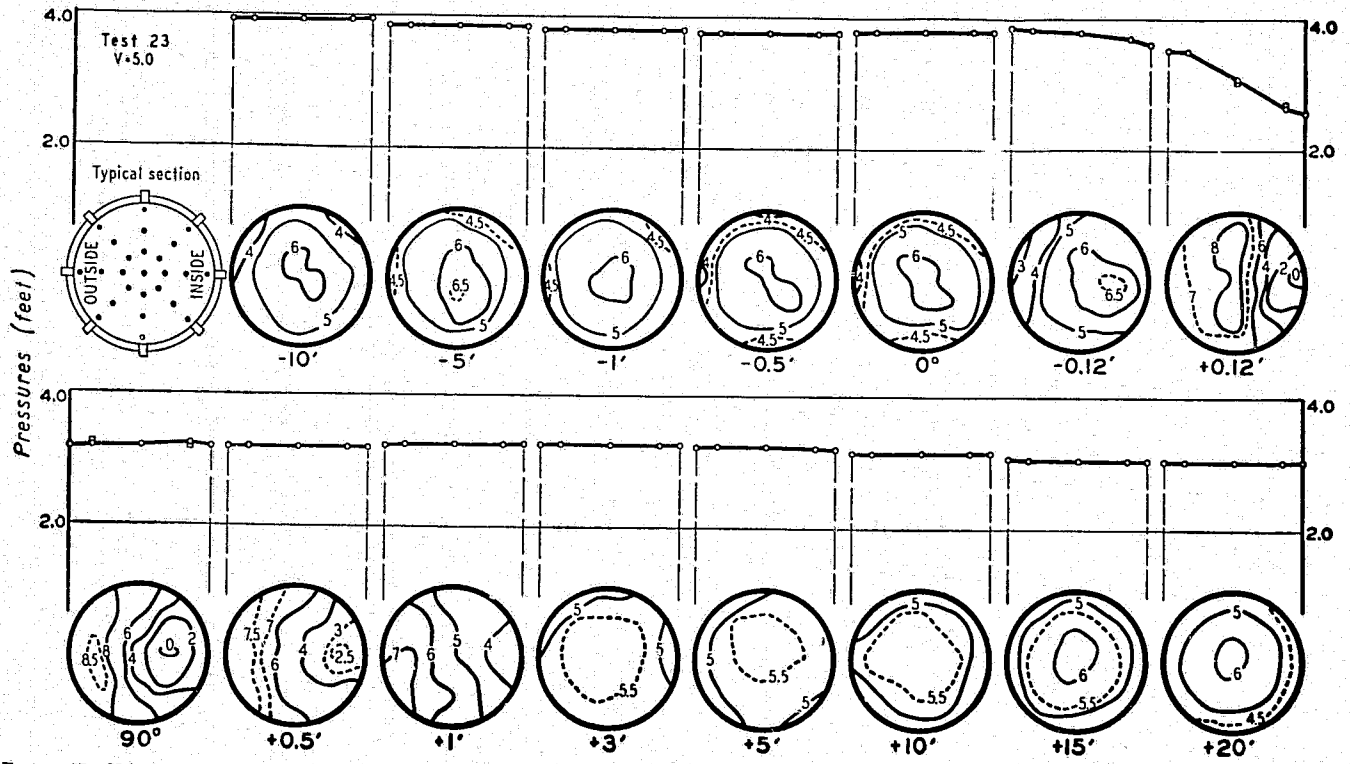

FIGURE 57.—Velocity distribution and peripheral pressures in miter bend with approximately uniform velocity distribution in approach tangent; mean velocity, 5 feet per second.

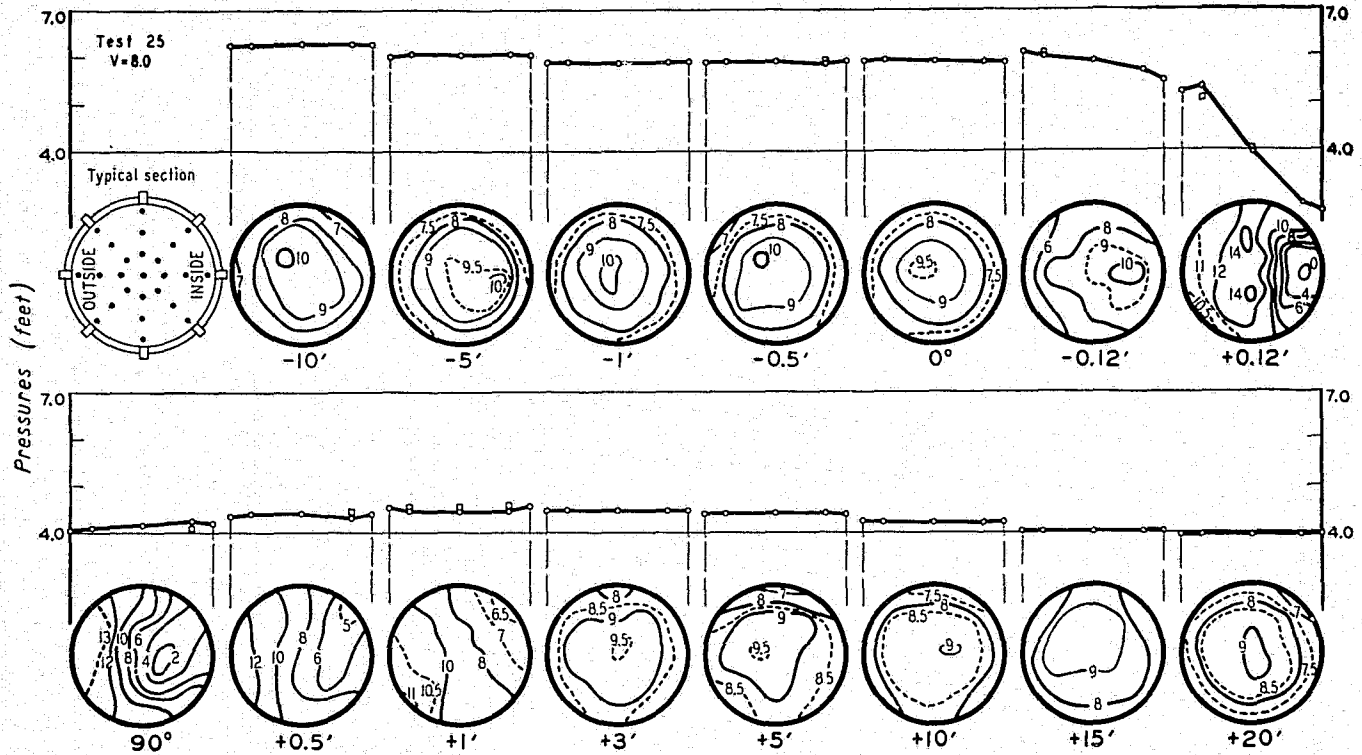

FIGURE 58.—Velocity distribution and peripheral pressures in miter bend with approximately uniform velocity distribution in approach tangent; mean velocity, 8 feet per second.

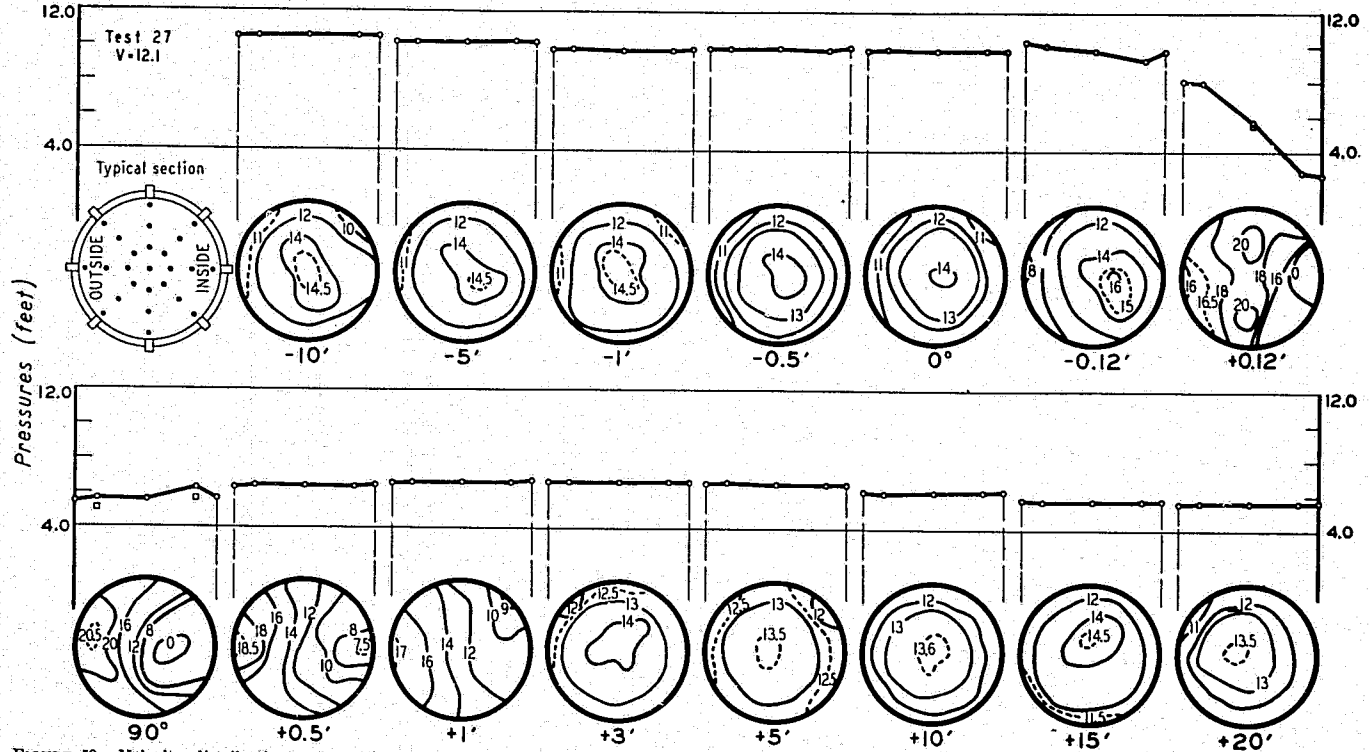

FIGURE 59.—Velocity distribution and peripheral pressures in miter bend with approximately uniform velocity distribution in approach tangent; mean velocity, 12.1 feet per second.

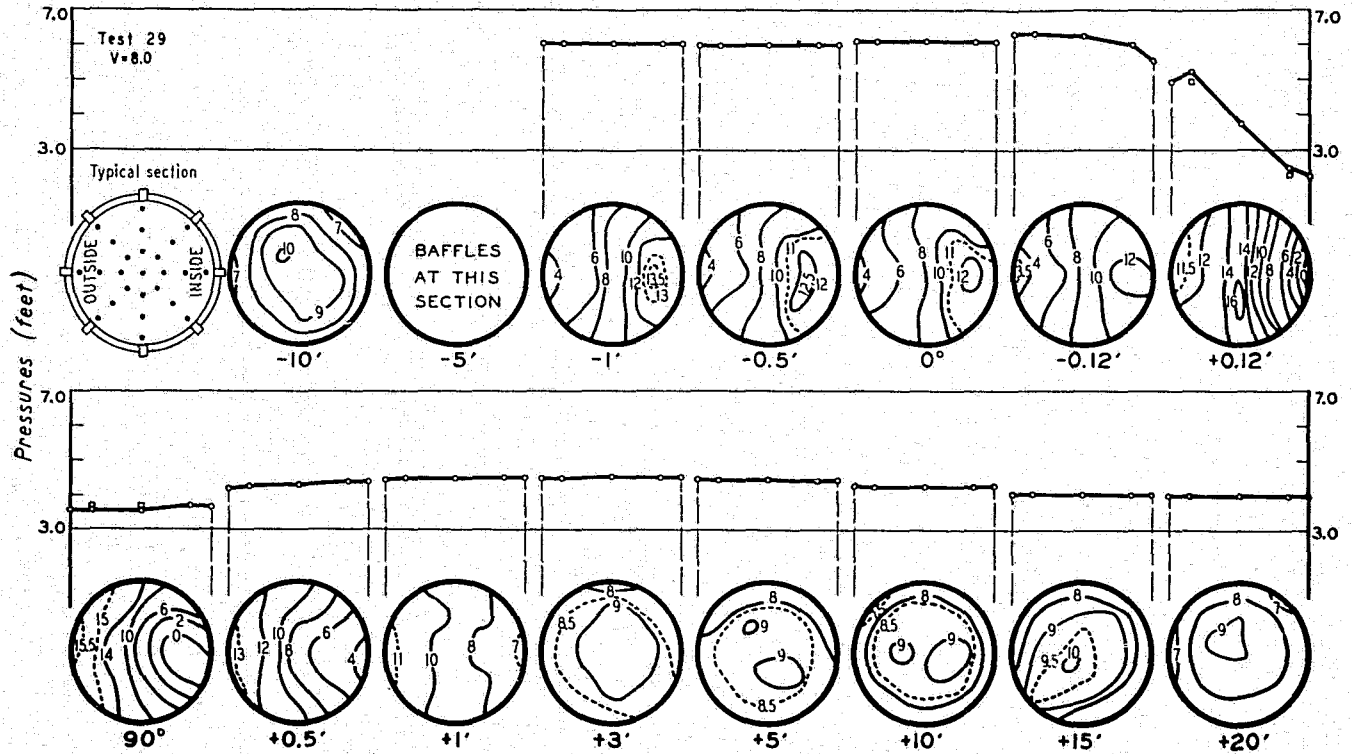

FIGURE 60.—Velocity distribution and peripheral pressures in miter bend with velocity in approach tangent high toward inner side; mean velocity, 8 feet per second.

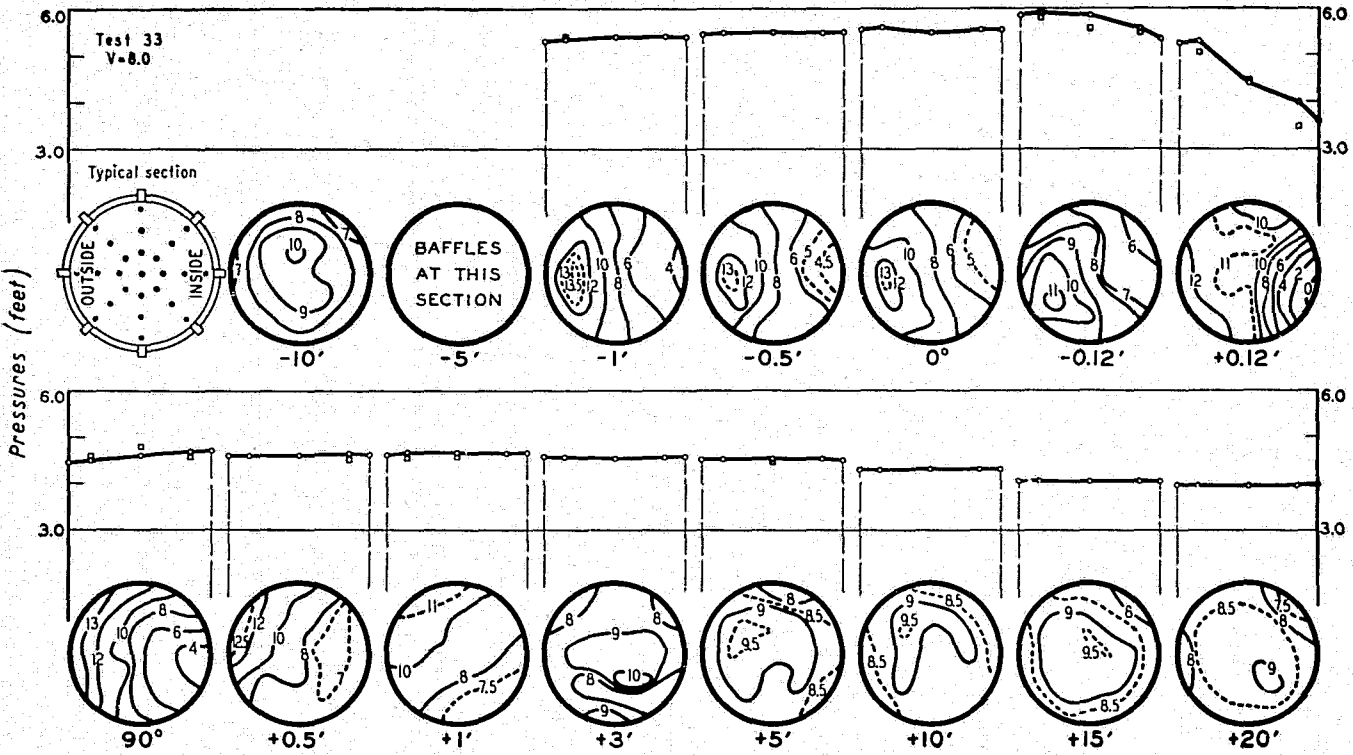

FIGURE 61.—Velocity distribution and peripheral pressures in miter bend with velocity in approach tangent high toward outer side; mean velocity, 8 feet per second.

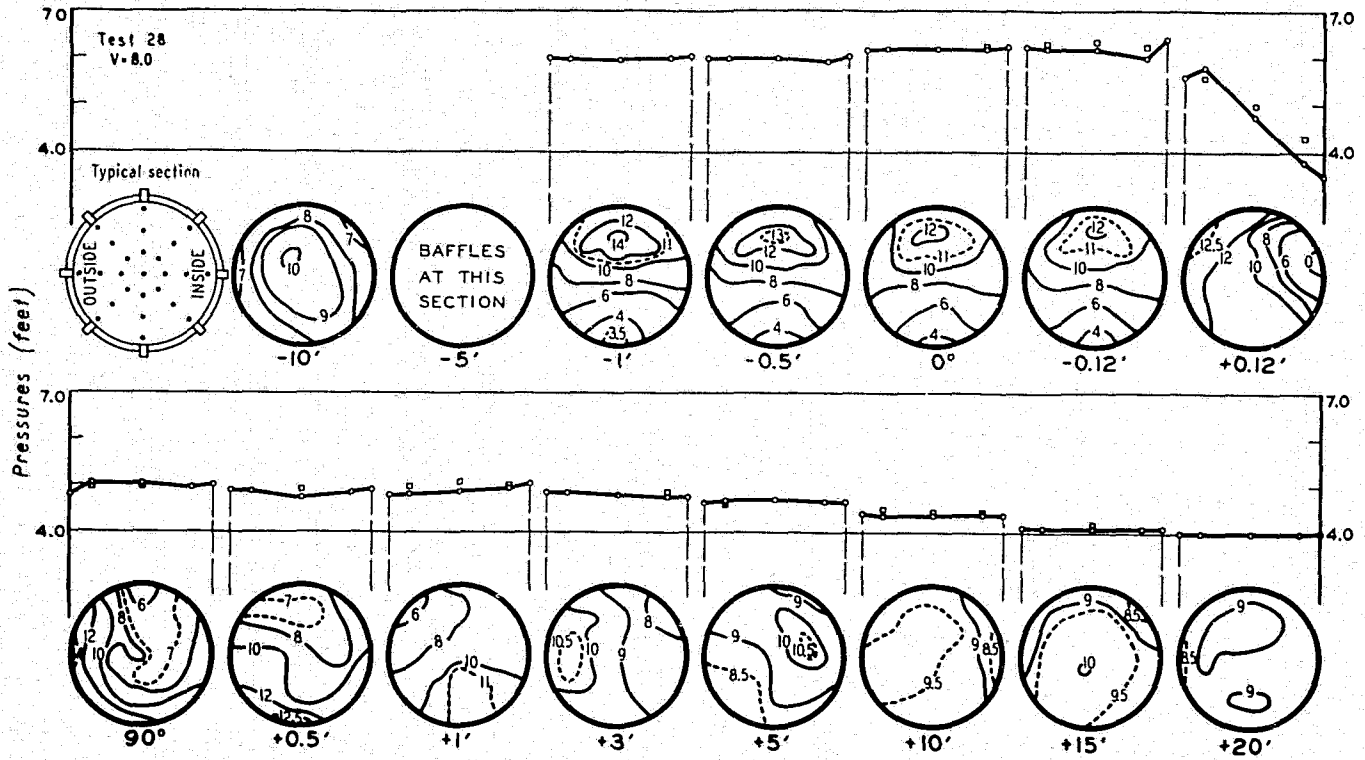

FIGURE 62.—Velocity distribution and peripheral pressures in miter bend with velocity in approach tangent high at top; mean velocity, 8 feet per second.

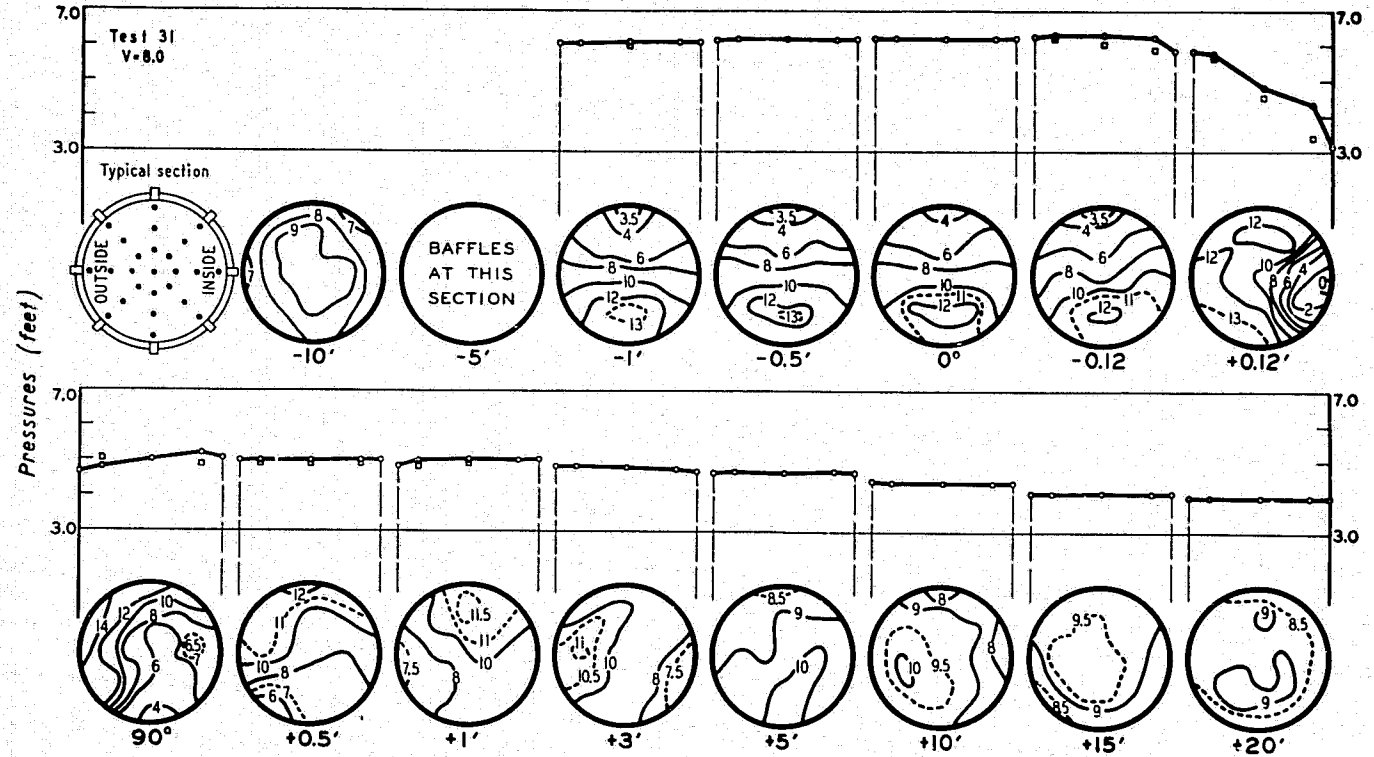

FIGURE 63.—Velocity distribution and peripheral pressures in miter bend with velocity in approach tangent high at bottom; mean velocity, 8 feet per second.

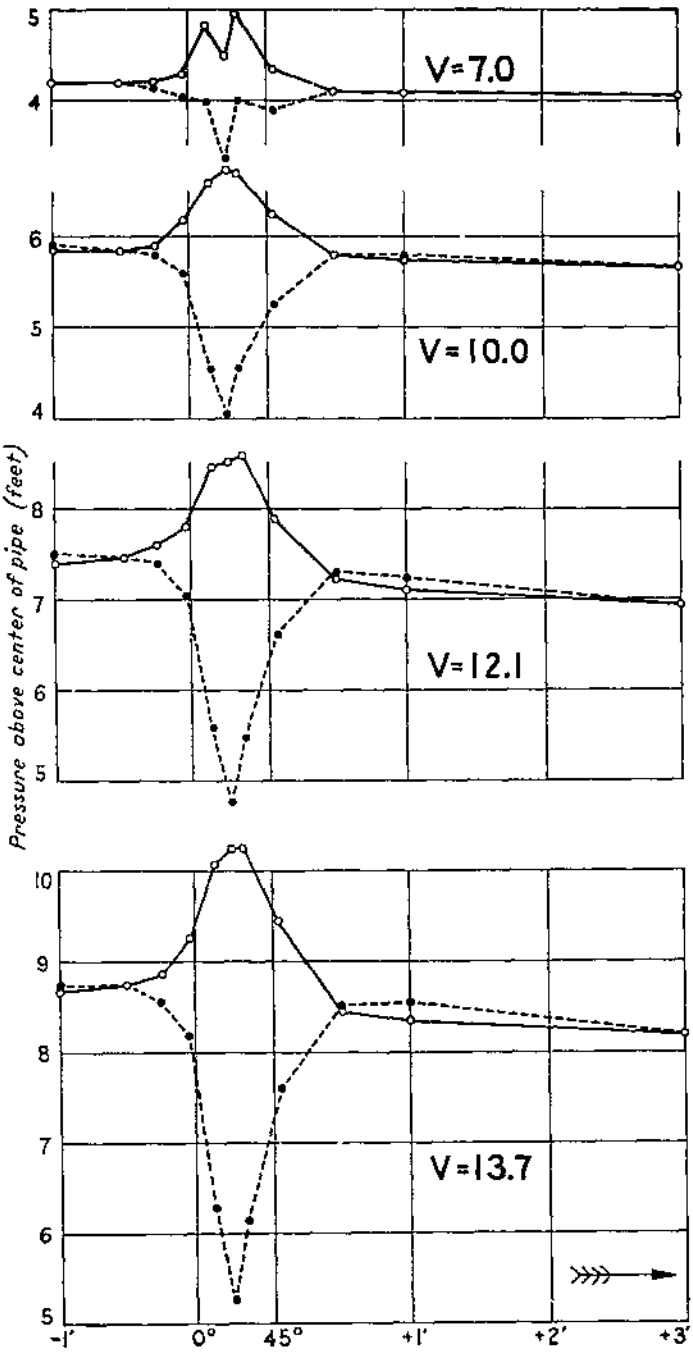

FIGURE 64.—Pressures along inner side (broken line) and outer side (solid line) of 45° bend with uniform velocity distribution in approach tangent.

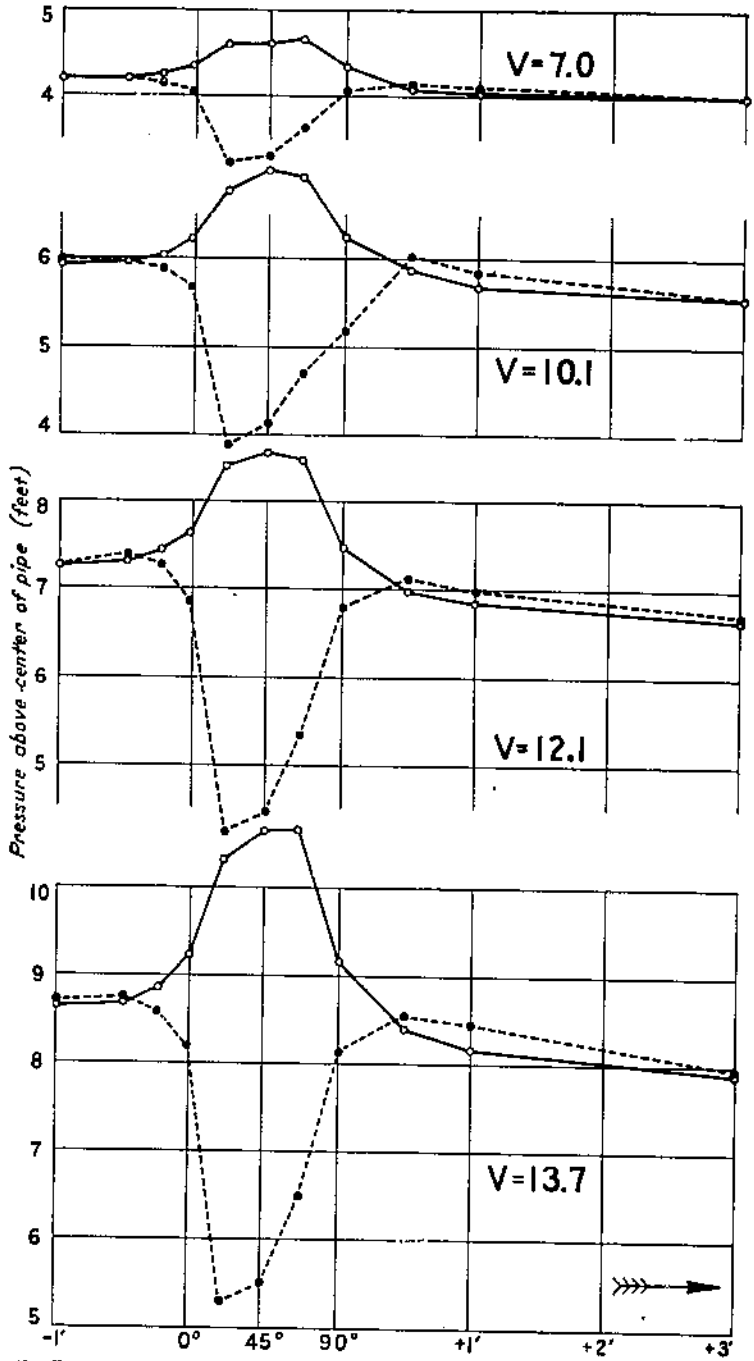

FIGURE 65.—Pressures along inner side (broken line) and outer side (solid line) of standard bend with uniform velocity distribution in approach tangent.

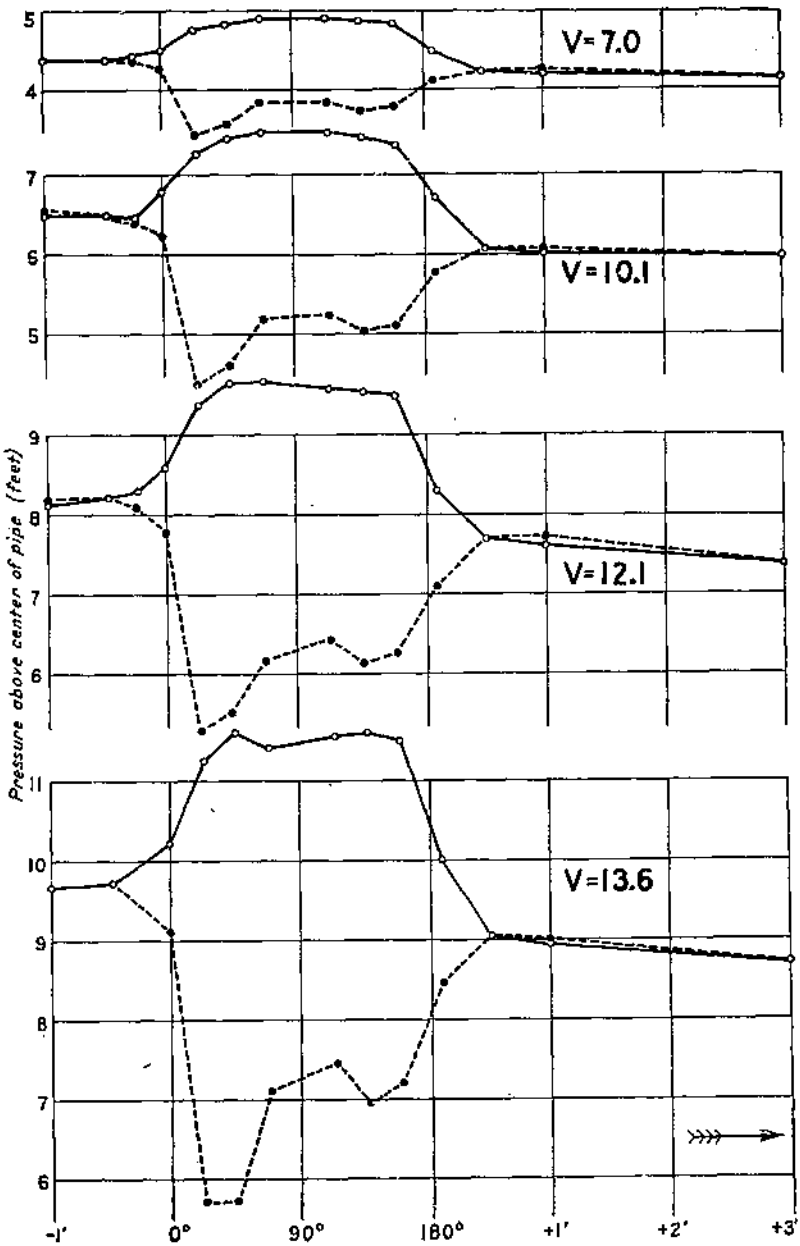

FIGURE 65.—Pressures along inner side (broken line) and outer side (solid line) of 180° continuous-curvature bend with uniform velocity distribution in approach tangent.

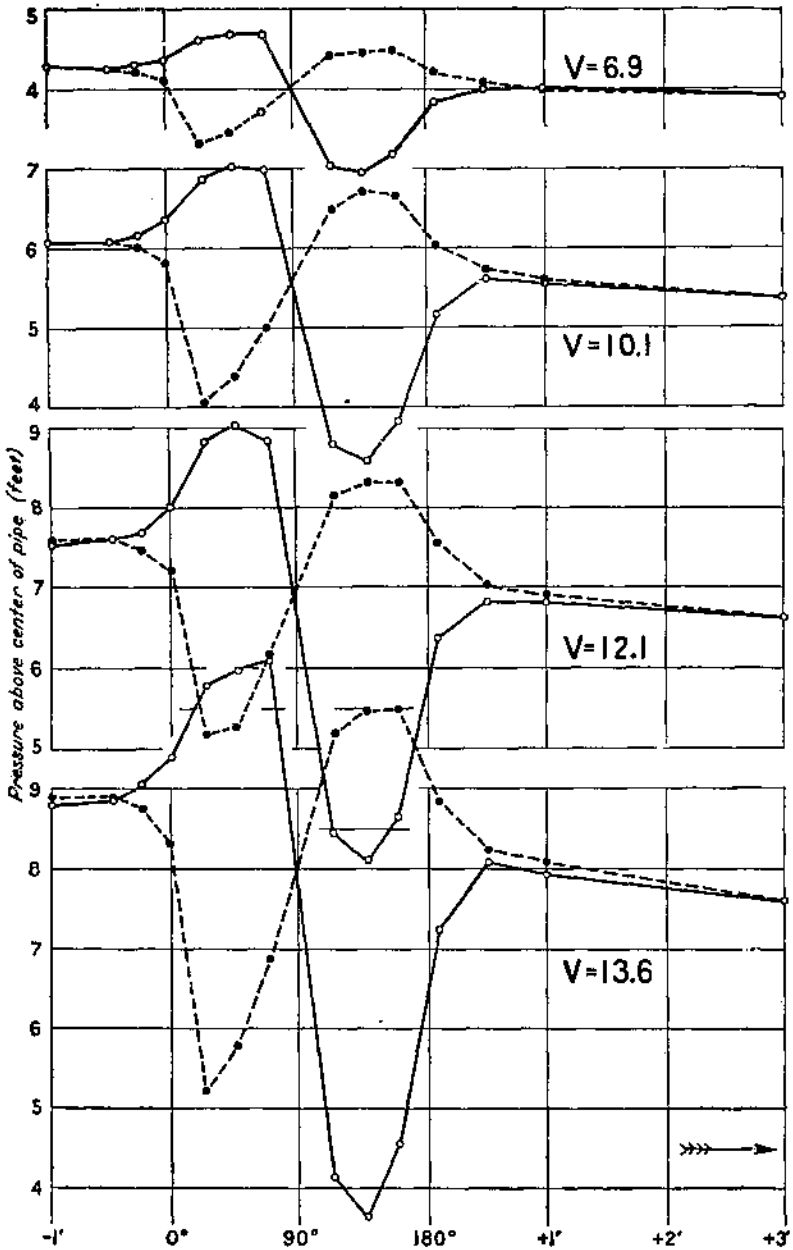

FIGURE 67.—Pressures along inner side (broken line) and outer side (solid line) of 180° reversed-curvature bend with uniform distribution in approach tangent.

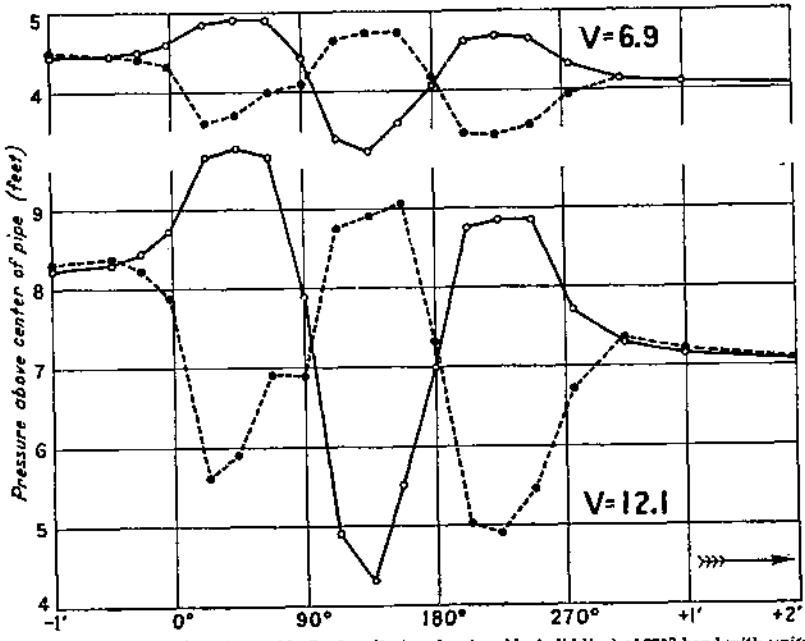

FIGURE 68.—Pressures along inner side (broken line) and outer side (solid line) of 270° bend with uniform velocity distribution in approach tangent.

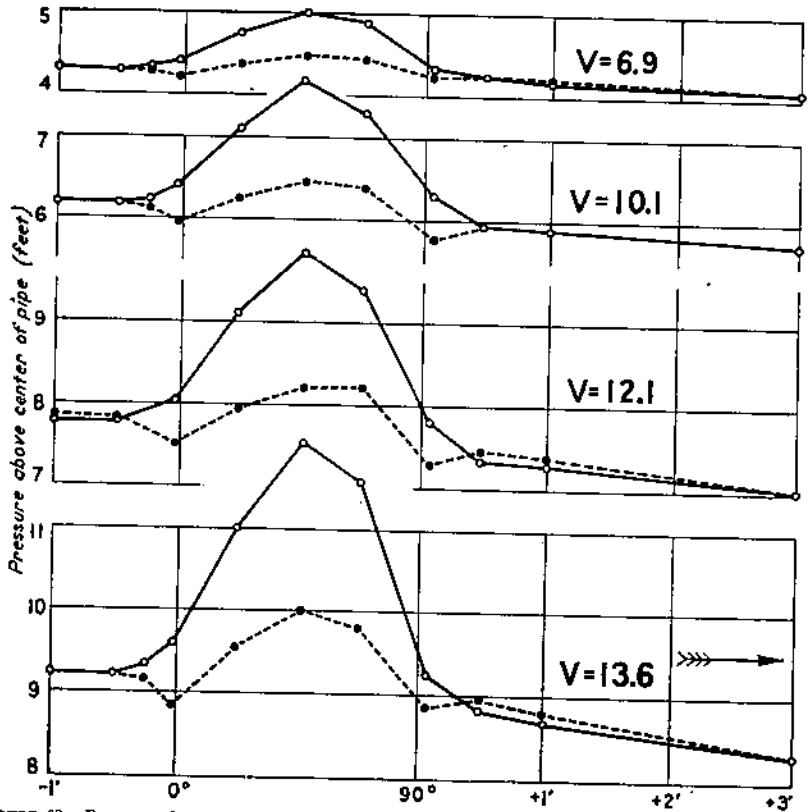

FIGURE 69.—Pressures along inner side (broken line) and outer side (solid line) of type M bend with uniform velocity distribution in approach tangent.

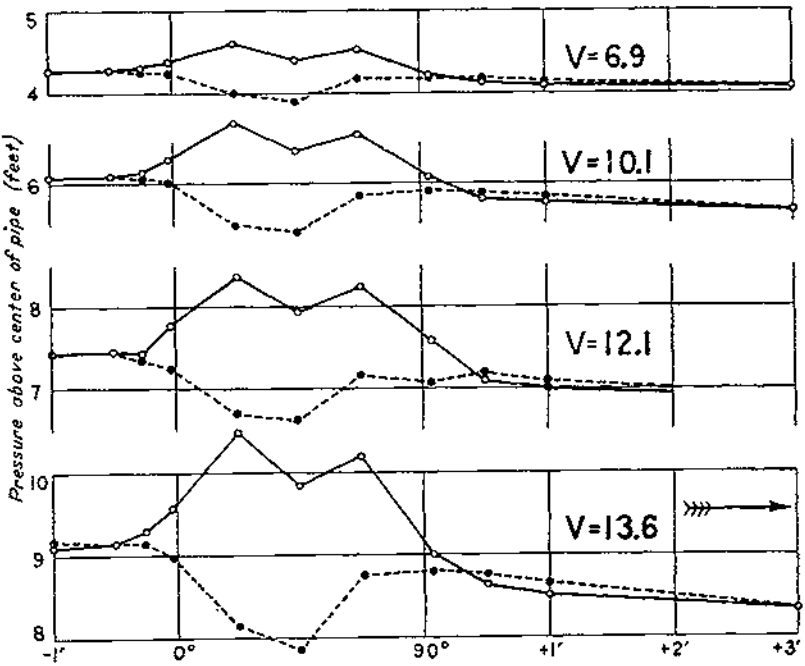

FIGURE 70.—Pressures along inner side (broken line) and outer side (solid line) of type N bend with uniform velocity distribution in approach tangent.

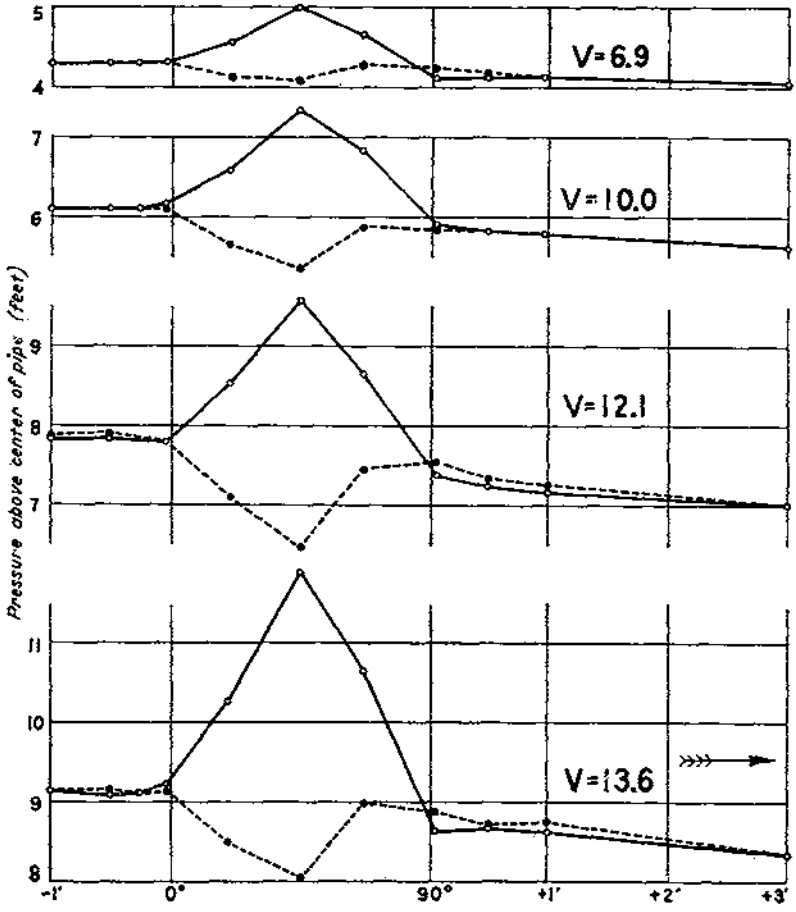

FIGURE 71.—Pressures along inner side (broken line) and outer side (solid line) of type W bend with uniform velocity distribution in approach tangent.

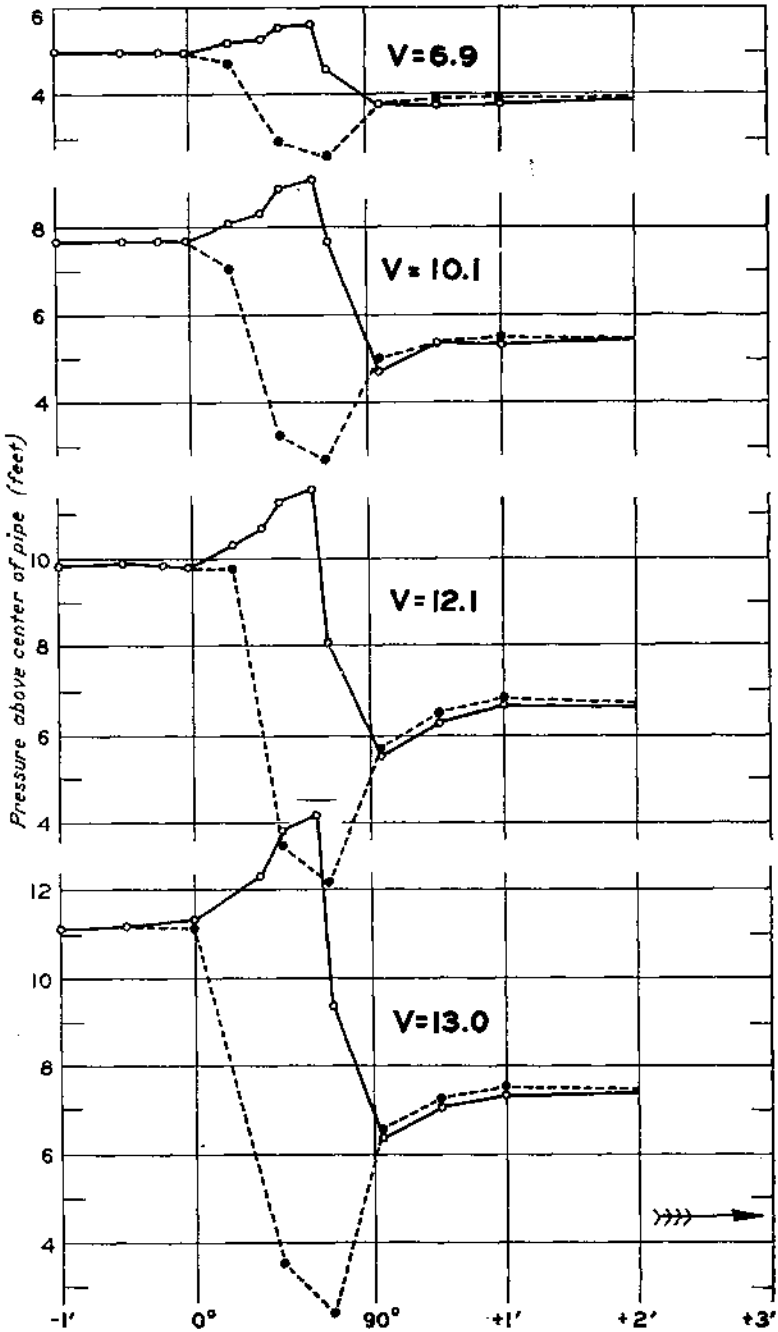

FIGURE 72.—Pressures along inner side (broken line) and outer side (solid line) of miter bend with uniform velocity distribution in approach tangent.

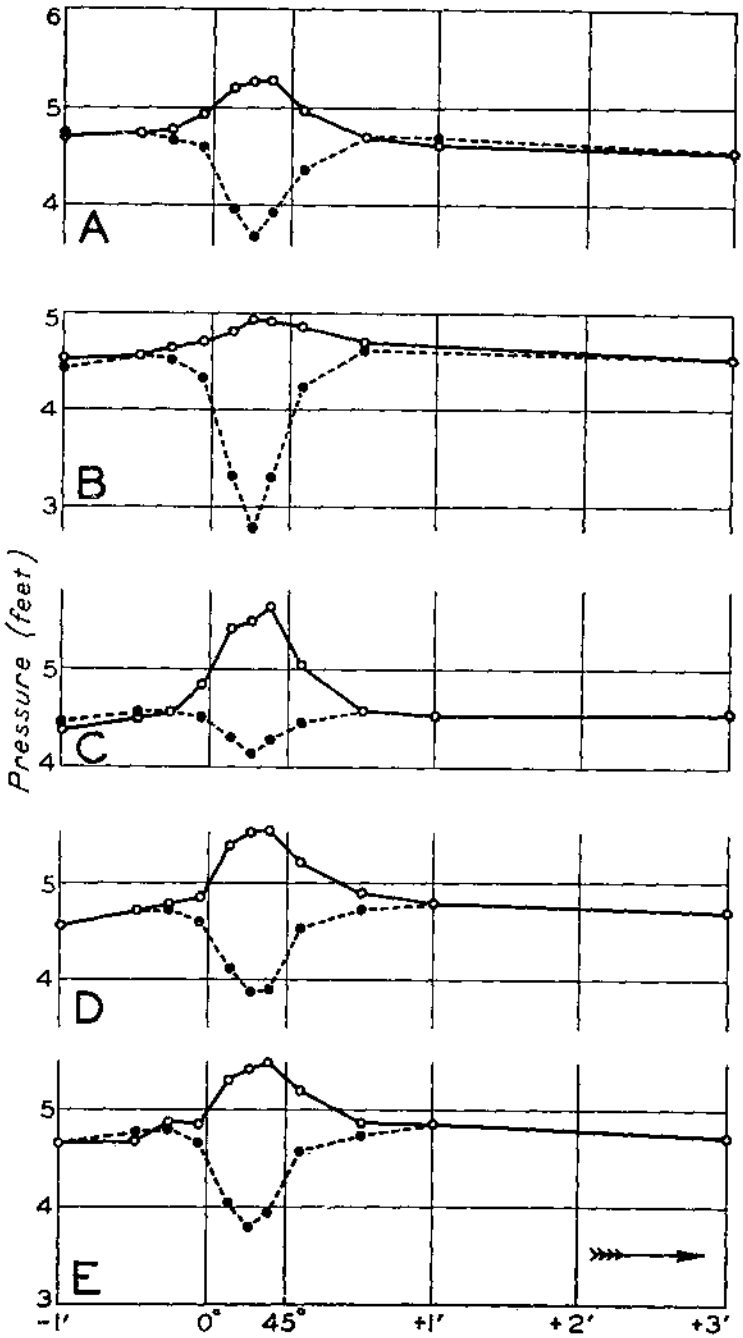

FIGURE 73.—Pressures along inner side (broken line) and outer side (solid line) of 45° bend with mean velocity 8 feet per second and velocity distribution in approach tangent: *A*, Uniform; *B*, high toward inner side; *C*, high toward outer side; *D*, high at top; *E*, high at bottom.

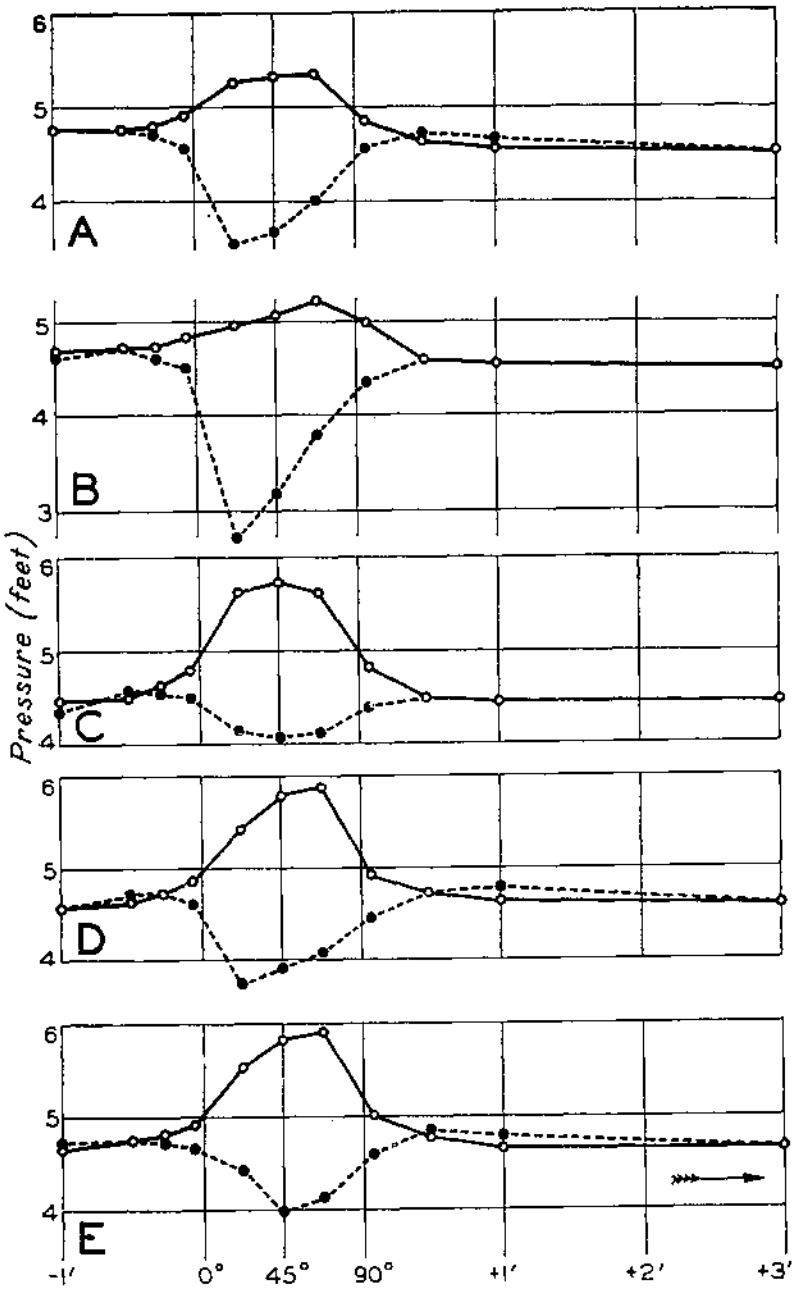

FIGURE 74.—Pressures along inner side (broken line) and outer side (solid line) of standard bend with mean velocity 8 feet per second and velocity distribution in approach tangent: *A*, Uniform; *B*, high toward inner side; *C*, high toward outer side; *D*, high at top; *E*, high at bottom.

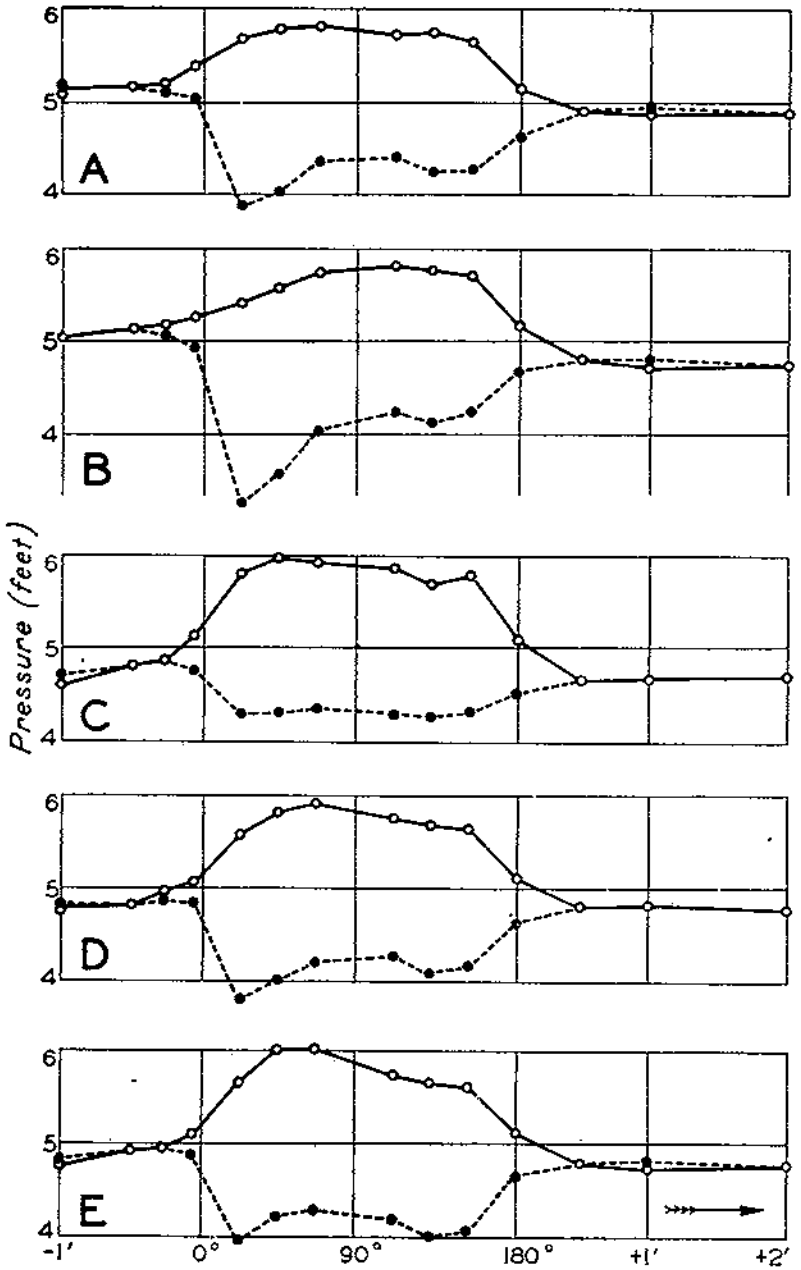

FIGURE 75.—Pressures along inner side (broken line) and outer side (solid line) of 180° continuous-curvature bend with mean velocity 8 feet per second and velocity distributions in approach tangent: *A*, Uniform; *B*, high toward inner side; *C*, high toward outer side; *D*, high at top; *E*, high at bottom.

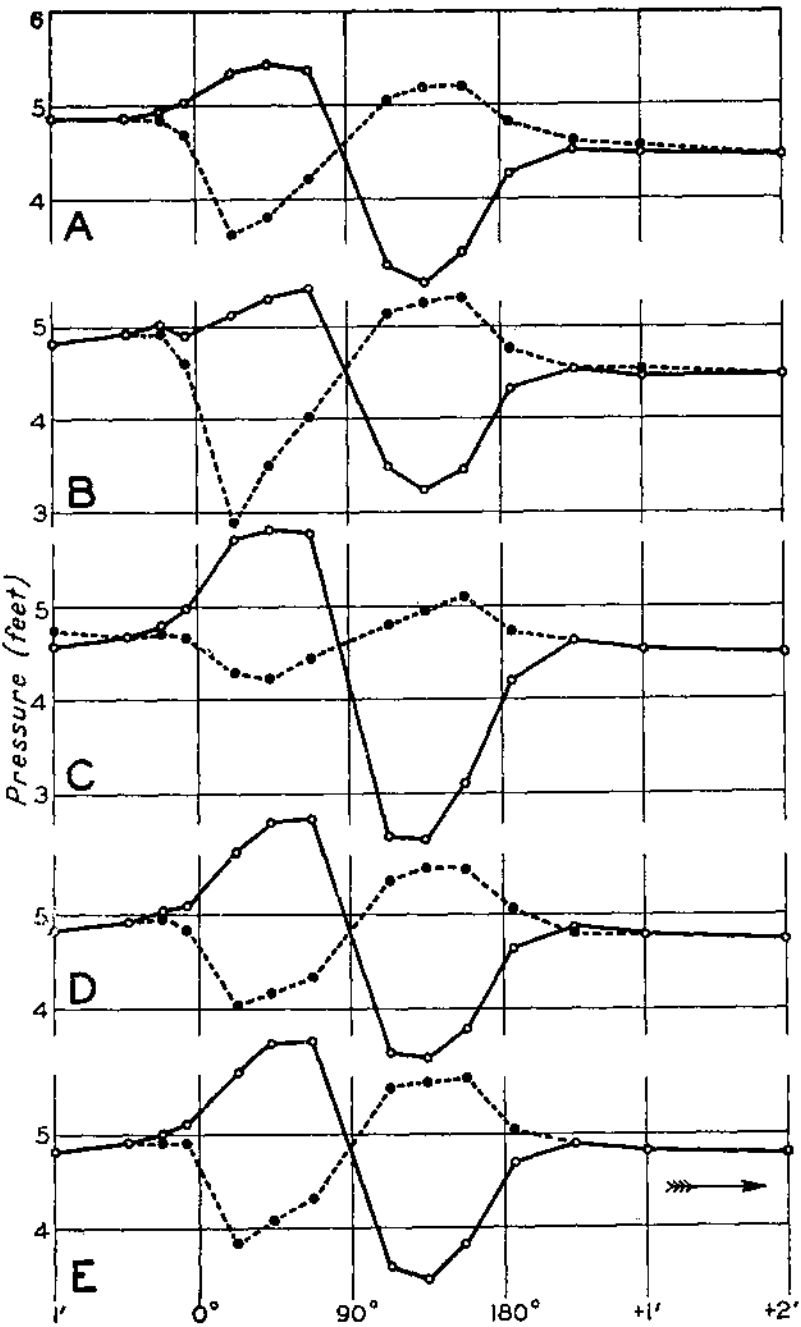

FIGURE 76.—Pressures along inner side (broken line) and outer side (solid line) of 180° reversed-curvature bend with mean velocity 8 feet per second and velocity distributions in approach tangent: *A*, Uniform; *B*, high toward inner side; *C*, high toward outer side; *D*, high at top; *E*, high at bottom.

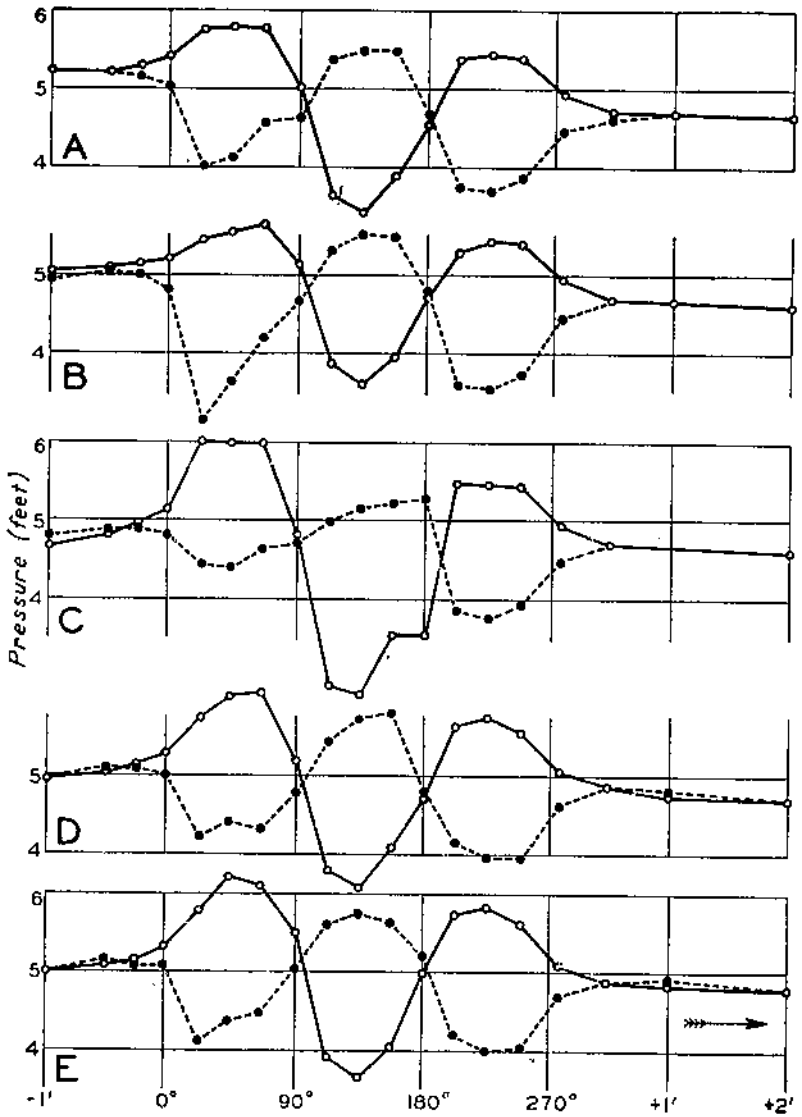

FIGURE 77.—Pressures along inner side (broken line) and outer side (solid line) of 270° bend with mean velocity 8 feet per second and velocity distributions in approach tangent: *A*, Uniform; *B*, high toward inner side; *C*, high toward outer side; *D*, high at top; *E*, high at bottom.

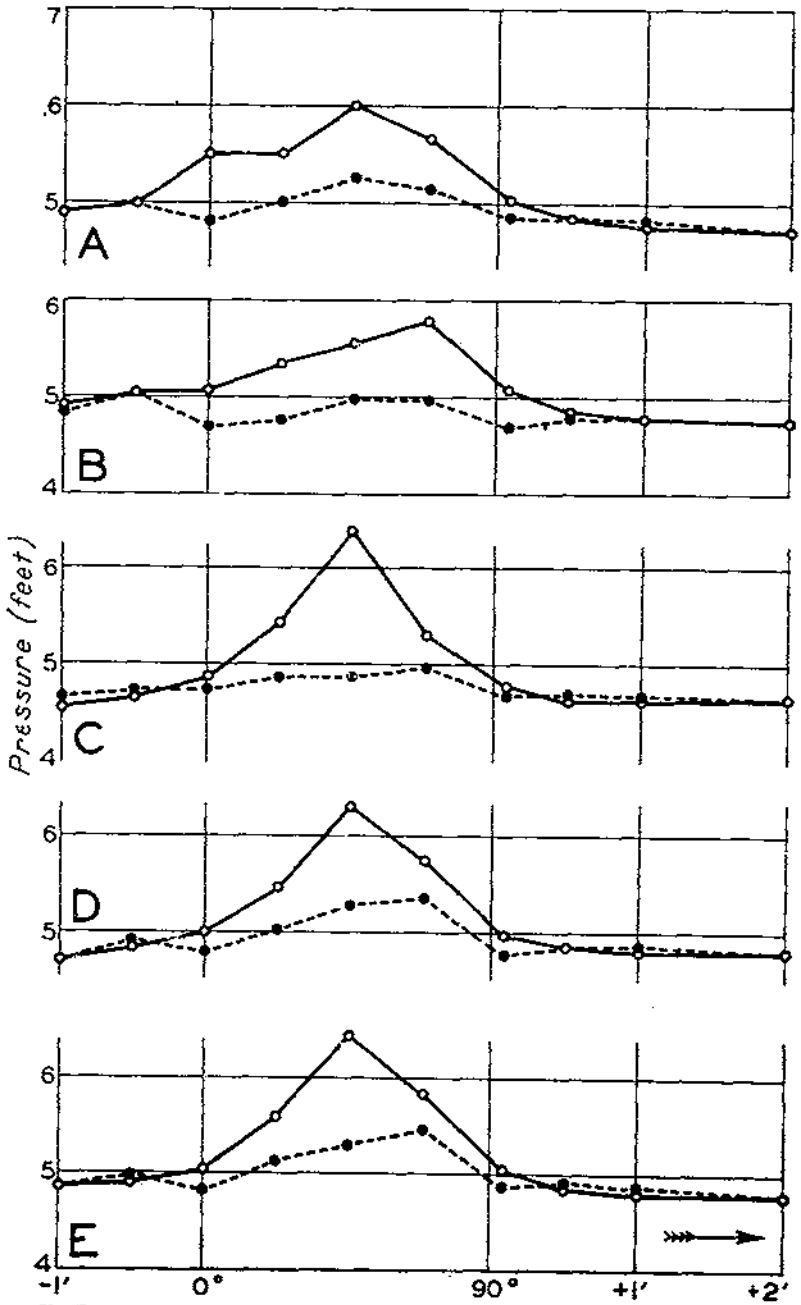

FIGURE 78.—Pressures along inner side (broken line) and outer side (solid line) of type M bend with mean velocity 8 feet per second and velocity distributions in approach tangent: *A*, Uniform; *B*, high toward inner side; *C*, high toward outer side; *D*, high at top; *E*, high at bottom.

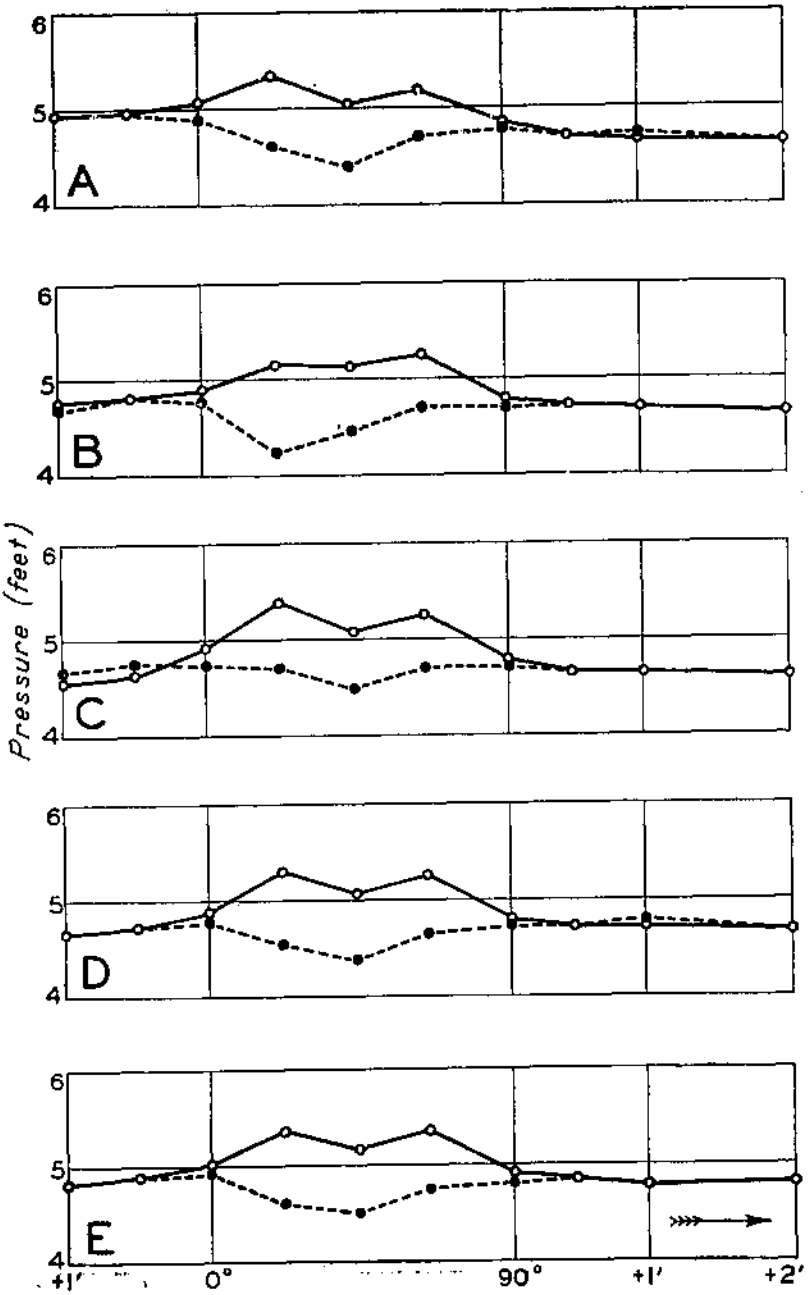

FIGURE 79.—Pressures along inner side (broken line) and outer side (solid line) of type N bend with mean velocity 8 feet per second and velocity distributions in approach tangent: *A*, Uniform; *B*, high toward inner side; *C*, high toward outer side; *D*, high at top; *E*, high at bottom.

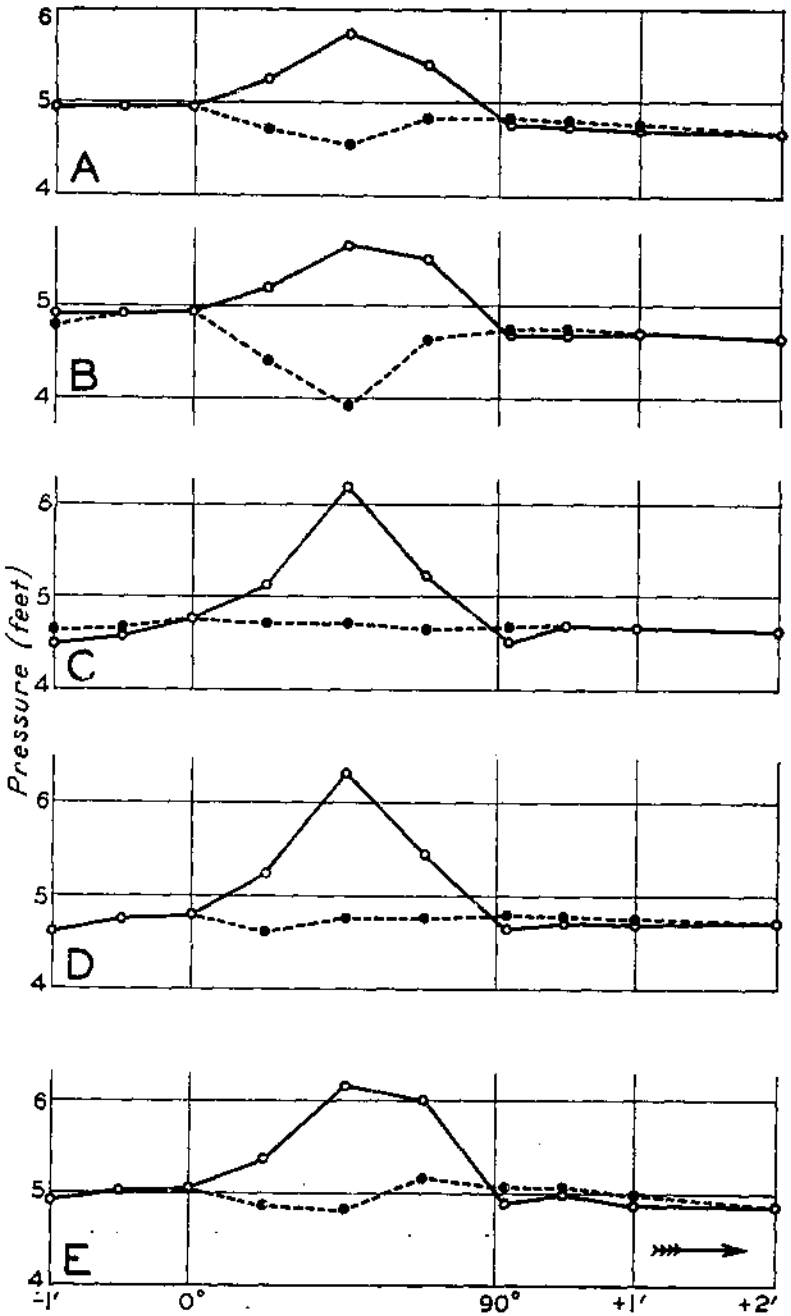

FIGURE 80.—Pressures along inner side (broken line) and outer side (solid line) of type W bend with mean velocity 8 feet per second and velocity distributions in approach tangent: *A*, Uniform; *B*, high toward inner side; *C*, high toward outer side; *D*, high at top; *E*, high at bottom.

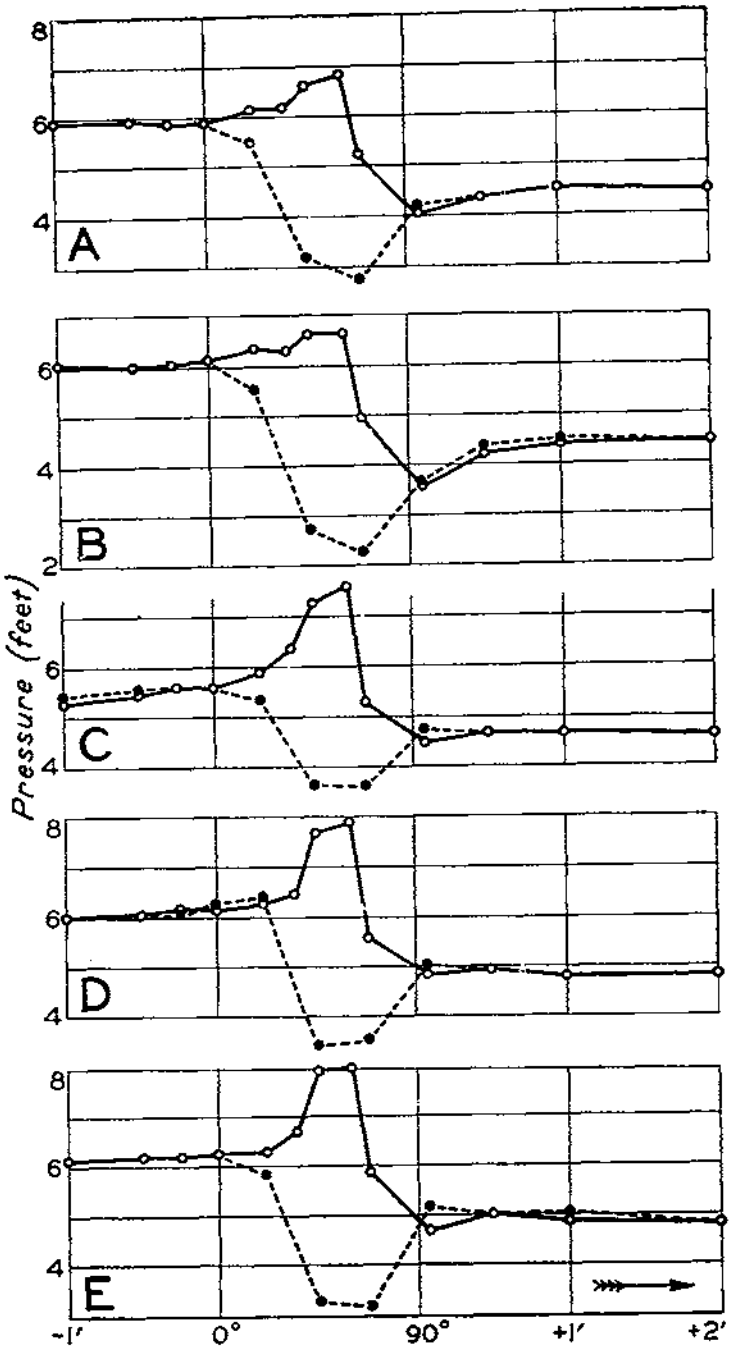

FIGURE 81.—Pressures along inner side (broken line) and outer side (solid line) of miter bend with mean velocity 8 feet per second and velocity distributions in approach tangent: *A*, Uniform; *B*, high toward inner side; *C*, high toward outer side; *D*, high at top; *E*, high at bottom.

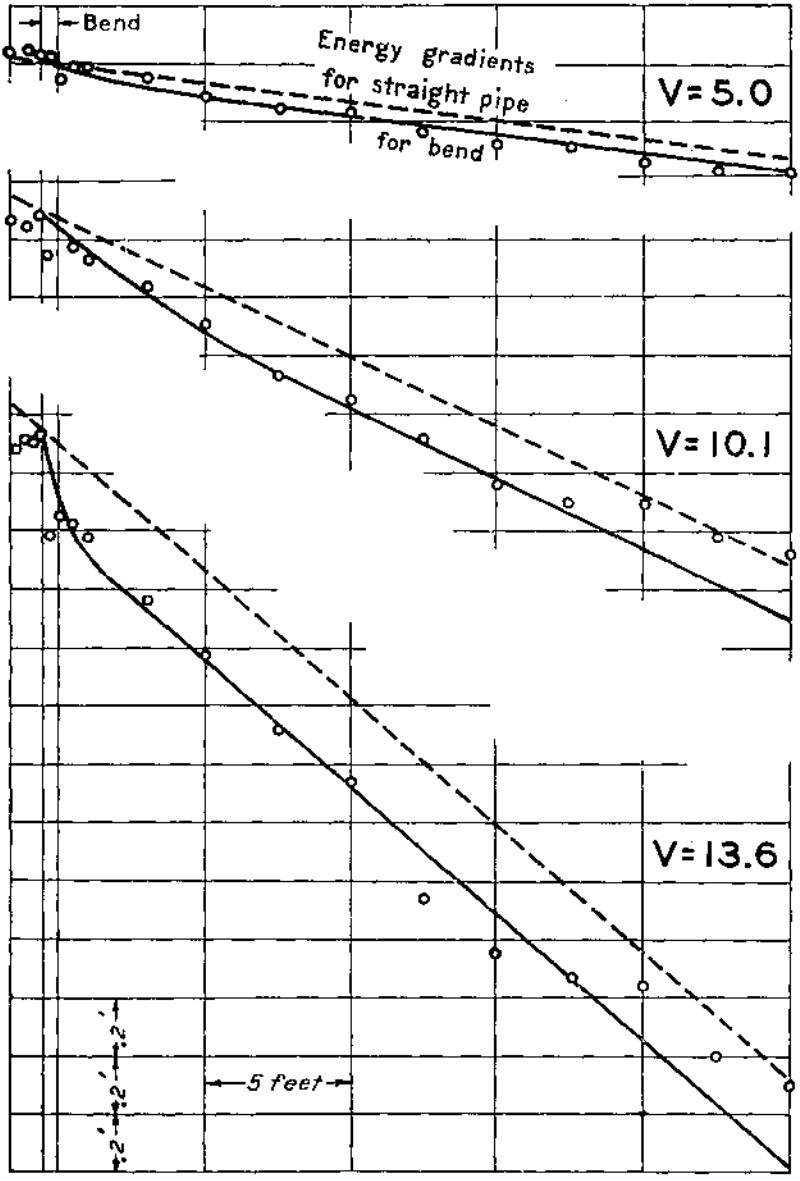

FIGURE 82.—Loss of head in 45° bend with uniform velocity distribution in approach tangent.

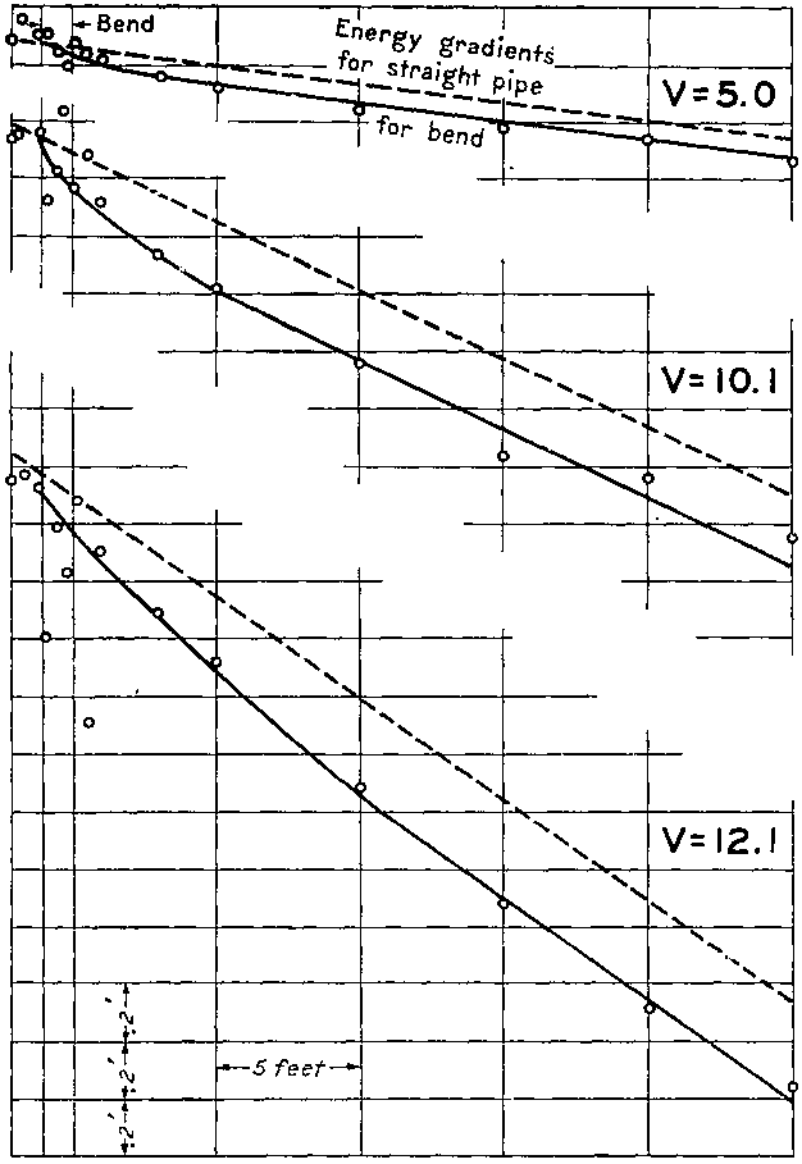

FIGURE 53.—Loss of head in standard bend with uniform velocity distribution in approach tangent.

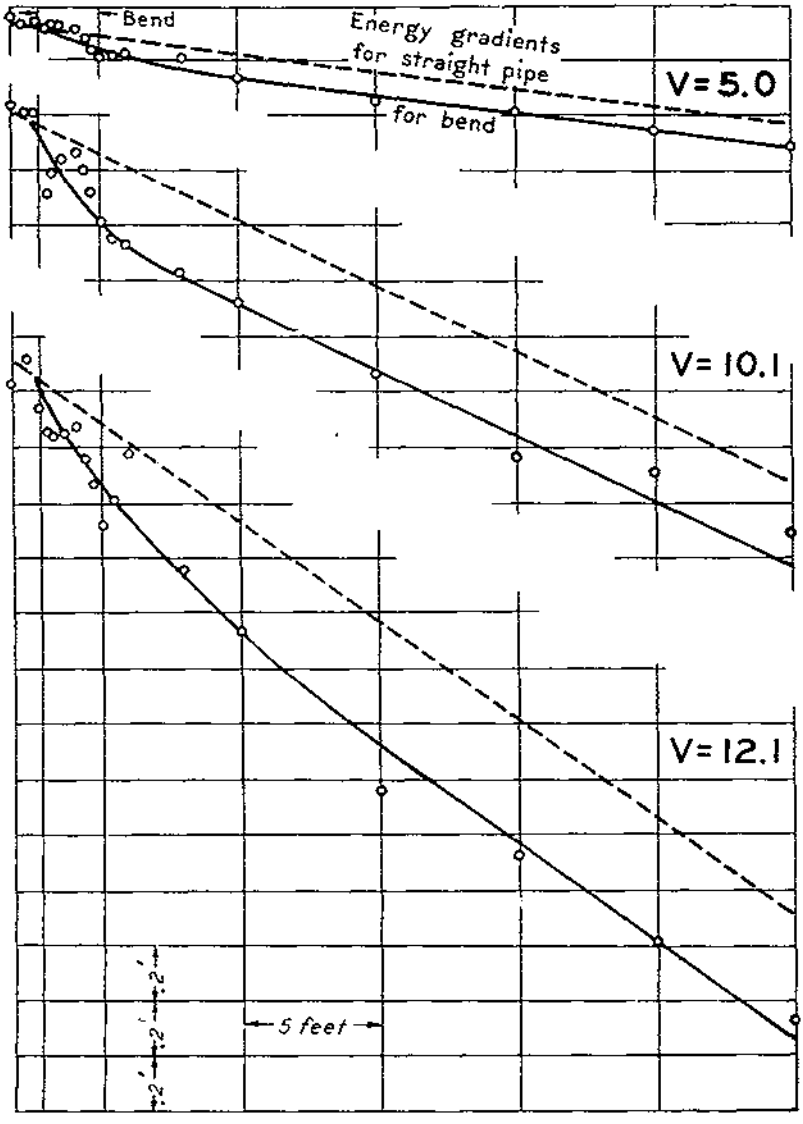

FIGURE 84.—Loss of head in 180° continuous-curvature bend with uniform velocity distribution in approach tangent.

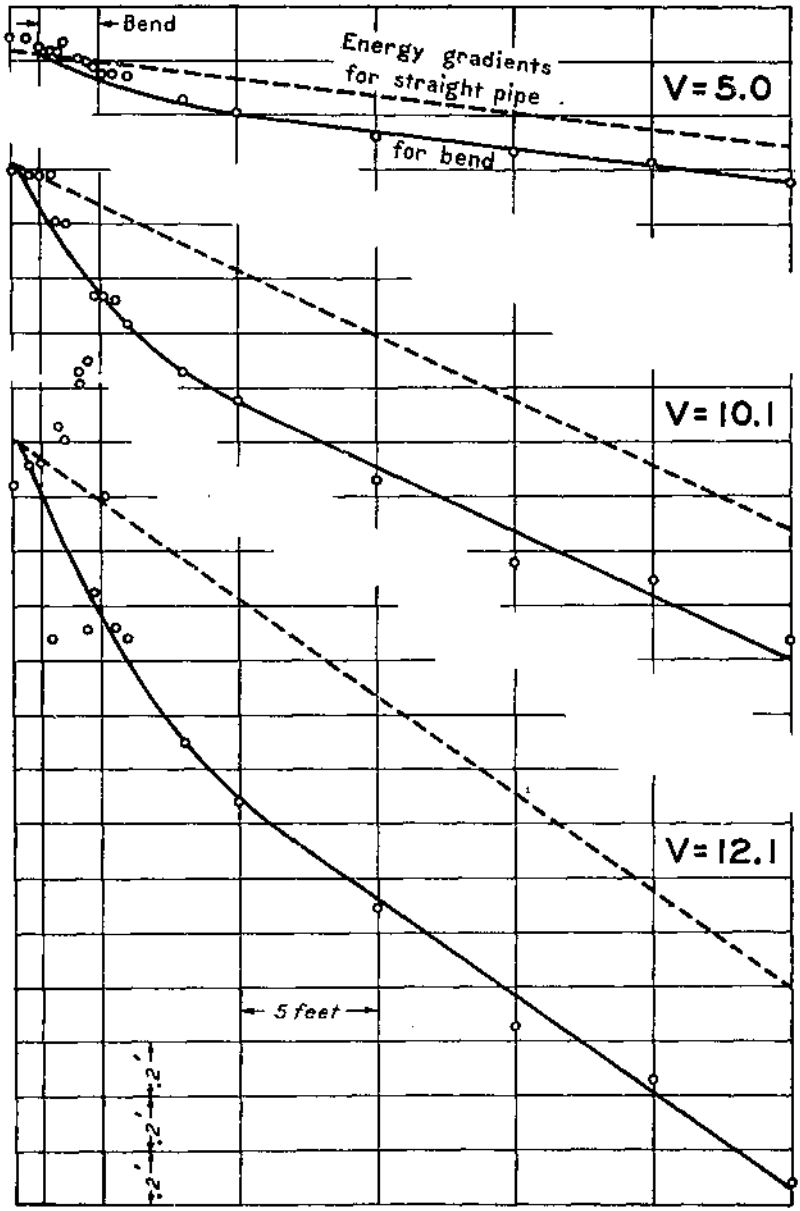

FIGURE 85.—Loss of head in 180° reversed-curvature bend with uniform velocity distribution in approach tangent.

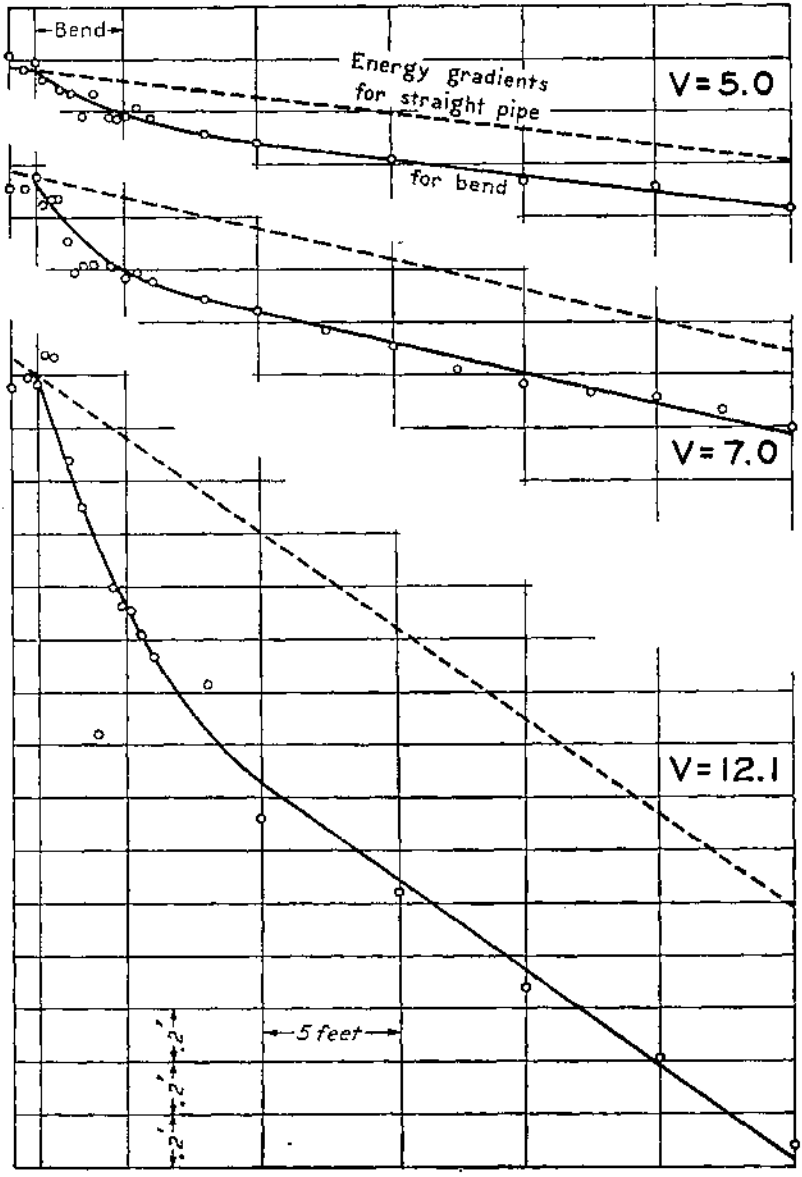

FIGURE 86.—Loss of head in 270° bend with uniform velocity distribution in approach tangent.

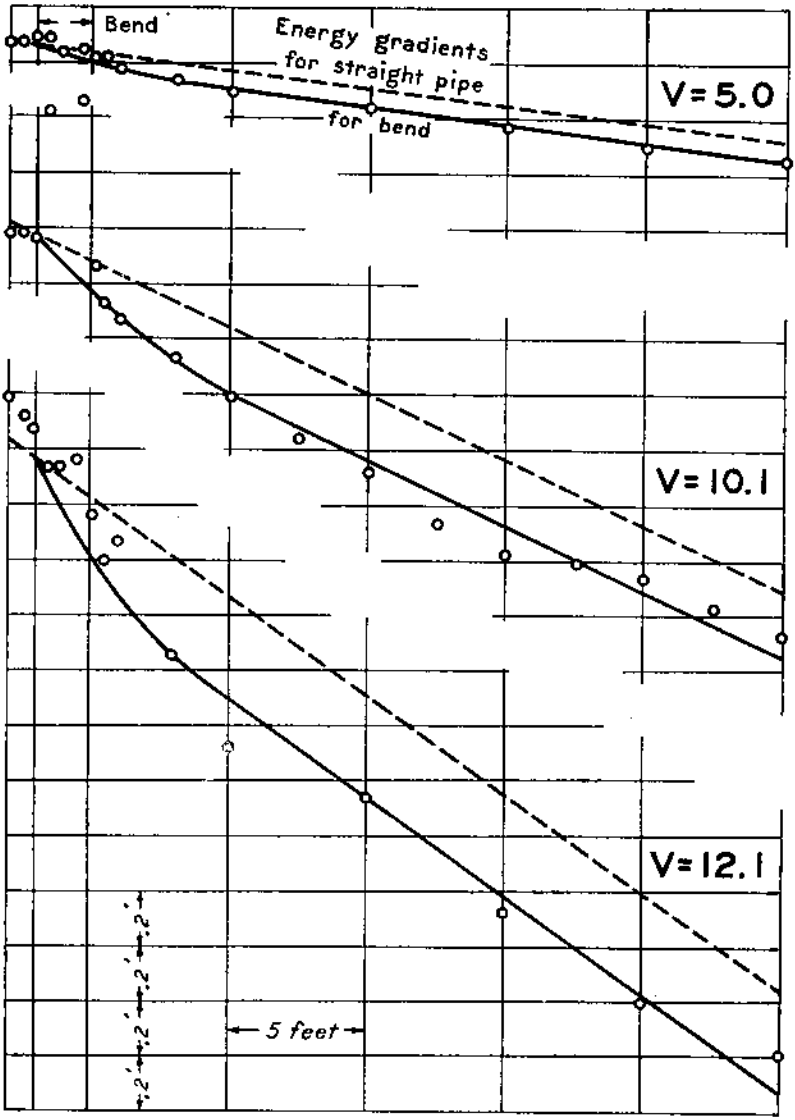

FIGURE 87.—Loss of head in type M bend with uniform velocity distribution in approach tangent.

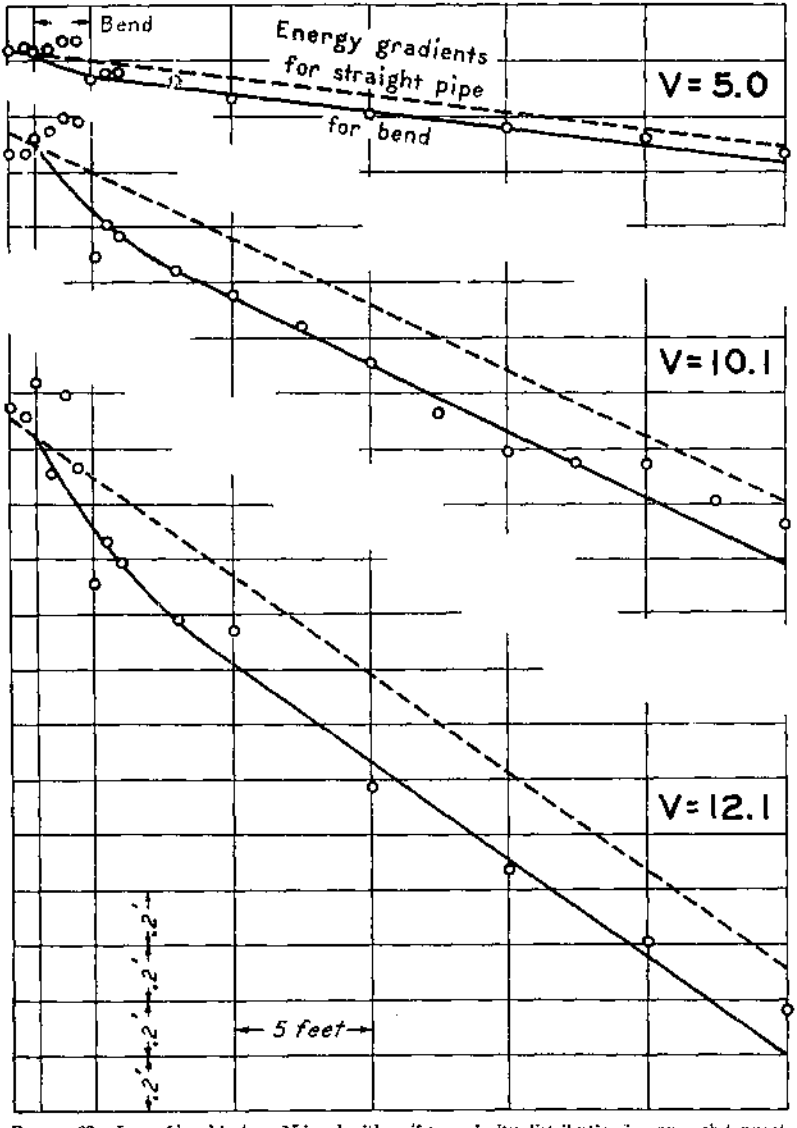

FIGURE 88.—Loss of head in type N bend with uniform velocity distribution in approach tangent.

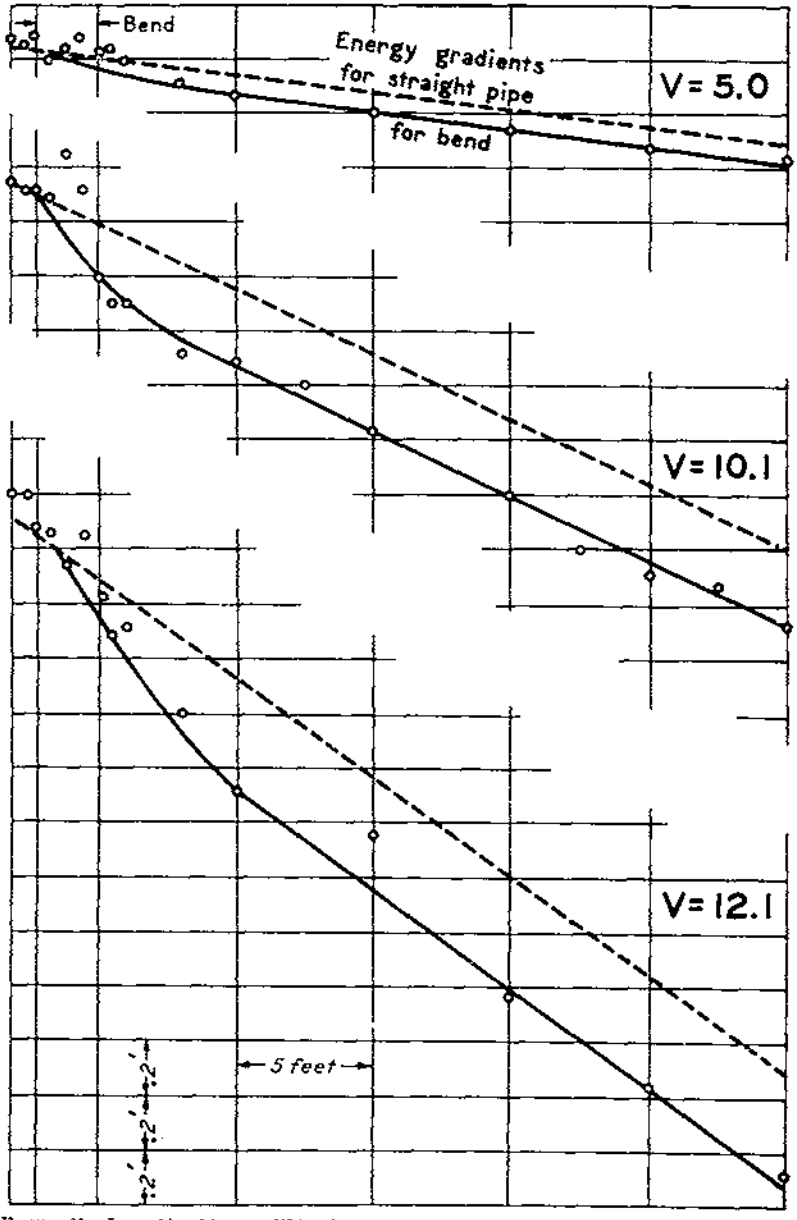

FIGURE 89.—Loss of head in type W bend with uniform velocity distribution in approach tangent.

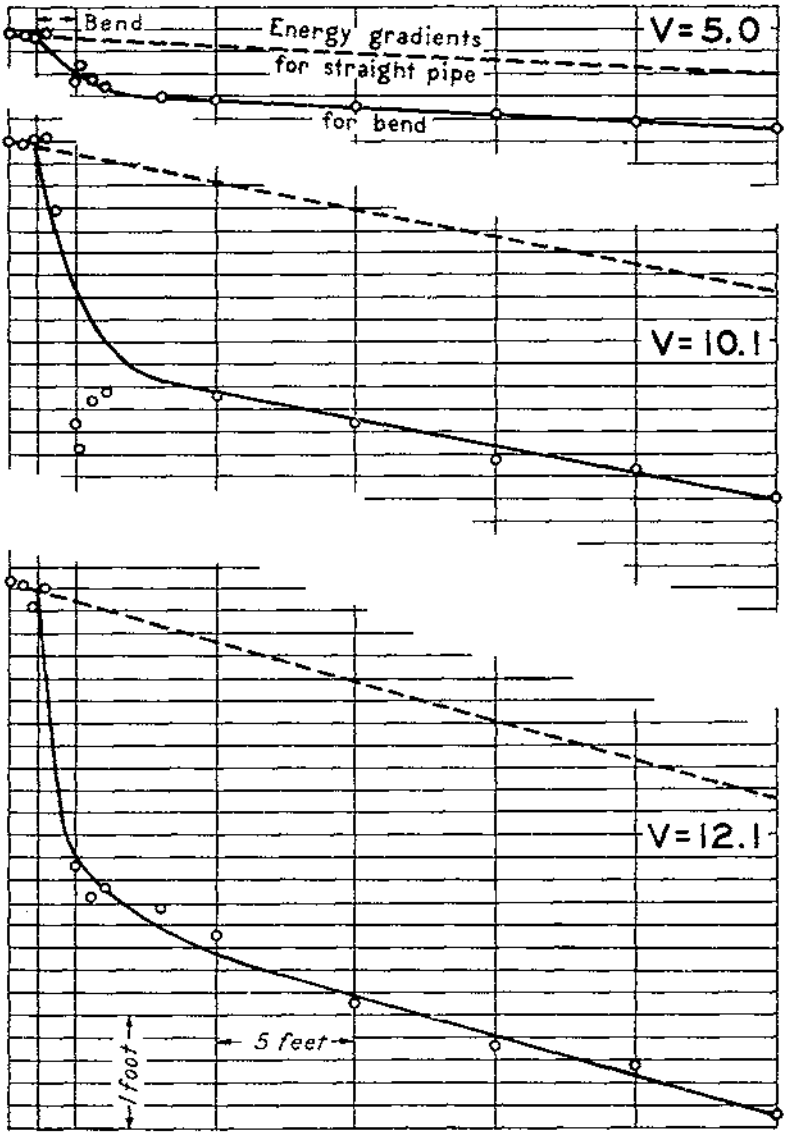

FIGURE 90.—Loss of head in miter bend with uniform velocity distribution in approach tangent.

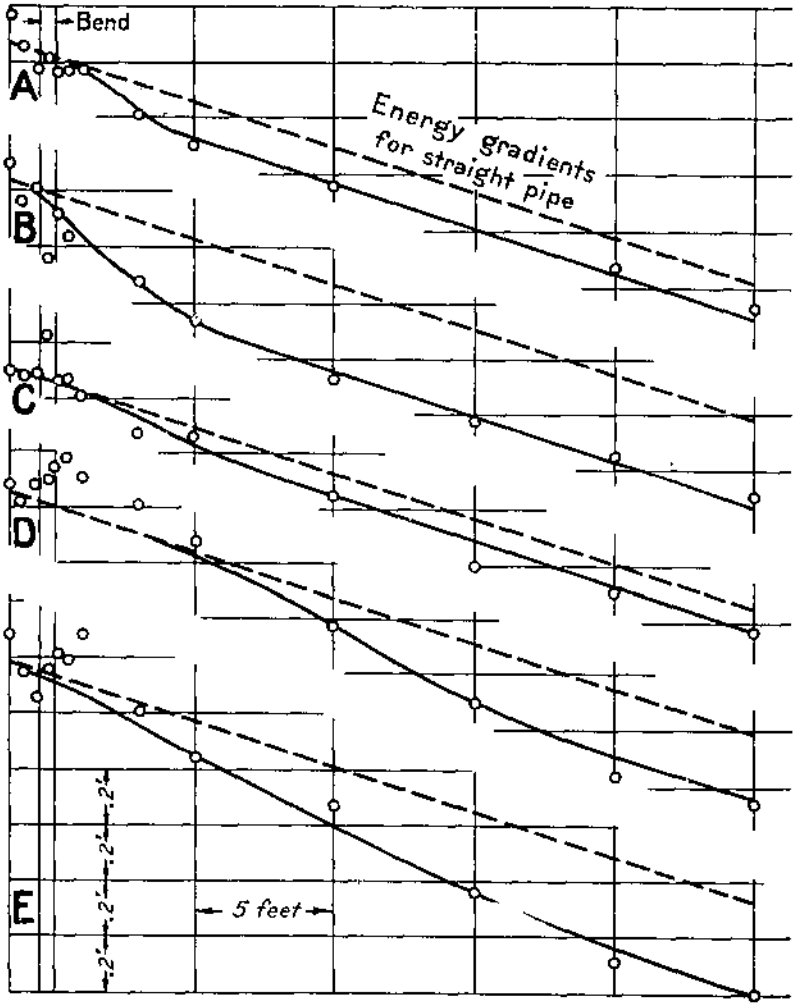

FIGURE 61.—Loss of head in 45° bend with mean velocity 8 feet per second and velocity distributions in approach tangent: *A*, Uniform; *B*, high toward inner side; *C*, high toward outer side; *D*, high at top; *E*, high at bottom.

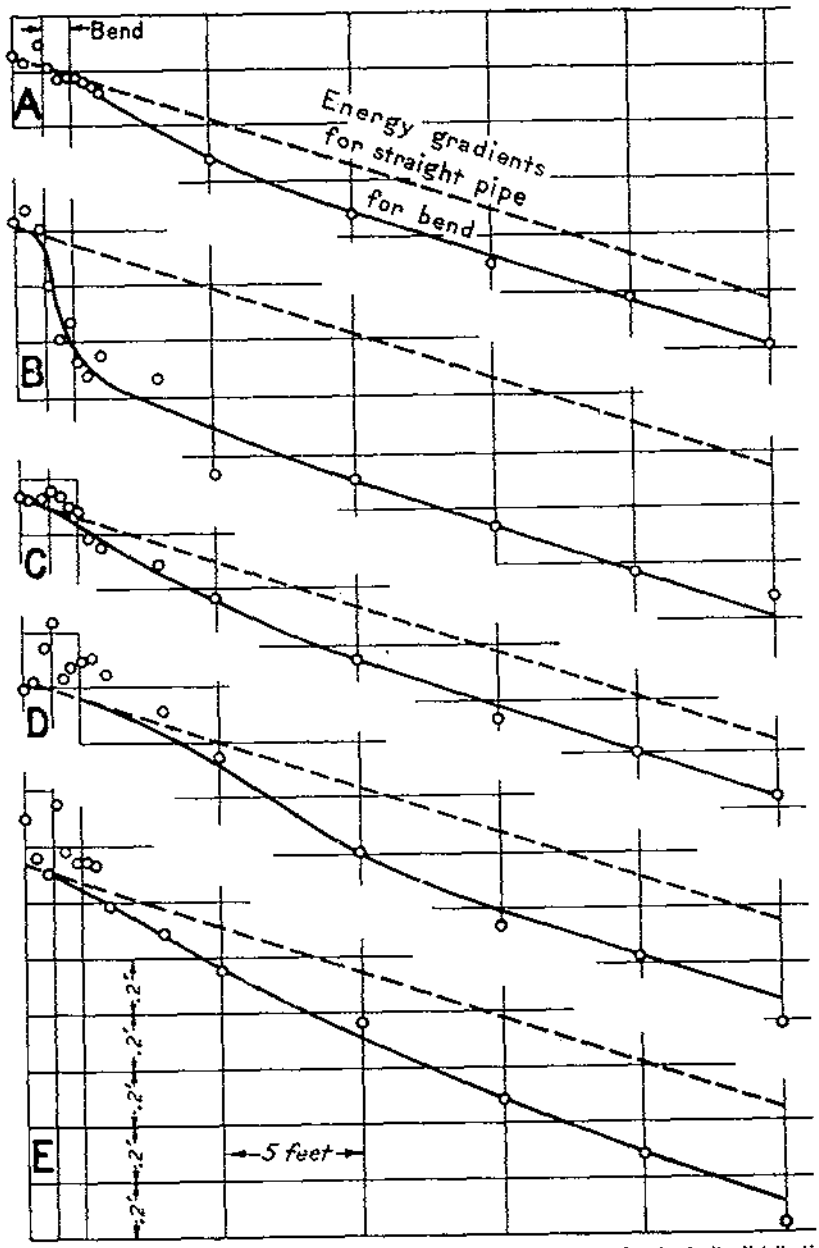

FIGURE 92.—Loss of head in standard bend with mean velocity 8 feet per second and velocity distributions in approach tangent: *A*, Uniform; *B*, high toward inner side; *C*, high toward outer side; *D*, high at top; *E*, high at bottom.

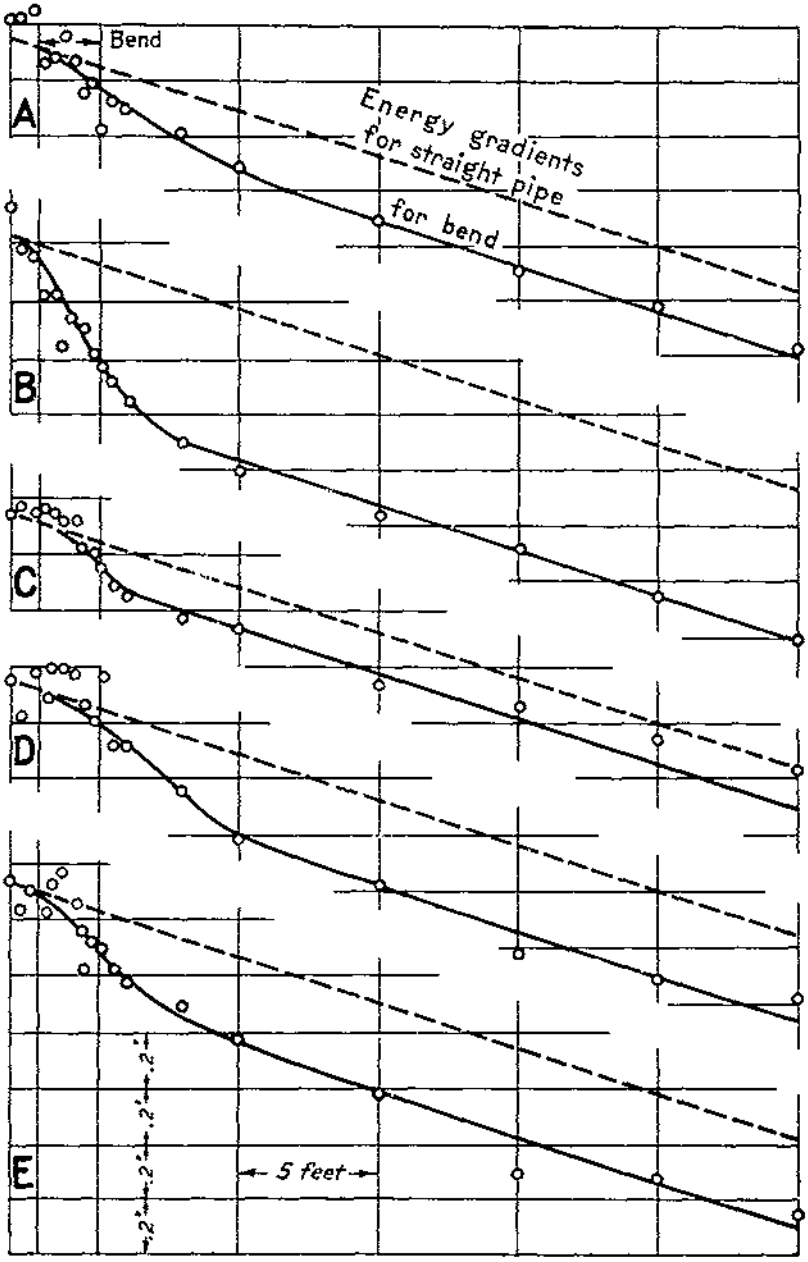

FIGURE 93.—Loss of head in 180° continuous-curvature bend with mean velocity 8 feet per second and velocity distributions in approach tangent: *A*, Uniform; *B*, high toward inner side; *C*, high toward outer side; *D*, high at top; *E*, high at bottom.

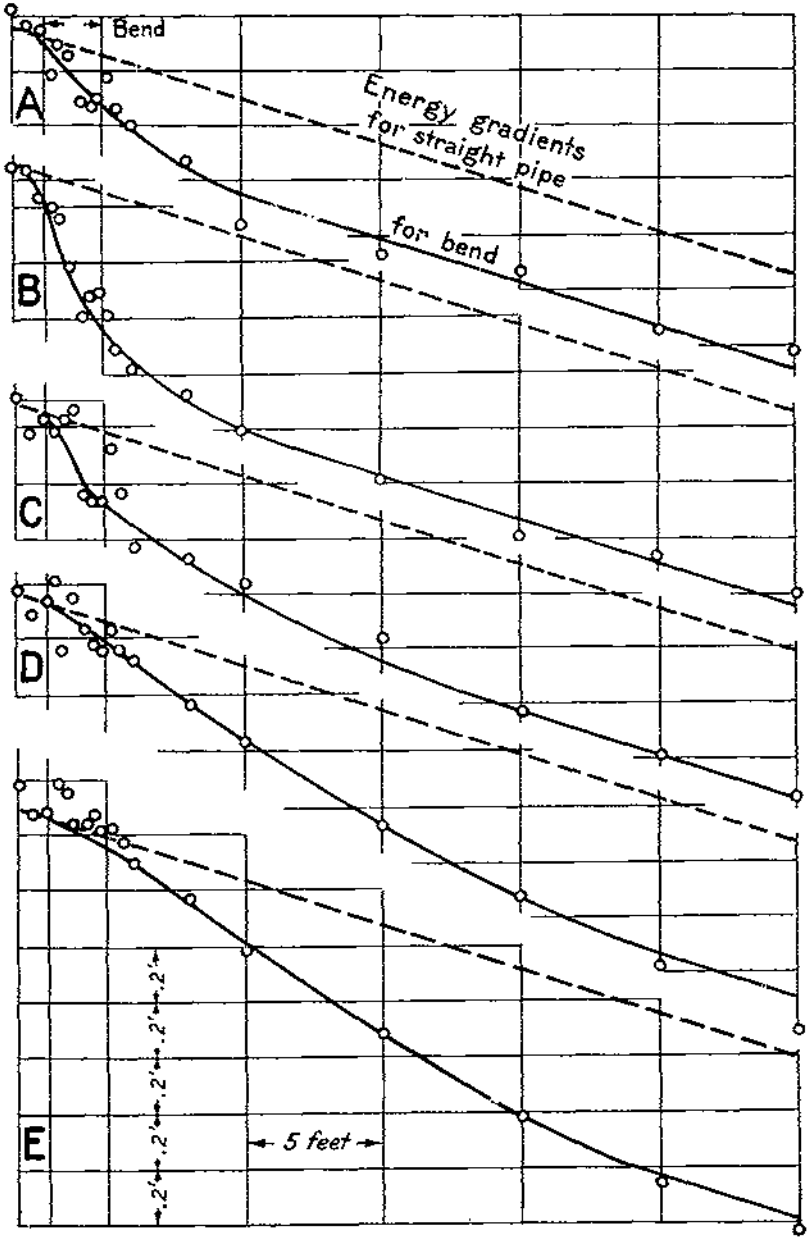

FIGURE 94.—Loss of head in 180° reversed-curvature bend with mean velocity 8 feet per second and velocity distributions in approach tangent: *A*, Uniform; *B*, high toward inner side; *C*, high toward outer side; *D*, high at top; *E*, high at bottom.

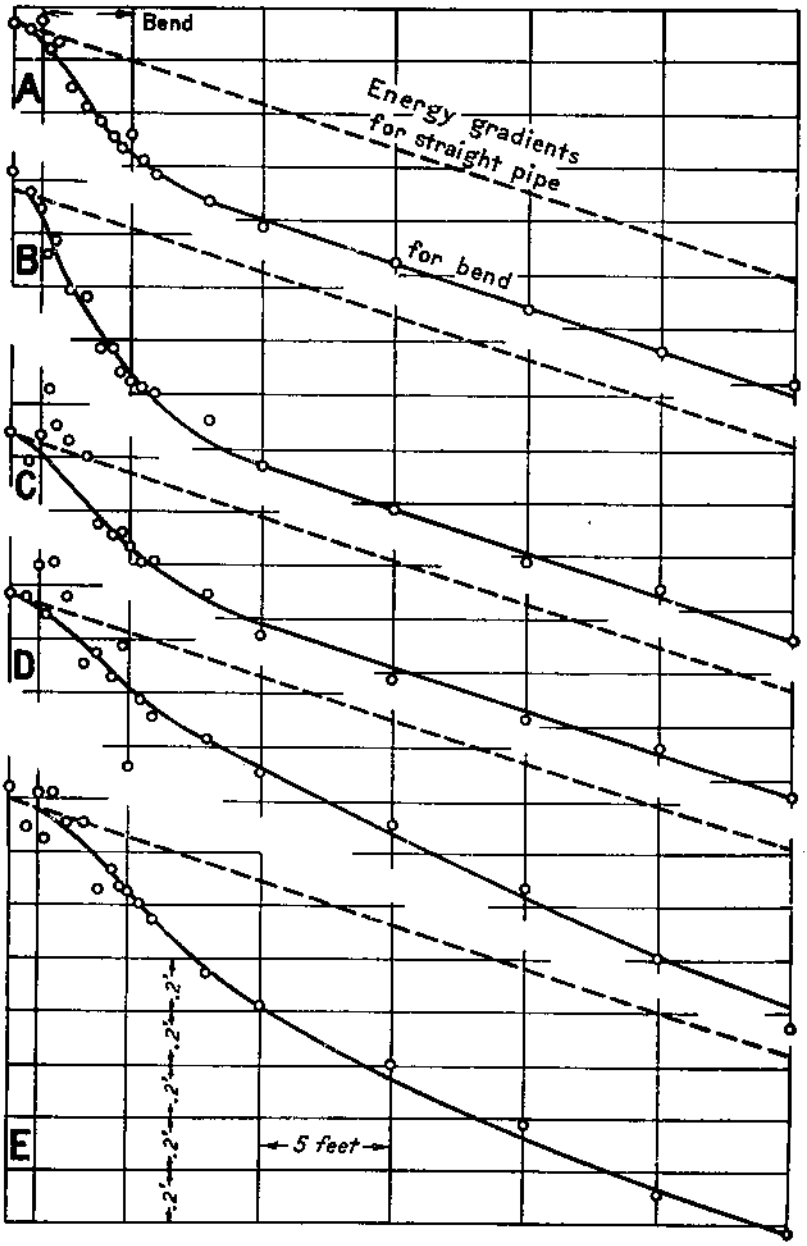

FIGURE 95.—Loss of head in 270° bend with mean velocity 8 feet per second and velocity distributions in approach tangent: *A*, Uniform; *B*, high toward inner side; *C*, high toward outer side; *D*, high at top; *E*, high at bottom.

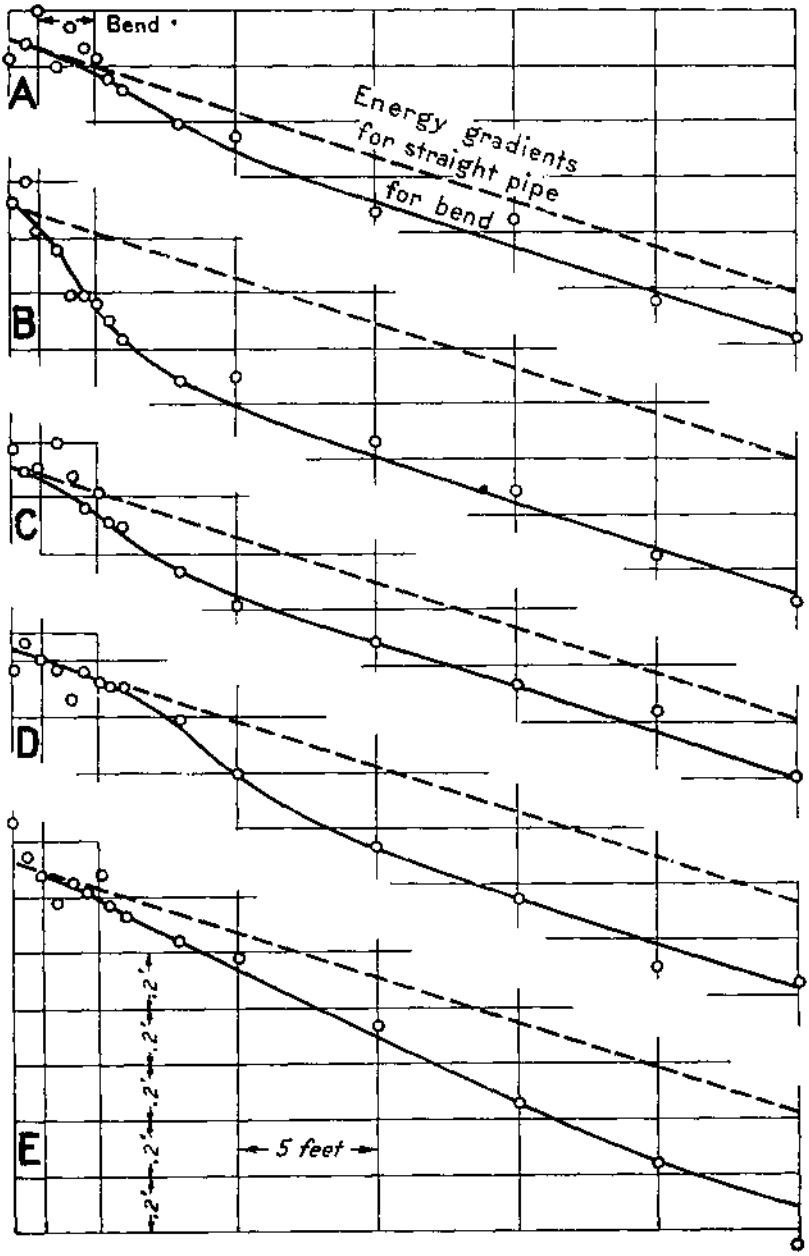

FIGURE 96.—Loss of head in type M bend with mean velocity 6 feet per second and velocity distributions in approach tangent: *A*, Uniform; *B*, high toward inner side; *C*, high toward outer side; *D*, high at top; *E*, high at bottom.

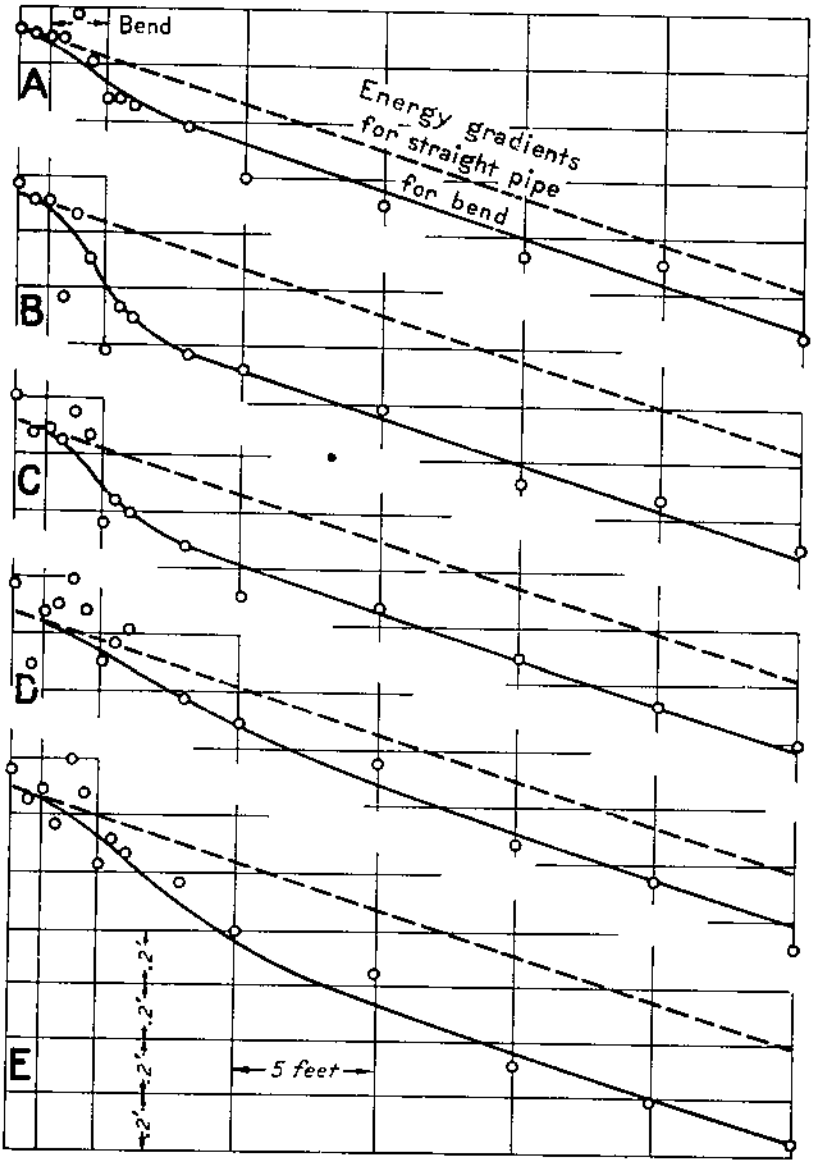

FIGURE 97.—Loss of head in type N bend with mean velocity 8 feet per second and velocity distributions in approach tangent: *A*, Uniform; *B*, high toward inner side; *C*, high toward outer side; *D*, high at top; *E*, high at bottom.

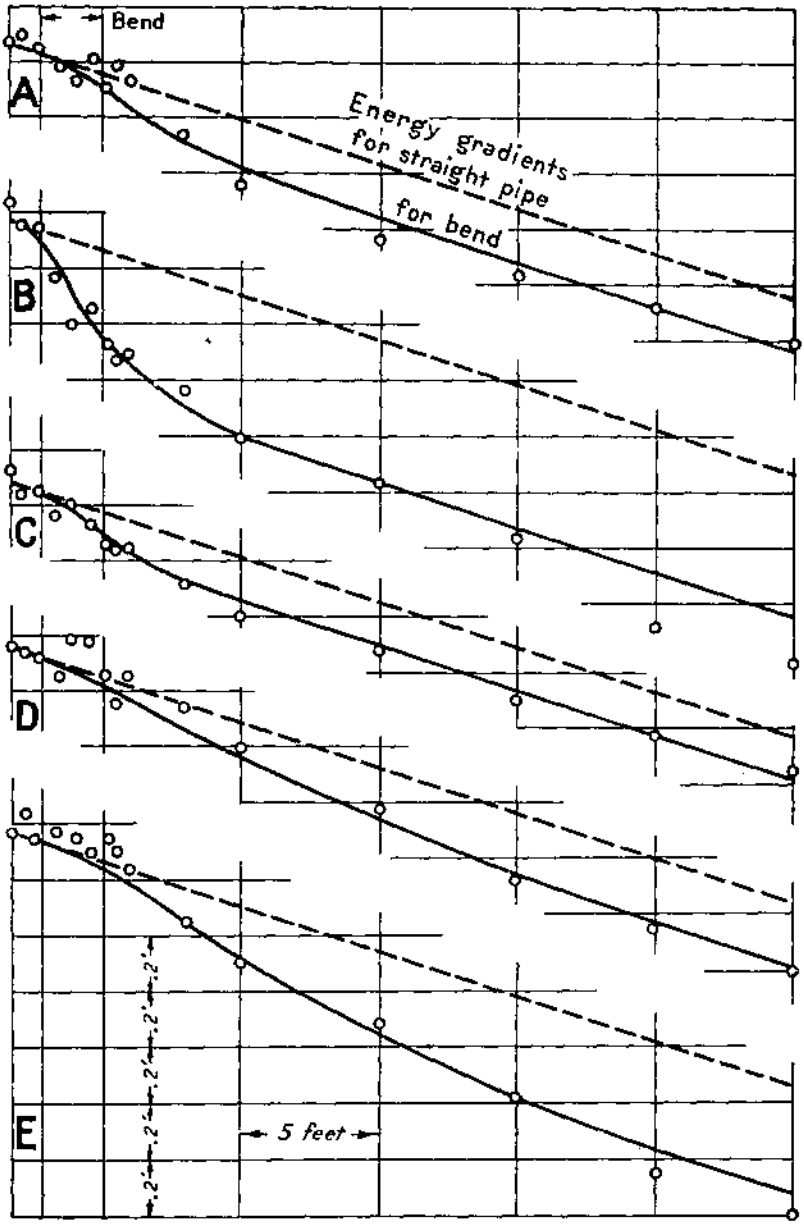

FIGURE 98.—Loss of head in type W bend with mean velocity 8 feet per second and velocity distributions in approach tangent: *A*, Uniform; *B*, high toward inner side; *C*, high toward outer side; *D*, high at top; *E*, high at bottom.

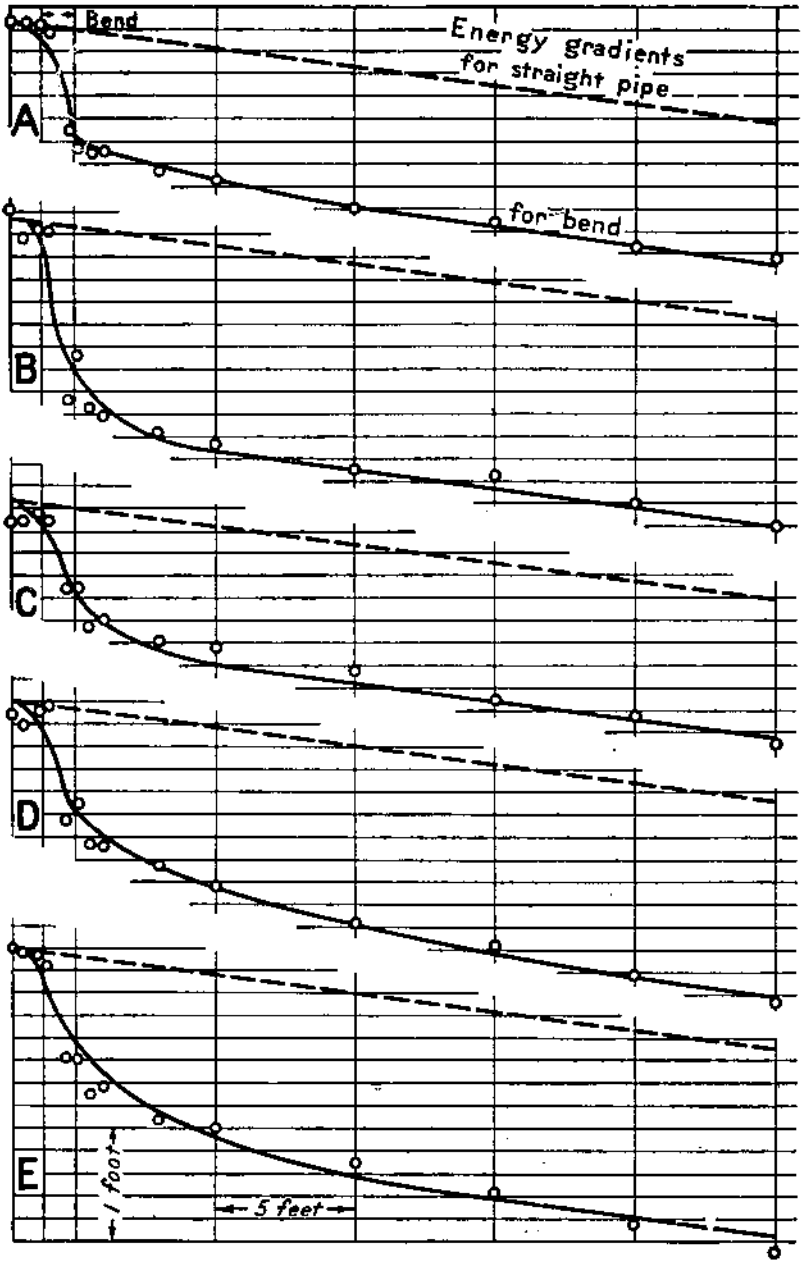

FIGURE 99.—Loss of head in miter bend with mean velocity 8 feet per second and velocity distributions in approach tangent: *A*, Uniform; *B*, high toward inner side; *C*, high toward outer side; *D*, high at top; *E*, high at bottom.

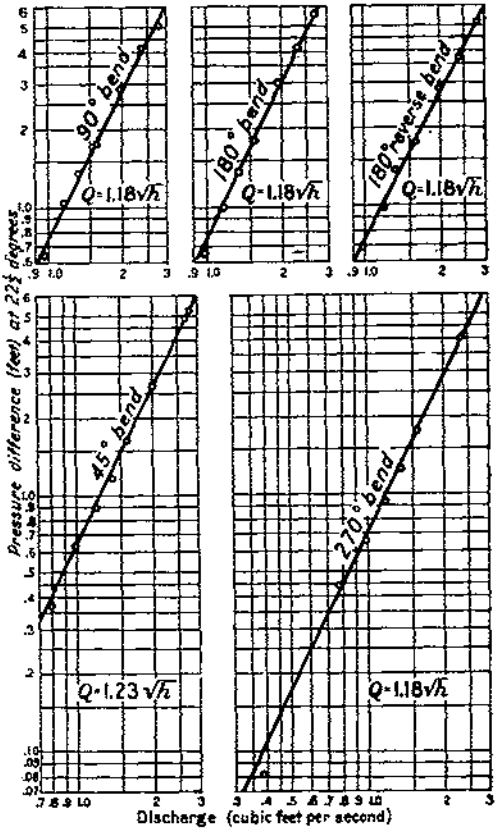

FIGURE 100.—Discharge through round-pipe bends for pressure differences at section 22½°.

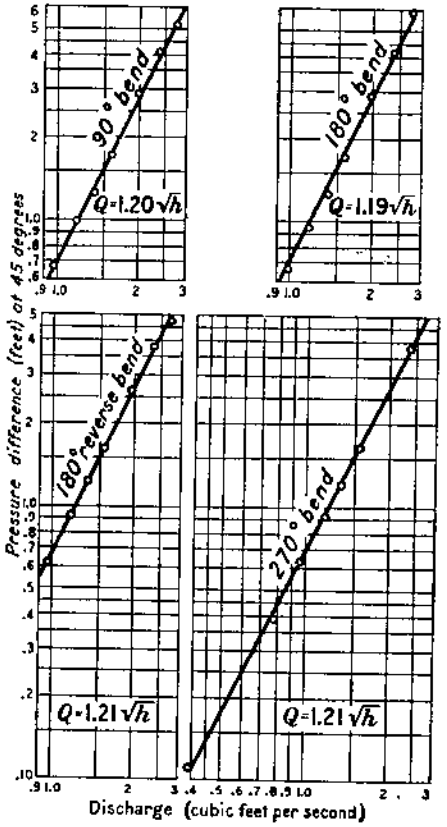

FIGURE 101.—Discharge through round-pipe bends for pressure differences at section 45°.

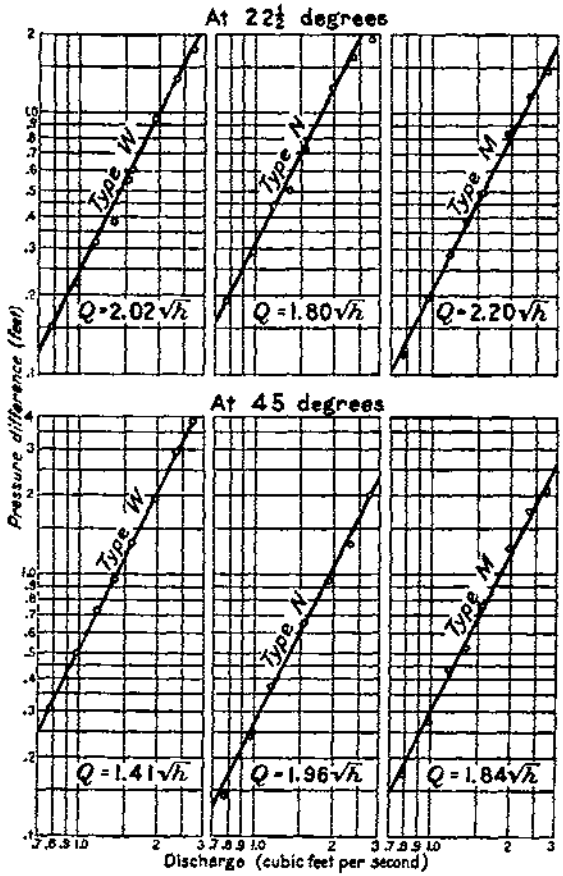

FIGURE 102.—Discharge through special-shape bends for pressure differences at sections 22½° and section 45°.

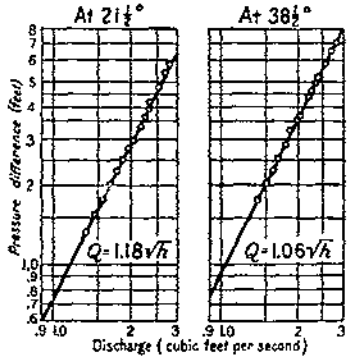

FIGURE 103.—Discharge through cast-iron 90° bend for pressure differences at sections 21½° and 38½°.

ORGANIZATION OF THE UNITED STATES DEPARTMENT OF AGRICULTURE WHEN THIS PUBLICATION WAS LAST PRINTED

Secretary of Agriculture	HENRY A. WALLACE.
Under Secretary	M. L. WILSON.
Assistant Secretary	HARRY L. BROWN.
Director of Extension Work	C. W. WARBURTON.
Director of Finance	W. A. JUMP.
Director of Information	M. S. EISENHOWER.
Director of Personnel	W. W. STOCKBERGER.
Director of Research	JAMES T. JARDINE.
Solicitor	MASTIN G. WHITE.
Agricultural Adjustment Administration	H. R. TOLLEY, *Administrator.*
Bureau of Agricultural Economics	A. G. BLACK, *Chief.*
Bureau of Agricultural Engineering	S. H. MCCRORY, *Chief.*
Bureau of Animal Industry	JOHN R. MOHLER, *Chief.*
Bureau of Biological Survey	IRA N. GABRIELSON, *Chief.*
Bureau of Chemistry and Soils	HENRY G. KNIGHT, *Chief.*
Commodity Exchange Administration	J. W. T. DUVEL, *Chief.*
Bureau of Dairy Industry	O. E. REED, *Chief.*
Bureau of Entomology and Plant Quarantine	LEE A. STRONG, *Chief.*
Office of Experiment Stations	JAMES T. JARDINE, *Chief.*
Food and Drug Administration	WALTER G. CAMPBELL, *Chief.*
Forest Service	FERDINAND A. SILCOX, *Chief.*
Bureau of Home Economics	LOUISE STANLEY, *Chief.*
Library	CLARIBEL R. BARNETT, *Librarian.*
Bureau of Plant Industry	FREDERICK D. RICHEY, *Chief.*
Bureau of Public Roads	THOMAS H. MACDONALD, *Chief.*
Farm Security Administration	W. W. ALEXANDER, *Administrator.*
Soil Conservation Service	H. H. BENNETT, *Chief.*
Weather Bureau	WILLIS R. GREGG, *Chief.*

This bulletin is a contribution from

Bureau of Agricultural Engineering	S. H. MCCRORY, *Chief.*
Division of Drainage	L. A. JONES, *Chief.*

U. S. GOVERNMENT PRINTING OFFICE: 1937

END